

The biostratigraphy and palaeogeography of acritarchs, chitinozoans, and cryptospores from the Upper Ordovician Ghelli Formation, Khoshyeilagh region, southern Caspian Sea, Alborz Mountains, northern Iran

Mohammad Ghavidel-Syooki

To cite this article: Mohammad Ghavidel-Syooki (28 Apr 2025): The biostratigraphy and palaeogeography of acritarchs, chitinozoans, and cryptospores from the Upper Ordovician Ghelli Formation, Khoshyeilagh region, southern Caspian Sea, Alborz Mountains, northern Iran, Palynology, DOI: [10.1080/01916122.2025.2475253](https://doi.org/10.1080/01916122.2025.2475253)

To link to this article: <https://doi.org/10.1080/01916122.2025.2475253>

 View supplementary material 

 Published online: 28 Apr 2025.

 Submit your article to this journal 

 Article views: 38

 View related articles 

 View Crossmark data 



The biostratigraphy and palaeogeography of acritarchs, chitinozoans, and cryptospores from the Upper Ordovician Ghelli Formation, Khoshyeilagh region, southern Caspian Sea, Alborz Mountains, northern Iran

Mohammad Ghavidel-Syooki

Institute of Petroleum Engineering, School of Chemical Engineering, College of Engineering, University of Tehran, Tehran, Iran

ABSTRACT

In the Khoshyeilagh region, 70 km north of Shahroud city, northern Iran, a siliciclastic succession of Lower Palaeozoic strata, including the Lalun, Mila, Lashkarak, and Ghelli formations, occurs alongside igneous rocks. These strata contain various organic-walled microfossils, including acritarchs, chitinozoans, cryptospores, scolecodonts, and graptolite remains. This study assesses the biostratigraphical significance of marine microfauna (chitinozoans), microflora (acritarchs), and terrestrial cryptospores in this part of the Alborz Mountains. Eighty-eight surface samples were collected from the above-mentioned formations, with six samples found to be barren due to red sediments or igneous rocks. The remaining samples yielded 118 palynomorph taxa: 55 species of acritarchs (28 genera), 48 species of chitinozoa (18 genera), and 15 cryptospore species (10 genera). Scolecodonts and graptolite remains were observed but not studied in detail. No palynomorphs were found in the Lalun, Mila, and Lashkarak formations, while the Ghelli Formation contained well-preserved, abundant organic-walled microfossils. These findings suggest that the Alborz Mountains were part of the Peri-Gondwana palaeo-province during the Late Ordovician. The co-occurrence of acritarchs, chitinozoans, and cryptospores in the Ghelli Formation indicates their potential for global chronostratigraphical correlation. The palynological assemblages suggest a shallow inner shelf environment during the Late Ordovician in the Khoshyeilagh region. Two hiatuses were identified: between the Lalun and Lashkarak formations and between the Ghelli and Soltan Meidan formations. This study also introduces 15 new morphotypes, including 10 new species of acritarchs and five new species of chitinozoa, detailed in the systematics sections.

KEYWORDS

Biostratigraphy; Upper Ordovician; chitinozoans; acritarchs; cryptospores; Khoshyeilagh region; Alborz Mountains; Caspian Sea; Northern Iran

1. Introduction

Palaeozoic sedimentary rocks extensively outcrop in the Alborz Mountain Range of northern Iran, forming substantial thicknesses (Figure 1). However, they have received limited biostratigraphical attention in the last several decades due to the scarcity of marine macrofossils. Although a general stratigraphical framework for the Palaeozoic of the Alborz Mountains has been proposed (Afshar-Harb 1975, 1994), precise stratigraphical correlations among the Lower Palaeozoic formations, and consequently the overall stratigraphical arrangement of the Alborz Mountain, remain uncertain due to the absence of detailed biostratigraphical evidence. In recent years, the utilisation of organic-walled microfossils such as acritarchs, chitinozoans, and miospores has proven significant for accurately dating and mapping the Iranian Palaeozoic formations, as well as for analysing their palaeogeographical connections (Ghavidel-Syooki 1995; Ghavidel-Syooki and Winchester-Seeto 2002; Ghavidel-Syooki and Vecoli 2007, 2008; Ghavidel-Syooki and Piri-Kangarshahi 2023, 2024). This paper examines the stratigraphical

relationships and biostratigraphical (palynological) age of the Ordovician sedimentary sequences with interbedded basalts in the Khoshyeilagh region. This study aims to date the Ordovician sediments in the Khoshyeilagh area precisely. Furthermore, the outcomes of this research will enhance the documentation of Ordovician palynomorphs (acritarchs, chitinozoans, and cryptospores) in this relatively unexplored Iranian region.

2. Geological setting and lithostratigraphy

The study examines the Khoshyeilagh region, where an anticline encompasses Khoshyeilagh village, about 70 km north of Shahroud in the Alborz Mountains, northern Iran. The area spans coordinates 36°30'–37°0'N and 55°30'–55°0'E, accessible via a paved road between Shahroud and Azadshahr cities (Figures 1–3). The Palaeozoic strata, totalling 7366 m, include the Lalun (412 m), Top Quartzite Member of the Mila (62 m), Lashkarak (290 m), Ghelli (3936 m), Soltan Meidan Basaltic Complex (SMBC) (710 m), Padeha (288 m), Khoshyeilagh (1188 m), and Mobarak

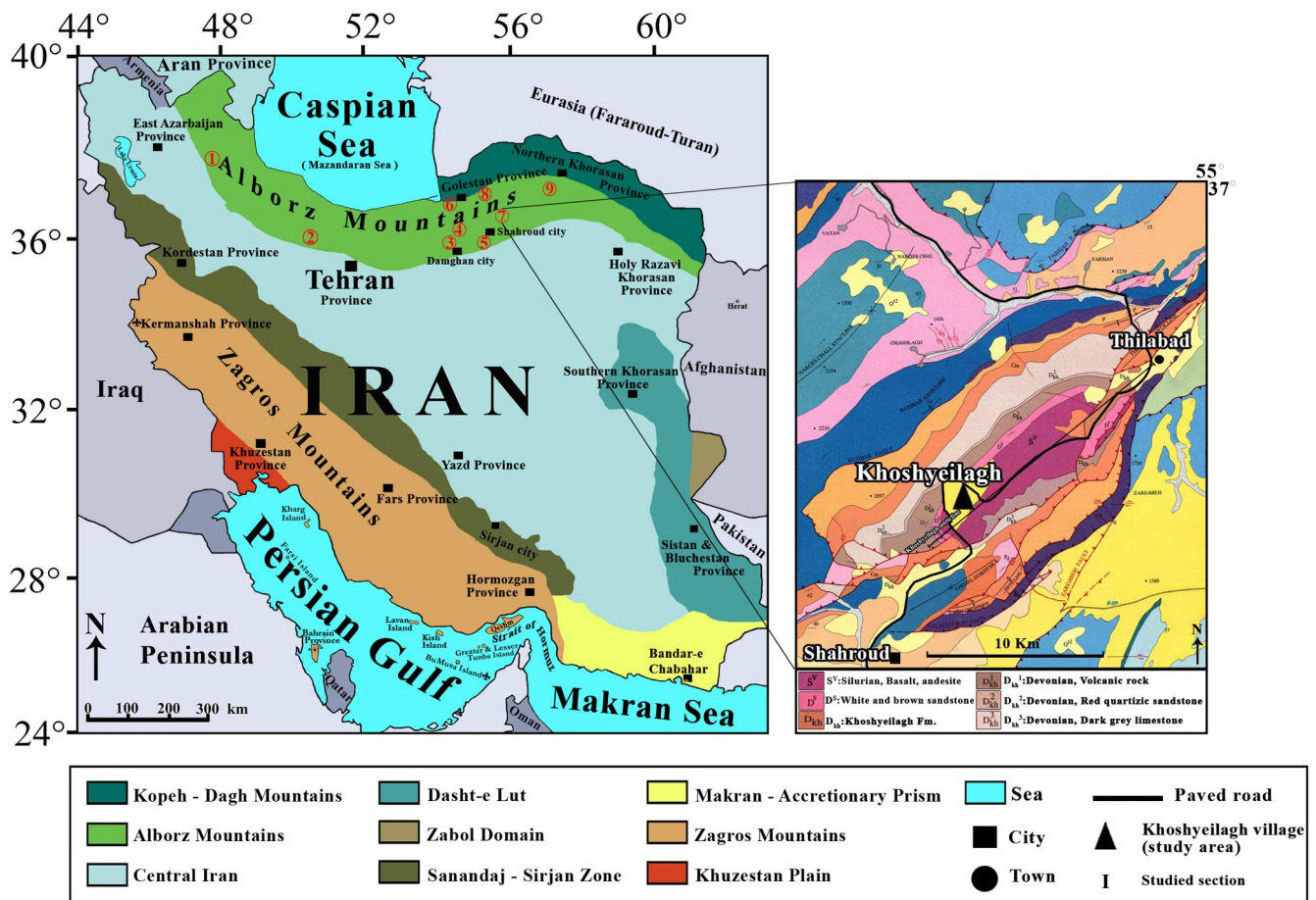


Figure 1. The geographical setting of the study area and other notable localities of Palaeozoic outcrops within the Alborz Mountains. These include: 1 = Alam Kuh; 2 = Hasanakdar; 3 = Gerdkuh; 4 = Simeh-Kuh; 5 = Deh-Molla; 6 = Deraznow (Gorgan Schists); 7 = Khoshyeilagh region (Khoshyeilagh village); 8 = Fazel Abad (Kholin Darreh); 9 = Kuh-e Saluk (Ghelli village and Plermis Gorge). Source from: Ghavidel-Syooki and Piri-Kangarshahi 2024.

(480 m) formations. While the Upper Palaeozoic formations (Padeha, Khoshyeilagh, Mobarak) have established biostratigraphical ages, the Lower Palaeozoic units lack diagnostic fossils.

This study documents the Lalun, Mila, and Lashkarak formations for the first time in the Khoshyeilagh anticline ('Jozak Farm' locality, see Figure 3), where a spring emerges from the Top Quartzite Member of the Mila Formation. It also confirms the Lashkarak Formation and identifies three divisions of the Ghelli Formation: lower siliciclastic (556 m), basaltic flow (3025 m), and upper detrital (355 m). The upper detrital succession has been variably assigned to the Shirgesht (Stampfli 1978), Lashkarak (Bozorgnia 1973), or Ghelli formations (Afshar-Harb 1994; Ghavidel-Syooki et al. 2011a). The Lashkarak and Shirgesht formations date to the Early Ordovician (Bozorgnia 1973; Ghavidel-Syooki 1995, 2000, 2001), whereas the Ghelli Formation is Late Ordovician at its type locality (Ghavidel-Syooki 1997, 2000, 2001; Ghavidel-Syooki and Winchester-Seeto 2002; Ghavidel-Syooki et al. 2011a; Ghavidel-Syooki and Piri-Kangarshahi 2024).

The SMBC, mainly trachybasalt-trachyandesite, remains age-uncertain. Jenny (1977) could not use K-Ar dating due to alteration but tentatively assigned a Silurian age based on its position between the Ghelli and Padeha formations. Later, U-Pb zircon dating from SMBC conglomerate pebbles suggested a Late Silurian (Gorstian) age (Ghavidel-Syooki et al. 2011a).

The SMBC (710 m) unconformably overlies the Ghelli Formation and is capped by the early Frasnian Padeha Formation. Only 13 m of the SMBC is sedimentary, with a 7-m pebbly conglomerate at its base. The upper detrital Ghelli Formation (355 m) consists of silty and grey shale (Figure 3), unconformably overlain by the SMBC. A brown, rounded, pebbly conglomerate and red-purple shales characterise the basal part of the upper detrital segment of the Ghelli Formation (Figure 3F). Despite the presence of trace fossils and ripple marks, marine macrofauna remains absent (Bozorgnia 1973; Afshar-Harb 1994; this study).

3. Materials and methods

Palynological analysis was conducted on 88 outcrop samples, with 82 obtained from the Ghelli Formation and five from the Lalun to Lashkarak formations (Figure 2). Each sample was assigned a National Iranian Oil Company Code number with the prefix MG, encompassing a range from MG-1 to MG-88. Palynomorphs were extracted from shale and siltstone samples following the palynological technique involving hydrochloric (HCl) and hydrofluoric (HF) acids (Sutherland 1994; Riding 2021). The purpose of this treatment was to eliminate carbonates and silicates, respectively. Residues were neutralised in distilled water after each acid treatment. The samples were not subjected to oxidation, and the



Figure 3. The Khoshyeilagh region, 70 km north of Shahroud city, exhibits various lithological features, including (A) the middle and upper member of the Ghelli Formation; (B) contact of the middle and upper members of the Ghelli Formation; (C) the Lalun Formation with its red-coloured components; (D) the 'Jozak Farm locality' of the Lalun Formation; (E) the top quartzite of the Mila Formation; (F) the basal conglomerate of the upper member of the Ghelli Formation; (G) the thick-bedded sandstone of the Lalun Formation; (H) sedimentary structure (load casts); (I) sedimentary structure (ripple marks) of the upper member of the Ghelli Formation in the Khoshyeilagh area.

organic residues were concentrated using density separation in a zinc bromide solution with a specific gravity of 1.95. Subsequently, the organic residue underwent sieving through a 15 μm nylon mesh sieve to remove finer debris and facilitate palynological analyses. The resulting palynological preparations were examined using transmitted light and scanning electron microscopy (SEM). The observed

acritarchs ranged from yellow to golden yellow, indicating a medium thermal alteration index ($\text{TAI} = 3.0\text{--}3.5$). This suggests a suitable organic maturation and implies potential oil generation in the shaly beds of the Ghelli Formation (Batten 1982, see fig. 1).

For reference and future research, the samples, slides, and SEM stubs from this study have been deposited in the

Iranian Natural History Museum, Department of Organisational Environment (DOE), under specific accession numbers ranging from DOEMG-1 to DOEMG-88 for samples and DOEStubMG-1 to DOEStubMG-88 for related stubs.

4. Systematics and biostratigraphy of palynomorph taxa

In the Khoshyeilagh region, the Upper Ordovician Ghelli Formation has yielded 10,179 palynomorph specimens. These specimens comprise 5,291 acritarchs, 3,686 chitinozoans, 128 scolecodonts, 198 graptolite remains, and 1,202 cryptospores (See [Supplementary data](#), S4–6). In total, 118 palynomorph taxa were identified, including 55 acritarch species in 28 genera, 48 chitinozoan species from 18 genera, and 15 cryptospore species in 10 genera. A detailed, alphabetical list of acritarchs is provided in the [Supplementary data](#) (S1). The chitinozoan microfauna is classified at a suprageneric level following the taxonomy of Paris et al. (1999), as documented in the [Supplementary data](#) (S2). The systematic palaeontology of cryptospores is detailed in the [Supplementary data](#) (S3) based on the morphological criteria established by Richardson (1996a, 1996b), Wellman and Richardson (1996), and Vecoli et al. (2011).

4.1. Systematics of new acritarch taxa

Many of the taxa under discussion correspond to well-known species. Therefore, I avoid providing an extensive formal systematic treatment. All measurements (in micrometres, μm) include minimum (mean) and maximum values. Detailed descriptions of new taxa are presented below.

Group INCERTAE SEDIS ACRITARCHA Evitt 1963

Genus *Baltisphaeridium* (Eisenack 1958) Eisenack 1969

Type species. *Baltisphaeridium longispinosum* Eisenack 1931

Baltisphaeridium tillabadensis sp. nov.

Plate 2, figure 21

Holotype. Plate 2, figure 21.

Type locality. Khoshyeilagh region, 70 km north of Shahrud city, south of the Caspian Sea within the Alborz Mountains in northern Iran.

Type stratum. Upper Ordovician (Sandbian) Ghelli Formation (MG-6 to MG-18).

Derivation of name. The name refers to the small town of Tillabad near the study area within the Alborz Mountains, in the north of Iran.

Dimensions. Diameter of vesicle 36 (38) 40 μm ; length of process 64 (67) 70 μm ; width of process 10 (11) 12 μm ;

diameter vesicle including processes 160 (164) 168 μm ; based on 10 measured specimens.

Description. The cyst is circular or oval, distinguished by four sturdy, identical hollow processes. These processes are notably narrowed at their base, forming a solid plug, and gradually taper towards their tips. The surfaces of both the vesicle wall and its processes are smooth. However, no excystment was detected during observation.

Remarks. *Baltisphaeridium tillabadensis* sp. nov. can be distinguished from other species of *Baltisphaeridium* primarily by its distinct number of processes and lack of ornamentation. While it resembles *Orthosphaeridium rectangulare* var. *quadricornis* Navidi-lzad et al. 2020, the former can be distinguished from differences in process type and its smaller overall size.

Baltisphaeridium iranense sp. nov.

Plate 2, figure 18

Holotype. Plate 2, figure 18.

Type locality. Khoshyeilagh region, 70 km north of Shahrud city, south of the Caspian Sea within the Alborz Mountains in northern Iran.

Type stratum. Upper Ordovician (Sandbian) Ghelli Formation (MG-6 to MG-18).

Derivation of name. *Baltisphaeridium iranense* sp. nov. is named after Iran, where this species was first described.

Dimensions. The diameter of the vesicle is 25 (31) 37 μm ; the length of the process is 32 (36) 40 μm ; the width of the process is 2.5 (3.5) 4.5 μm ; the total diameter, including processes, is 74 (77) 80 μm ; based on 10 measured specimens.

Description. The cyst exhibits a circular shape and is embellished with a variable count of processes, ranging from six to 10. These protrusions are distinctive and robust and display various forms, hollow and narrowed at their connection with the cyst. They remain detached from the cyst's interior due to a plug near their base. Gradually widening shortly above the plug, they taper to a pointed end. The processes are simple, bifurcated, or conical, or possess trifurcated branches, sometimes differing in size. The vesicle wall comprises a single layer with a smooth surface, while the processes' walls are either spiny or granular. Excystment occurs via a medium split.

Remarks. *Baltisphaeridium iranense* sp. nov. displays circular cysts adorned with simple, bifurcate, and trifurcate processes. While sharing similarities with *Baltisphaeridium perclarum* Loeblich and Tappan (1978), this new species stands out due to its smaller size, single vesicle wall layer, and one trifurcate process. Furthermore, Iranian specimens

resemble *Baltisphaeridium bramkaense* Górká (1979), albeit smaller and featuring only one trifurcate process.

Genus *Cornuferifusa* Jacobson and Achab 1985

Type species. *Cornuferifusa bifidipertica* Jacobson and Achab 1985

Cornuferifusa persianense sp. nov.

Plate 4, figures 7, 8

2011 *Cornuferifusa* sp. Ghavidel-Syooki et al. p. 259, p. III, fig. 1.

Holotype. Plate 4, figure 7.

Type locality. Khoshyeilagh region, 70 km north of Shahroud city, south of the Caspian Sea within the Alborz Mountains in northern Iran.

Type stratum. Upper Ordovician (Katian) Ghelli Formation (MG-75 to MG-88).

Derivation of the name. Originating from the Latin term 'Persia', which denotes the historical appellation of Iran.

Dimensions. Vesicle length 69 (71) 73 μm ; width of vesicle 16 (17.5) 19 μm ; length of polar process 15 (17) 19 μm ; width of process 1.8 (2) 2.2 μm ; processes in number 39–45; based on 10 specimens.

Description. The vesicle displays a symmetrical fusiform shape with bifurcate, hollow, conical polar processes. Adjacent to the polar regions, processes are simple, conical, curved, and bifurcated, albeit shorter than those at the poles. Both the vesicles and the processes feature thin walls with acuminate tips. Thirty-nine to 45 processes of uniform size emerge from the cysts. No excystment structure was observed.

Remarks. *Cornuferifusa persianense* sp. nov. resembles *Cornuferifusa bifidipertica* Jacobson and Achab (1985); however, it deviates from the latter in its size, process count, and less robust cysts. Furthermore, similarities exist with *Safirotheca safira* Vavrdová (1989). However, the Iranian species stands apart from those in the Czech Republic regarding size, process count, and variable morphology.

Genus *Dorsennidium* Wicander 1974 emend. Sarjeant and Stancliffe 1994

Type species. *Dorsennidium hamii* (Loeblich 1970) Sarjeant and Stancliffe 1994

Dorsennidium iranense sp. nov.

Plate 1, figure 16

Holotype. Plate 1, figure 16.

Type locality. Khoshyeilagh region, 70 km north of Shahroud city, south of the Caspian Sea within the Alborz Mountains in northern Iran.

Type stratum. Upper Ordovician (Katian) Ghelli Formation (MG-44 to MG-60).

Derivation of name. Refers to Iran, the country in which this species was first described.

Dimensions. Vesicle length excluding processes 28 (38) 48 μm ; width of vesicle 20 (23) 26 μm ; vesicle length including processes 60 (74) 88 μm ; length of apical process 40 (44) 48 μm ; width of apical process 11 (13) 15 μm .

Description. The vesicle's cyst displays an almost polygonal shape with convex sides or a bottle shape. Its processes are well-defined, elongated, and hollow, protruding from the cyst's surface. Usually, six to 15 spine-like processes extend freely into the vesicle's interior. These processes widen at the base, gradually tapering to sharp tips. The apical process is broader near its base compared to other processes, and three subsidiary spinelike processes extend from its closest taper point. No excystment structure was observed.

Remarks. *Dorsennidium iranense* sp. nov. exhibits a polygonal or bottle shape, adorned with 6–15 intricate processes. Its unique morphology and size distinguish it from other species within the genus.

Genus *Excultibrachium* Loeblich and Tappan 1978 emend. Turner 1984

Type species. *Excultibrachium concinnum* Loeblich and Tappan 1978

Excultibrachium jahandidehii sp. nov.

Plate 5, figures 1, 5; 2, 6; 3, 7; 4, 8; 9, 13

Holotype. Plate 5, figure 3.

Type locality. Khoshyeilagh region, 70 km north of Shahroud city, south of the Caspian Sea within the Alborz Mountains in northern Iran.

Type stratum. Upper Ordovician (Katian) Ghelli Formation (MG-31 to MG-43).

Derivation name. The species is named in honour of Mr Akbar Jahandideh, an employee of the Technical Faculty of Tehran University. He generously assisted me in capturing SEM photos during my research endeavours, for which I am sincerely grateful.

Dimensions. Total length, including from the tip of one process to the tip of another process, 101 (111) 121 μm ; diameter of vesicle 60 (63) 66 μm ; length of process 48 (52.5) 57 μm ; thickness of process 2.5 (3.7) 5 μm ; the number of processes 4–10.

Description. The vesicle exhibits a circular to subcircular outline. Processes are discrete, numbering 4–10, cylindrical and

homomorphic, hollow, without accessible communication with the vesicle interior, and sealed at the base by a plug. These processes arise at 90° from the vesicle wall, tapering from the proximal end to the point of furcation, where they divide into four to six tines, typically four, which are long and flexible, all within a single plane. The vesicle surface is smooth, while the process wall is either scabrous or faveolate. Excystment occurs via a medium split. Herein, I affirm my agreement with the definition of the genus *Excultibrachium* as provided by Loeblich and Tappan (1978), encompassing all its characteristics. *Excultibrachium jahandidehii* sp. nov. bears a resemblance to *Excultibrachium concinnum* (Loeblich and Tappan 1978) found in the Upper Ordovician (Caradocian) Eden Formation, USA (Loeblich and Tappan 1978). However, the former can be distinguished from the latter based on the number of appendices and dimensions. American specimens exhibit processes numbering from 18 to 28, whereas *Excultibrachium jahandidehii* sp. nov. features 4–10 processes, dividing into four to six tines. Moreover, the Iranian specimens exhibit similarities to *Excultibrachium oligocladatum*, documented from the Ordovician Caradoc Series in Shropshire, England (Turner 1984), and the Ashgillian of Anticosti Island, Québec, Canada (Jacobson and Achab 1985). However, the Iranian specimens differ in the number of processes (4–10) and their dimensions compared to those from England (16–26).

Remarks. A species of *Excultibrachium jahandidehii* features circular to subcircular vesicles and sturdy hollow processes (4–10); each branch divides four to six times within a single plane. These elongated processes exhibit flexibility, terminating in fine threads at their distal ends and feature a plug at their proximal ends.

Genus *Inflatarium* Le Hérisse et al. 2015

Type species. *Inflatarium trilobatum* Le Hérisse et al. 1915

Inflatarium alborzensis (Ghavidel-Syooki and Piri-Kangarshahi 2024) comb. nov.

Plate 1, figures 4, 5; Plate 4, figures 13–15; 17, 18; 20–22
2011b *Veryhachium* sp. cf. *V. triangulatum* Ghavidel-Syooki, et al. p. 259, pl. VII, fig. 2.

2021 *Inflatarium trilobatum* Ghavidel-Syooki and Piri-Kangarshahi, p. 15, pl. IX, figs. 1, 2.

2024 *Inflatarium trilobatum* Ghavidel-Syooki and Piri-Kangarshahi

Holotype. Plate 1, figure 4.

Type locality. Khoshyeilagh region, 70 km north of Shahroud city, south of the Caspian Sea within the Alborz Mountains in northern Iran.

Type stratum. The Upper Ordovician (Katian), Ghelli Formation (MG-44 to MG-60).

Derivation of name. The name refers to the Alborz Mountains, which stretch from the north-west to the north-east of Iran.

Dimensions. Longer lobe 44 (64) 84 µm; shorter lobe 37 (57.5) 78 µm; length of terminate spine 5 (9) 13 µm. Based on 20 measured specimens.

Description. The cyst presents as a hollow, inflated structure consisting of three rounded lobes, all situated within a single plane. These lobes are nearly identical in size and perpendicular to the axis of the cyst. The sides of the cyst may be straight, convex, or concave. Its wall is characteristically thin and smooth. The pylome is split and positioned centrally within the cyst. Each lobe terminates with a spinose ornamentation.

Remarks. The cyst is lobated, resulting from the fusion of three lobes. The rounded terminations of these lobes each bear a spinose ornament. While this species has similarities to *Inflatarium trilobatum* Le Hérisse et al. (2015) in having inflated vesicles and global coalescence, it differs in terms of its larger size, equivalent lobes, the presence of straight, convex, or concave sides, and the presence of one spinose ornament in the terminating lobes.

Genus *Navifusa* Combaz et al. 1967 ex Eisenack et al. 1976

Type species. *Navifusa navis* (Eisenack) Combaz et al. 1967

Navifusa caspiansis sp. nov.

Plate 1, figures 6, 7

Holotype. Plate 1, figure 6.

Type locality. Khoshyeilagh region, 70 km north of Shahroud city, south of the Caspian Sea within the Alborz Mountains in northern Iran.

Type stratum. The Upper Ordovician (Katian) Ghelli Formation (MG-44 to MG-60).

Derivation of name. *Navifusa caspiansis* sp. nov. is named after the Caspian Sea, the largest lake in the world, located between Asia and Europe.

Dimensions. Long diameter 34 (42) 48 µm; short diameter 15 (17) 19 µm; 10 specimens were measured.

Description. *Navifusa caspiansis* sp. nov. is characterised by a naviform vesicle with subparallel sides and rounded polar ends. This species tends to cluster in specific samples of the Ghelli Formation within the study area. Based on measurements from 10 specimens, the vesicle length ranges from 34 to 48 µm, and the vesicle width ranges from 15 to 19 µm. The vesicle wall is thin and slightly distorted due to folding, with abundantly scattered punctae ornamenting the surface. No excystment structure was observed.

Remarks. *Navifusa caspiansis* sp. nov. has a similar outline to *Navifusa ancepsipuncta* Loeblich (1970), *Navifusa punctata* Loeblich and Tappan (1978), and *Navifusa similis* (Eisenack

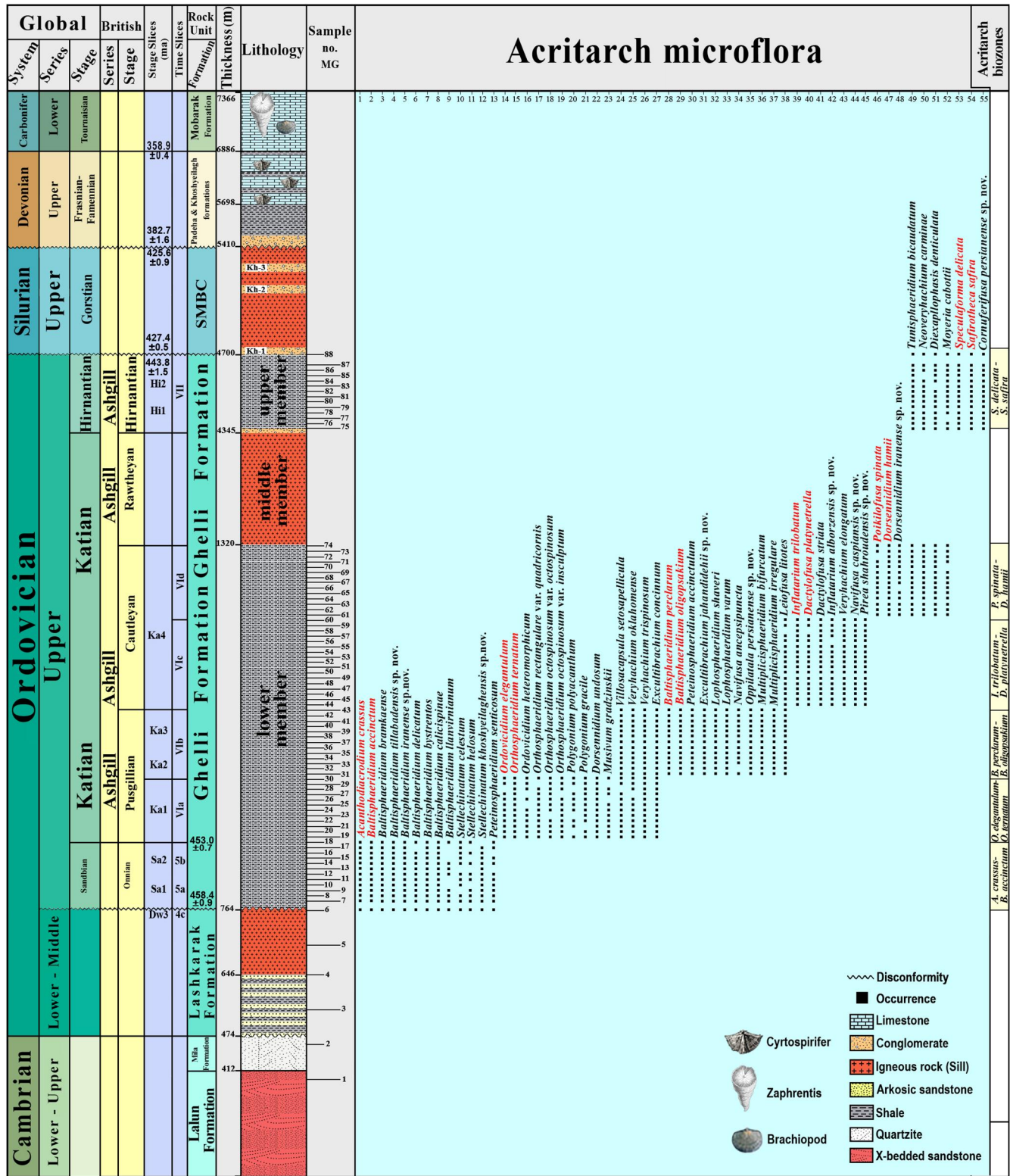


Figure 4. The lithology and stratigraphical distribution of acritarch taxa within the Ghelli Formation at the Khoshyeilagh region, northern Shahroud city, in the southern Caspian Sea, the Alborz Mountains of the north of Iran. Biostratigraphically significant species are highlighted in red font, and numbers correspond to those at the top of this figure. 1. *Acanthodiacrodiium crassum*; 2. *Baltisphaeridium accinctum*; 3. *Baltisphaeridium bramkaense*; 4. *Baltisphaeridium tillabadensis* sp. nov.; 5. *Baltisphaeridium iranense* sp. nov.; 6. *Baltisphaeridium delicatum*; 7. *Baltisphaeridium bystrentos*; 8. *Baltisphaeridium calcicispinae*; 9. *Baltisphaeridium oligopsakium*; 10. *Stellechinatum celestum*; 11. *Stellechinatum helosum*; 12. *Stellechinatum khoshyeilaghensis* sp. nov.; 13. *Peteinosphaeridium senticosum*; 14. *Ordovicidium elegantulum*; 15. *Orthosphaeridium ternatum*; 16. *Ordovicidium heteromorphicum*; 17. *Orthosphaeridium rectangulare* var. *quadricornis*; 18. *O. octospinosum* var. *Octospinosum*; 19. *O. octospinosum* var. *Insculptum*; 20. *Polygonium polyacanthum*; 21. *Polygonium gracile*; 22. *Dorsennidium undosum*; 23. *Musivium gradzinskii*; 24. *Villosacapsula setosapellucula*; 25. *Veryhachium oklahomense*; 26. *V. Trispinosum*; 27. *Excultibrachium concinnum*; 28. *Baltisphaeridium perclarum*; 29. *Baltisphaeridium oligopsakium*; 30. *Peteinosphaeridium accinctulum*; 31. *Excultibrachium jahandidehii* sp. nov.; 32. *Lophosphaeridium shaveri*; 33. *Lophosphaeridium varum*; 34. *Navifusa ancepsipuncta*; 35. *Oppilatala persianense* sp. nov.; 36. *Multiplicisphaeridium bifurcatum*; 37. *Multiplicisphaeridium irregulare*; 38. *Leiofusa litotes*; 39. *Inflatarium trilobatum*; 40. *Dactylofusa platynetrella*; 41. *Dactylofusa striata*; 42. *Inflatarium alborzensis* sp. nov.; 43. *Veryhachium elongatum*; 44. *Navifusa caspiensis* sp. nov.; 45. *Pirea shahroudensis* sp. nov.; 46. *Poikilofusa spinata*; 47. *Dorsennidium hamii*; 48. *Dorsennidium iranense* sp. nov.; 49. *Tunisphaeridium bicaudatum*; 50. *Neoverhachium carminae*; 51. *Diexaplophasis denticulata*; 52. *Moyeria cabottii*; 53. *Speculaformis delicata*; 54. *Safirotheca safira*; 55. *Cornuferifusa persianense* sp. nov.

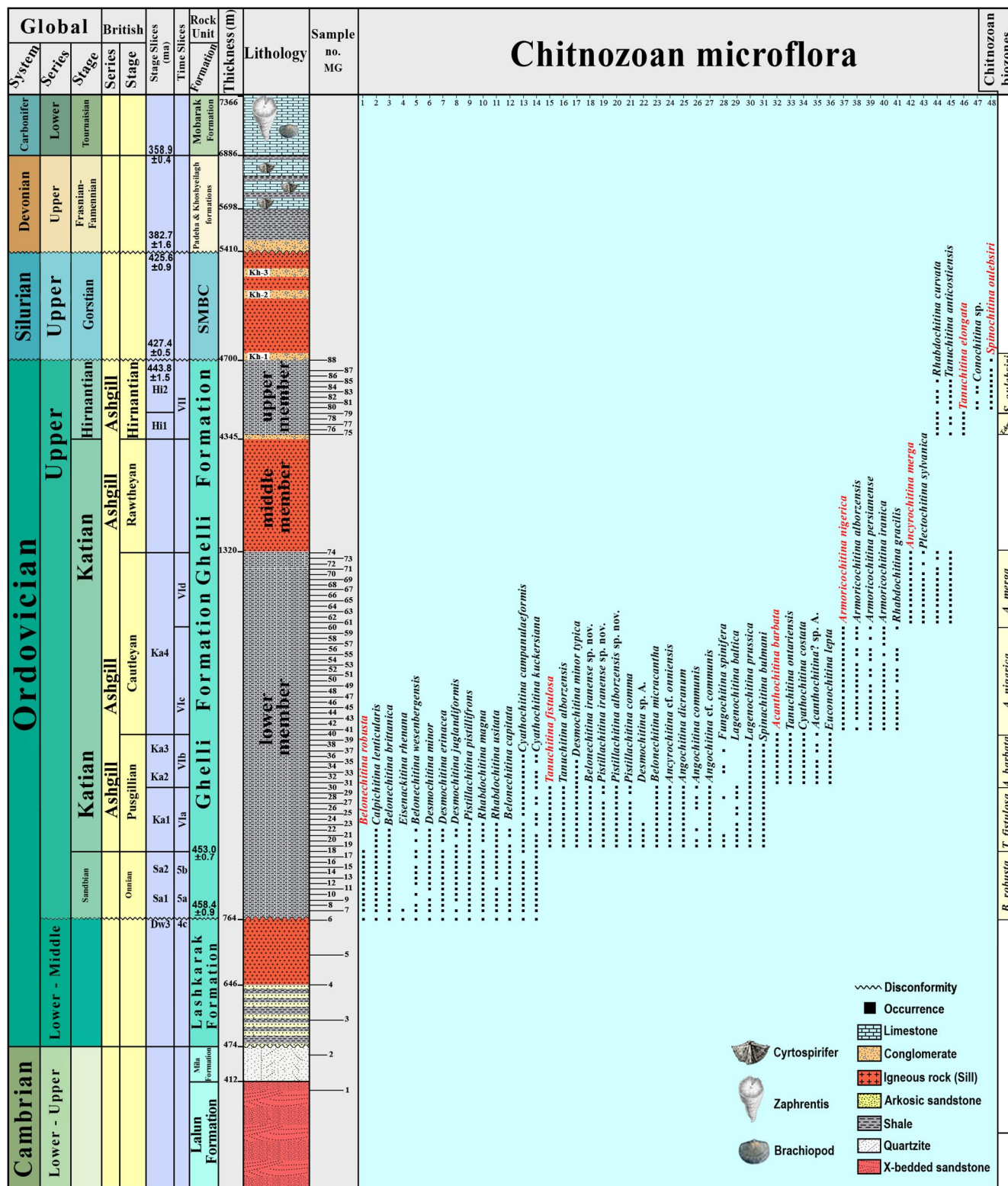


Figure 5. The lithology and stratigraphical distribution of chitinozoan taxa throughout the Ghelli Formation at the Khoshyeilagh region, northern Shahroud city, in the southern Caspian Sea, the Alborz Mountains of the north of Iran. Biostratigraphically significant species are highlighted in red font, and numbers preceding species names correspond to those at the top of this figure. 1. *Belonechitina robusta*; 2. *Calpichitina lenticularis*; 3. *Belonechitina britannica*; 4. *Eisenackitina rhenana*; 5. *Belonechitina wesenbergensis*; 6. *Desmochitina minor*; 7. *Desmochitina erinacea*; 8. *Desmochitina juglandiformis*; 9. *Pistillachitina pistillifrons*; 10. *Rhabdochitina magna*; 11. *Rhabdochitina usitata*; 12. *Belonechitina capitata*; 13. *Cyathochitina campanulaeformis*; 14. *Cyathochitina kuckersiana*; 15. *Tanuchitina fistulosa*; 16. *Tanuchitina alborzensis*; 17. *Desmochitina minor typica*; 18. *Belonechitina iranense* sp. nov.; 19. *Pistillachitina iranense* sp. nov.; 20. *Pistillachitina alborzensis* sp. nov.; 21. *Pistillachitina comma*; 22. *Desmochitina* sp. A; 23. *Belonechitina micracantha*; 24. *Ancyrochitina cf. onniensis*; 25. *Angochitina dicranum*; 26. *Angochitina communis*; 27. *Angochitina cf. communis*; 28. *Fungochitina spinifera*; 29. *Lagenochitina baltica*; 30. *Lagenochitina prussica*; 31. *Spinachitina bulmani*; 32. *Acanthochitina barbata*; 33. *Tanuchitina ontariensis*; 34. *Cyathochitina costata*; 35. *Acanthochitina?* sp. A; 36. *Euconochitina leptia*; 37. *Armoricochitina nigerica*; 38. *Armoricochitina alborzensis*; 39. *Armoricochitina persianense*; 40. *Armoricochitina iranica*; 41. *Rhabdochitina gracilis*; 42. *Ancyrochitina merga*; 43. *Plectochitina sylvanica*; 44. *Rhabdochitina curvata*; 45. *Tanuchitina anticostiensis*; 46. *Tanuchitina elongata*; 47. *Conochitina* sp.; 48. *Spinachitina oulebsiri*.

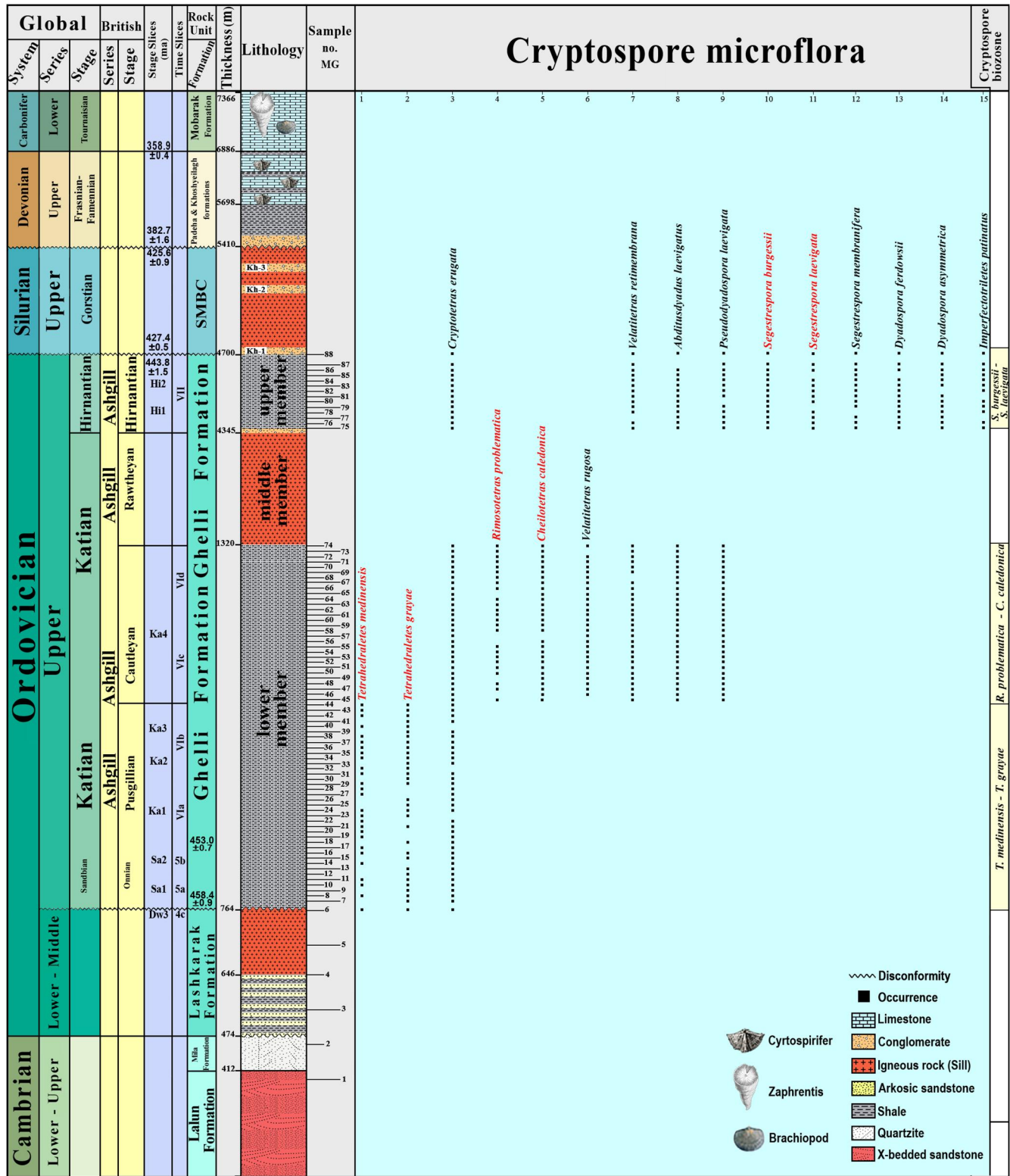


Figure 6. The lithology and stratigraphical distribution of cryptospore taxa within the Ghelli Formation at the Khosheyilagh region, northern Shahroud city, in the southern Caspian Sea, the Alborz Mountains of northern Iran. Biostratigraphically significant species are highlighted in red font, and numbers preceding species names correspond to those at the top of this figure. 1. *Tetraedraletes medimensis*; 2. *Tetraedraletes grayae*; 3. *Cryptotetras erugata*; 4. *Rimosotetras problematica*; 5. *Cheilotetras caledonica*; 6. *Velatitetras rugosa*; 7. *Velatitetras retimembrana*; 8. *Abditusdyadospora laevigata*; 9. *Pseudodyadospora laevigata*; 10. *Segestrespora burgessii*; 11. *Segestrespora laevigata*; 12. *Segestrespora membranifera*; 13. *Dyadospora ferdowsii*; 14. *Dyadospora asymmetrica*; 15. *Imperfectotriletes patinatus*.

1963) Turner 1984. However, the Iranian species differs from these taxa due to its significantly smaller size. Additionally, specimens resembling *Navifusa similis* have been

documented in the Quwarah Member of the Sarah Formation and the Baq'a Shale Member in the Arabian Peninsula (Le Hérisse et al. 2015; see Plate VIII, figure 4).

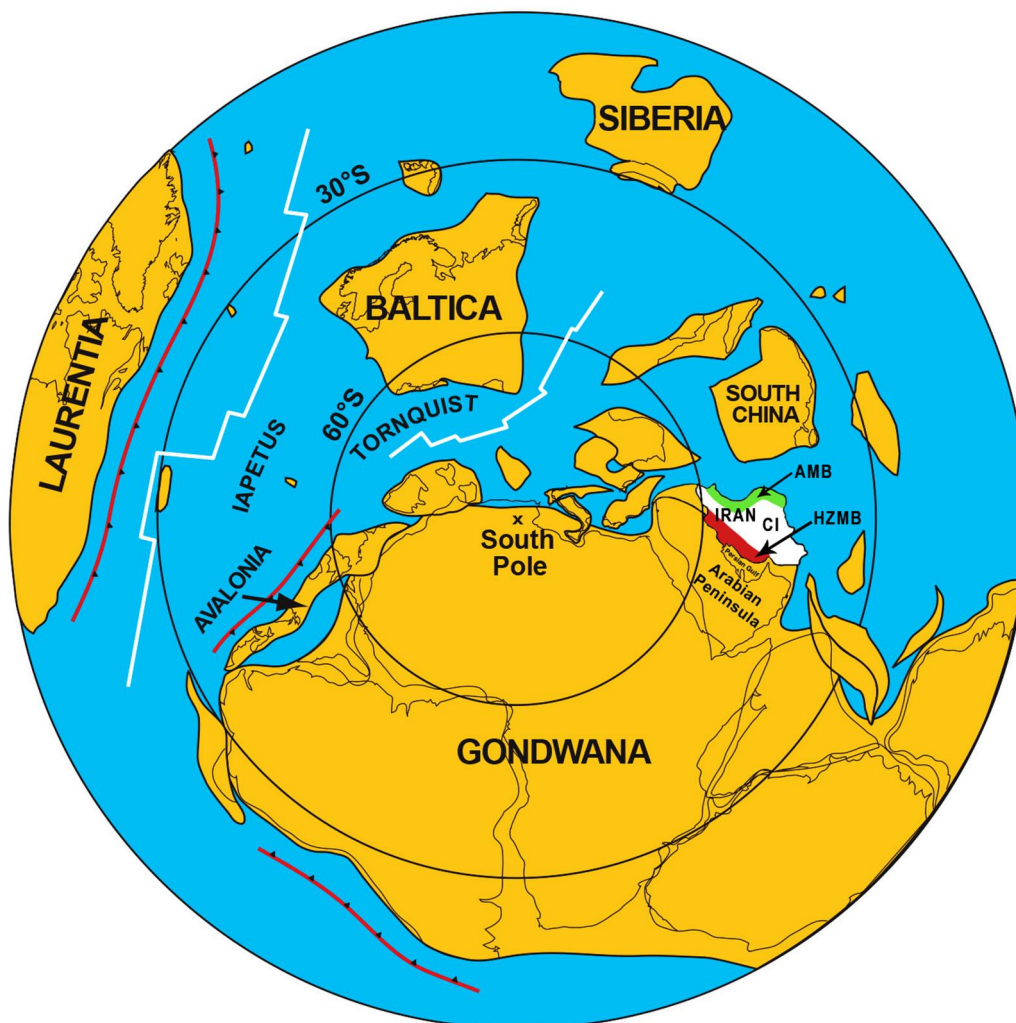


Figure 7. The palaeogeographical reconstruction of continental mass distribution during Ordovician times, along with the positioning of different parts of Iran, is depicted in the figure, adapted with slight modifications from Servais et al. (2009, fig. 2) and Cocks and Torsvik (2002, fig. 1). HZMB indicates the High Zagros Mountain Belt (Ghavidel-Syooki 2021, 2023), while AMB denotes the Alborz Mountain Belt (Ghavidel-Syooki 2016, 2017a, 2017b, 2017c; Ghavidel-Syooki and Piri-Kangarshahi 2023, 2024). CI refers to Central Iran (Ghavidel-Syooki 2003; Ghavidel-Syooki and Piri-Kangarshahi 2021).

However, the former can be distinguished from the latter due to its smaller size.

Genus *Oppilatata* Loeblich and Wicander 1976

Type species. *Oppilatata vulgaris* Loeblich and Wicander 1976

Oppilatata persianense sp. nov.

Plate 3, figure 12

2015 *Oppilatata* sp. Le Hérisse et al. p. 35, pl. VII, figs. 5, 6.

Holotype. Plate 3, figure 11.

Type locality. Khoshyeilagh region, 70 km north of Shahroud city, south of the Caspian Sea within the Alborz Mountains in northern Iran.

Type stratum. The Upper Ordovician (Katian) Ghelli Formation (MG-31 to MG-43).

Derivation of name. Originating from the Latin term 'Persia', which denotes the historical appellation of Iran.

Dimensions. Diameter of the central body 38 (41) 44 µm; length of processes 36 (40) 44 µm; width of processes 3 (3.5) 4 µm; 15 specimens were measured.

Description. The vesicle's cyst is spherical, with a thick wall, and smooth. There are 14–16 homomorphous processes, uniformly distributed. The processes are cylindrical and divide near their tip into two long, filose, and flexible branches, sometimes secondarily divided into two smaller branches. The processes communicate freely with the vesicle's interior. Their wall is thin and unornamented. The excystment structure is medium split.

Remarks. *Oppilatata persianense* sp. nov. shows similarities to *Oppilatata biscula* (Le Hérisse et al. 2001). However, the former differs in its fewer processes and the larger size of the vesicle.

Genus *Pirea* Vavrdová 1972

Type species. *Pirea dubia* Vavrdová 1972

***Pirea shahroudensis* sp. nov.**

Plate 1, figures 1, 2

2015 *Pirea* sp. Le Hérisse et al. 2015. p. 31, pl. III, figs. 5, 6.**Holotype.** Plate 1, figure 2.**Type locality.** Khoshyeilagh region, 70 km north of Shahroud city, south of the Caspian Sea within the Alborz Mountains in northern Iran.**Type stratum.** The Upper Ordovician (Katian) Ghelli Formation (MG-44 to MG-60).**Derivation of name.** *Pirea shahroudensis* sp. nov. is named after Shahroud City, which is located in the southern part of the study area.**Dimensions.** Length of vesicle 50 µm; width of vesicle 17 µm; 20 specimens were measured.**Description.** The cyst exhibits an elongated shape with a short, conical apical horn. This species tends to cluster in specific samples of the Ghelli Formation within the study area. All specimens from the Ghelli Formation display thin-walled, ovoid vesicles adorned with finely granulated, evenly distributed ornamentation. A slight constriction occurs at the neck, where the vesicle meets the horn. The horn terminates in a rounded fashion. Similar specimens (Plate 1, figures 6 and 7) have been documented in the Quwarah Member of the Sarah Formation and the Baq'a Shale Member in the Arabian Peninsula (Le Hérisse et al. 2015).**Remarks.** *Pirea shahroudensis* sp. nov. resembles *Pirea ornata* Cramer and Díez (1977) due to its ornamentation of dense granules on the vesicle. However, the former can be distinguished from the latter by its lack of striations on both the vesicle and the horn.Genus ***Stellechinatum*** Turner 1984**Type species.** *Stellechinatum celestum* (Martin) Turner 1984*Stellechinatum khoshyeilaghensis* sp. nov.

Plate 6, figure 11

Holotype. Plate 6, figure 11.**Type locality.** Khoshyeilagh region, 70 km north of Shahroud city, south of the Caspian Sea within the Alborz Mountains in northern Iran.**Type stratum.** The Upper Ordovician Ghelli Formation (MG-6 to MG-18).**Derivation of name.** The name refers to the Khoshyeilagh area within the Alborz Mountains, northern Iran.**Dimensions.** Diameter of the vesicle 35 (40) 45 µm; length of the processes 58 (62) 66 µm; width of the processes 12 (14)

16 µm; total length 167 µm, including two processes; the number of processes is 5–7; four specimens were measured.

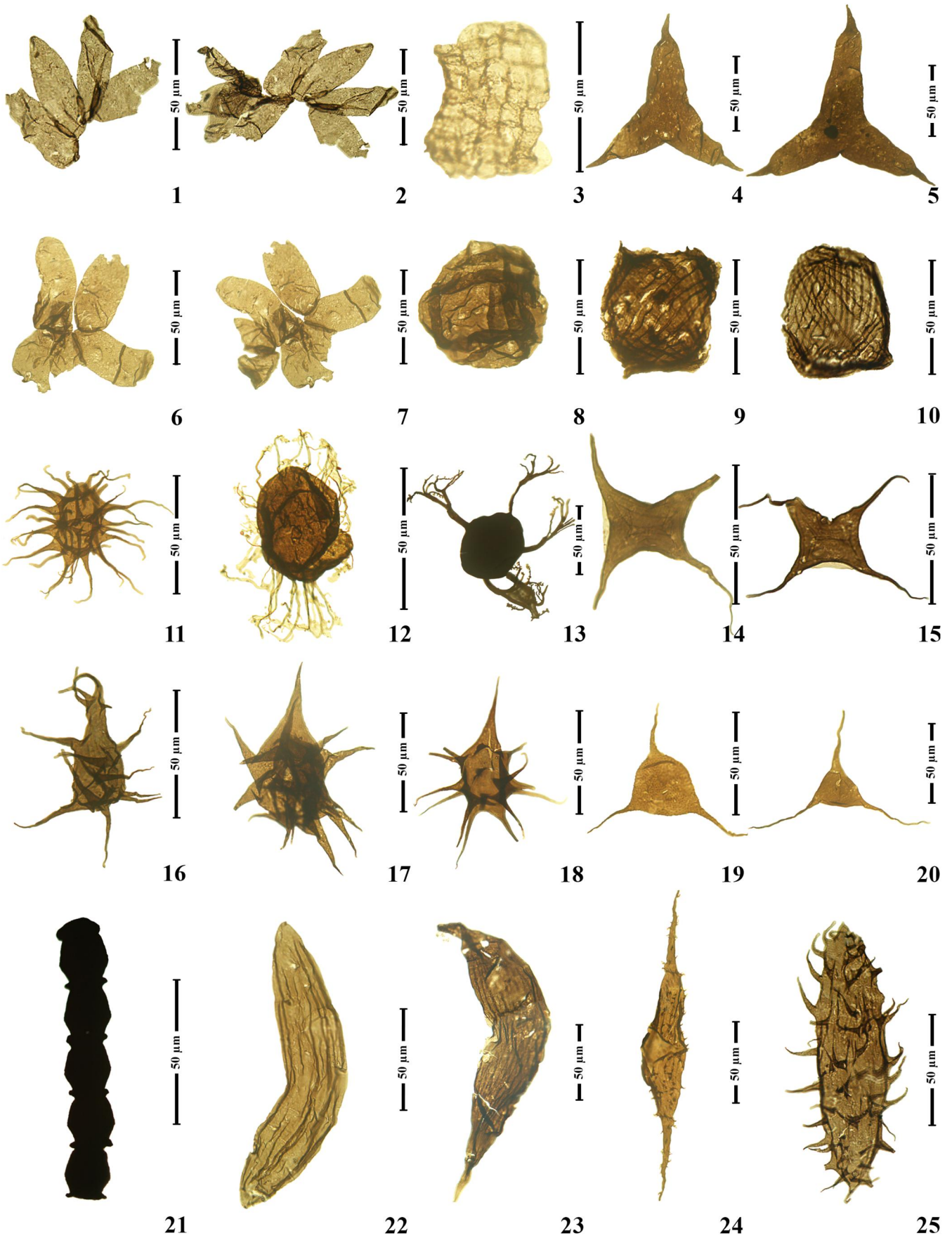
Description. The vesicle has a polygonal outline and is formed by merging wide process bases. The walls of both the cyst and processes are thick and single-layered. Based on observations of five specimens, 5–7 conical-shaped processes are present, which are hollow and superficial with acuminate ends. These processes open into the interior cavity and may vary in length and width. They are ornamented with slender spines, while the surface of the vesicle itself is smooth.**Remarks.** *Stellechinatum khoshyeilaghensis* sp. nov. differs from other species of *Stellechinatum* in its larger size and the presence of smaller spines in the processes.

4.2. Acritarch biostratigraphy

The Lower Palaeozoic rock units of the Alborz Mountains, including the Mila, Lashkarak, Ghelli, and Niur formations, have been extensively studied by several palynologists (Ghavidel-Syooki 1995, 2001, 2006, 2008, 2016, 2017a, 2017b; Ghavidel-Syooki and Winchester-Seeto 2002; Ghavidel-Syooki and Vecoli 2007; Ghavidel-Syooki and Piri-Kangarshahi 2023, 2024). The present study focuses on the Lalun, Mila (Middle–Late Cambrian), and Ghelli (Upper Ordovician) formations in the Khoshyeilagh region. Measurements and sampling were conducted to gather data on the first appearance datum (FAD) and last appearance datum (LAD) of each acritarch taxon. In total, 55 acritarch species, representing 28 genera, were identified, defining six acritarch assemblage biozones, as described below.

4.2.1. *Acanthodiacrodium crassus*–*Baltisphaeridium accinctum* assemblage biozone (time slices 5a–5b)

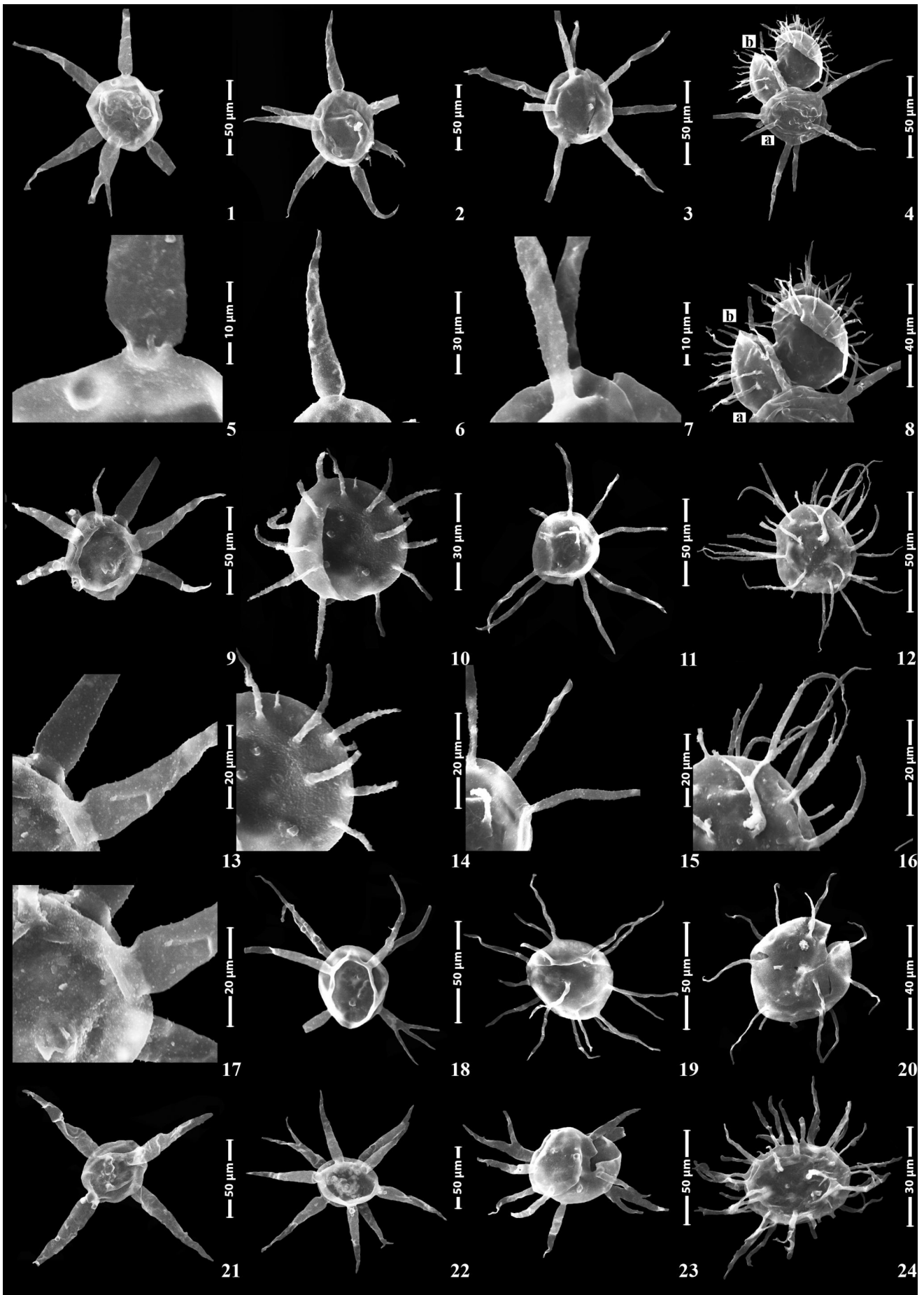
This acritarch assemblage biozone is defined by the co-occurrence of *Acanthodiacrodium crassus* (Loeblich and Tappan 1978) Vecoli (1999), and *Baltisphaeridium accinctum* (Loeblich and Tappan 1978). It appears in the basal part of the Ghelli Formation within the Khoshyeilagh region, persisting through samples MG-6 to MG-18, corresponding to a thickness of 105 m. *Acanthodiacrodium crassus* (Plate 4, figures 1–6) is present throughout MG-6 to MG-18 in the Ghelli Formation. This species has been previously documented in various regions, including the Sandbian–Katian stage slices Sa1–Ka1 (time slices 5a–Vla) of the Eden Formation in Indiana, USA (Loeblich and Tappan 1978); Katian stage slices Ka2–Ka4 (time slices Vlb–Vld) in Missouri, USA (Miller 1991); and the Sandbian–Katian of Anticosti Island, Canada (Jacobson and Achab 1985). Additionally, it has been recorded from the Algerian Sahara (Vecoli 1999), Jordan (Keegan et al. 1990), the Arabian Peninsula (Jachowicz 1995; Le Hérisse et al. 2015), and many localities in Iran (Ghavidel-Syooki 1996, 2001, 2008, 2016, 2017a, 2017b, 2017c; Ghavidel-



Syooki and Piri-Kangarshahi 2021, 2024). Its presence within the study area suggests a correlation with the Sandbian stage slices Sa1–Sa2 (time slices 5a–5b). *Baltisphaeridium accinctum* (Plate 2, figures 4b, 8b) is identified for the first time in the Khoshyeilagh region (Figure 4; Supplementary data, S4). It has been recorded in a few localities, including the late Middle to early Late Ordovician (Darrivilian–early Sandbian, stage slices Dw3–Sa1 and time slices 4c–5a) in the Black River Member of the Bromide Formation, USA (Loeblich and Tappan 1978), and the Sandbian stage slices Sa1–Sa2 (time slices 5a–5b) in southern Sweden (Rubinstein and Vajda 2023). The associated acritarchs of this biozone include *Baltisphaeridium calicispinae*, *Baltisphaeridium bramkaense*, *Baltisphaeridium bystrentos*, *Baltisphaeridium delicatum*, *Baltisphaeridium llanvirnianum*, *Peteinosphaeridium senticosum*, *Stellechinatum celestum*, and *Stellechinatum helosum*, which are discussed below. *Baltisphaeridium bramkaense* (Plate 2, figures 1, 5; 2, 6; 23) first appears in sample MG-6 and continues into sample MG-18 of the Ghelli Formation in the Khoshyeilagh region (Figure 4). According to Górká (1979), *B. bramkaense* closely resembles *Baltisphaeridium perclarum* (Loeblich and Tappan 1978) but with broader processes and an ornamented vesicle, suggesting it could be a junior synonym of *B. perclarum*. The Iranian specimens show greater similarity to the Swedish specimens than those from the USA, although I refrain from considering these species synonyms pending a detailed taxonomic revision. Researchers have documented this species in various regions, including the late Middle–Late Ordovician (Darrivilian–Sandbian stage slices Dw1–Sa1 and time slices 4a–5a) in Estonia (Górká 1979; Uutela and Tynni 1991); late Middle–early Late Ordovician (late Darrivilian–early Late Ordovician stage slices Dw3–Sa1 and time slices 4c–5a) in Iran (Ghavidel-Syooki and Piri-Kangarshahi 2023); and Sandbian–early Katian stage slices Sa1–Ka1 (time slices 5a–V1a) in Sweden (Rubinstein and Vajda 2023). *Baltisphaeridium calicispinae* (Plate 2, figures 10, 15) is reported for the first time from the Ghelli Formation in the Khoshyeilagh region. It has been identified in samples MG-6 to MG-18 (Figure 4; Supplementary data, S4). This species has been documented in a few regions, including the early Caradocian (Sandbian stage slice Sa1 and time slice 5a) in Estonia (Górká 1969) and the Sandbian stage slices Sa1–Sa2 (time slices 5a–5b) in southern Sweden (Rubinstein and Vajda 2023). *Peteinosphaeridium senticosum* (Plate 5, figures 12, 16) is present in samples MG-6 to MG-18 of the Ghelli Formation in the Khoshyeilagh region (Figure 4;

Supplementary data, S4). This species was previously documented in North Africa in the Darrivilian stage slices Dw1–Dw3 (time slices 4a–4b) (Vecoli 1999). *Stellechinatum celestum* (Plate 3, figures 19, 20) is identified in samples MG-6 to MG-18 of the Ghelli Formation in the Khoshyeilagh region (Figure 4; Supplementary data, S4). Researchers have recorded *Stellechinatum celestum* in various localities, including the Floian–Darrivilian stage slices F1–Dw3 (time slices 2a–4c) in Montagne Noire, France (Martin 1973), the Algerian Sahara (Jardiné et al. 1974); the Darrivilian stage slices Dw1–Dw3 (time slices 4a–4c) in Belgium (Servais and Maletz 1992); the Darrivilian stage slices Dw1–Dw3 (time slices 4a–4c) in the Prague Basin, Czech Republic (Vavrdová 1977); the late Darrivilian–Sandbian stage slices Dw3–Sa2 (time slices 4c–5b) in North Wales, UK (Trythall et al. 1987); the early Sandbian stage slice Sa1 (time slice 5a) on the Arabian Peninsula (Jachowicz 1995); the Sandbian stage slices Sa1–Sa2 (time slices 5a–5b) in the Caradoc Series, type area, Shropshire, England (Turner 1984); the Darrivilian stage slices Dw1–Dw3 (time slices 4a–4c) in North Africa (Vecoli 1999); and the Darrivilian stage slices Dw1–Dw3 (4a–4c) in the Lashkarak Formation of the Simeh-Kuh area within the Alborz Mountains of northern Iran (Ghavidel-Syooki and Piri-Kangarshahi 2024). *Stellechinatum helosum* (Plate 3, figures 16, 17, 18) also occurs in samples MG-6 to MG-18 of the Ghelli Formation in the Khoshyeilagh region (Figure 4; Supplementary data, S4). This species is documented for the first time in this region. Previously, researchers had identified *Stellechinatum helosum* in the Sandbian stage slices Sa1–Sa2 (time slices 5a–5b) in Shropshire, England (Turner 1984). Additionally, three new species – *Baltisphaeridium tillabadenesis* sp. nov. (Plate 2, figure 21), *Baltisphaeridium iranense* sp. nov. (Plate 2, figure 18), and *Stellechinatum khoshyeilaghensis* sp. nov. (Plate 6, figure 11) – were identified, and they are restricted to this assemblage biozone. The presence of the *Acanthodiacrodium crassus*–*Baltisphaeridium accinctum* assemblage biozone, along with the associated acritarch taxa, indicates that the interval from MG-6 to MG-18 of the Ghelli Formation in the Khoshyeilagh region of northern Iran corresponds to the Sandbian stage slices Sa1–Sa2 (time slices 5a–5b). Notably, strata older than the upper part of the Ghelli Formation have not been reported from the Khoshyeilagh anticline. As a result, the lower and middle parts of the Ghelli Formation and the Lalun, Mila, and Lashkarak formations are recorded for the first time in the study section.

Plate 1. Figures 1, 2. *Pirea shahroudensis* sp. nov. (sample MG-44; three specimens); Figure 3. *Musivum gradzinskii* Wood and Turnau 2001 (sample MG-19; two specimens); Figures 4, 5. *Inflatarium alborzensis* Ghavidel-Syooki and Piri-Kangarshahi 2024 (sample MG-44; 10 specimens); Figures 6, 7. *Navifusa caspiensis* sp. nov. (sample MG-44; 10 specimens); Figure 8. *Lohosphaeridium shaveri* Loeblich and Tappan 1978 (sample MG-31; four specimens); Figures 9, 10. *Moyeria cabottii* (Cramer 1971) Miller and Eames 1982 (sample MG-61; two specimens); Figure 11. *Polygonium polyacanthum* (Eisenack 1963) Sarjeant and Stancliffe 1994 (sample MG-19; two specimens); Figure 12. *Tunisphaeridium bicaudatum* Le Hérisse et al. 2015 (sample MG-61; five specimens); Figure 13. *Excultibrachium concinnum* Loeblich and Tappan 1987 (sample MG-19; five specimens); Figures 14, 15. *Neoverhachium carminae* (Cramer) Cramer 1971 (sample MG-61; two specimens); Figure 16. *Dorsennidium iranensis* sp. nov. (sample MG-61; three specimens); Figures 17, 18. *Dorsennidium undosum* Wicander et al. 1999 (sample MG-19; five specimens); Figure 19. *Villosacapsula setosapellucula* (Loeblich) Loeblich and Tappan 1976 (sample MG-19; four specimens); Figure 20. *Verhachium elongatum* Downie 1963 (sample MG-44; nine specimens); Figure 21. *Desmochitina minor typica* Eisenack 1931 (sample MG-19; two specimens); Figures 22, 23. *Dactylofusa striata* (Staplin et al. 1965) Fensome et al. 1990 (sample MG-44; one specimen); Figure 24. *Poikilofusa spinata* (Staplin et al. 1965) emend. Loeblich and Tappan 1978 (sample MG-61; three specimens); Figure 25. *Safirotheca safira* Vavrdová 1989 (sample MG-75; three specimens).



4.2.2. *Ordoviciidum elegantulum*–*Orthosphaeridium ternatum* assemblage biozone (time slice VIa)

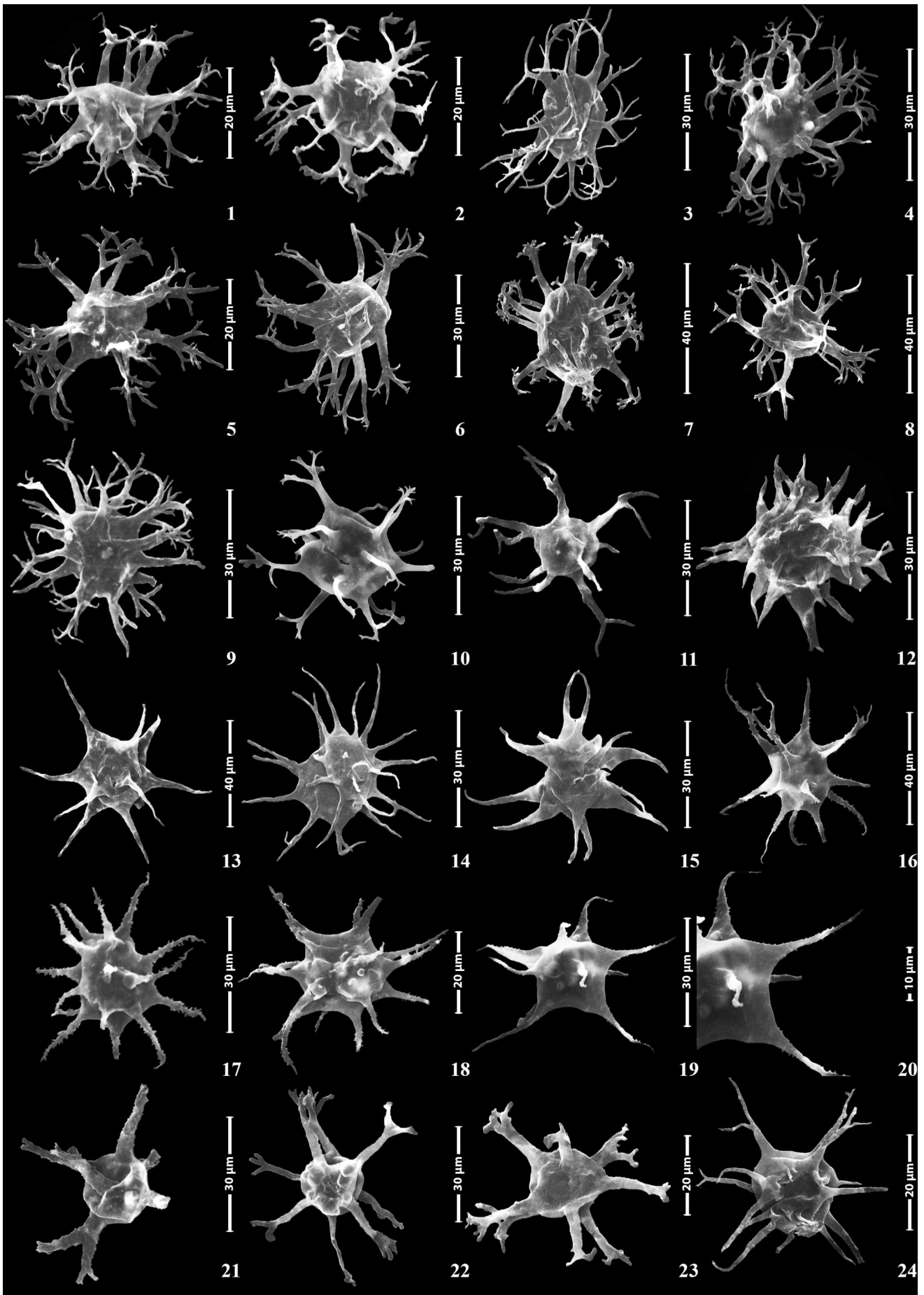
The co-occurrence of *Ordoviciidum elegantulum* Tappan and Loeblich (1971) and *Orthosphaeridium ternatum* (Burmam) Eisenack et al. (1976) defines this acritarch biozone in the Ghelli Formation (Khoshyeilagh region). It succeeds the preceding biozone and spans the MG-19 to MG-30 interval, covering 97 m of the stratigraphical column. *Ordoviciidum elegantulum* (Plate 5, figures 17, 18) occurs in intervals MG-19 to MG-30 of the Ghelli Formation in the Khoshyeilagh region (Figure 4; Supplementary data, S4). It has been documented from the late Darriwilian to Hirnantian across various localities, including Oklahoma and Indiana, USA (Tappan and Loeblich 1971; Colbath 1979), Shropshire, England (Turner 1984), China (Li and Wang 1997), the Arabian Peninsula and Iraq (Jachowicz 1995; Al-Ameri 2010), Sweden (Eiserhardt 1992; Rubinstein and Vajda 2023), the Prague Basin, Morocco, Algeria, Tunisia, and Libya (Elaouad-Debbaj 1988; Vavrdová 1988, 1989; Vecoli 1999, 2000), as well as Chad and south-eastern Libya (Le Hérisse et al. 2013). In Iran, it has been recorded from the Katian stage (Ghavidel-Syooki 2008, 2016; Ghavidel-Syooki et al. 2011a; Ghavidel-Syooki et al. 2014; Ghavidel-Syooki and Piri-Kangarshahi 2021, 2024). *Orthosphaeridium ternatum* (Plate 6, figure 10) appears in the MG-19 to MG-30 interval of the Ghelli Formation, Alborz Mountains, south of the Caspian Sea (Figure 4; Supplementary data, S4). It has been recorded from the Middle Ordovician (Dapingian, slices Dp1–Dp3, time slices 3a–3b) in Turkey (Paris et al. 2007); the late Darriwilian stage slice Dw3 (time slice 4c) in Germany (Burmam 1970a), France (Rauscher 1973), England (Booth 1979), the Arabian Peninsula (Le Hérisse et al. 2017), Iraq (Al-Ameri 2010), and North Gondwana (Vecoli and Le Hérisse 2004); the late Darriwilian stage slice Dw3 (time slice 4c) in the Lashkarak Formation, Alborz Mountains, Iran (Ghavidel-Syooki and Piri-Kangarshahi 2023, 2024); and the Sandbian–Katian stage slices Sa1–Ka4 (time slices 5a–VIId) in the Seyahou Formation, Zagros Mountains (Ghavidel-Syooki et al. 2011b) and the Ghelli Formation, Alborz Mountains (Ghavidel-Syooki 2017b).

The associated acritarch taxa in this biozone include *Dorsennidium undosum*, *Excultibrachium concinnum*, *Musivum gradzinskii*, *Ordoviciidum heteromorphicum*, *Orthosphaeridium rectangulare* var. *quadricornis*, *O. octospinosum* var. *octospinosum*, *O. octospinosum* var. *insculptum*, *Polygonium polyacanthum*, *Polygonium gracile*, *Villosacapsula setosapellicula*, *Veryhachium oklahomense*, and *V. trispinosum*, each of which is discussed below.

Dorsennidium undosum (Plate 1, figures 17, 18) is recorded for the first time from the Ghelli Formation (Khoshyeilagh region, Alborz Mountains, Iran) in the MG-19

to MG-30 interval (Figure 4; Supplementary data, S4). Previously, it was documented from the Caradocian–Ashgillian (Sandbian–Katian stage slices Sa1–Ka4, time slices 5a–VIId) in Kansas, USA (Wright and Meyers 1981) and the Richmondian (Katian stage slices Ka1–Ka4, time slices VIa–VIId) in Missouri, USA (Wicander et al. 1999). *Excultibrachium concinnum* (Plate 1, figure 13) is recorded for the first time from the Ghelli Formation (Khoshyeilagh region, Alborz Mountains, Iran) in the MG-19 to MG-30 interval and continues into the succeeding biozone (Figure 4; Supplementary data, S4). It has been documented from the Llanvirnian–Caradocian (late Darriwilian–Sandbian stage slices Dw3–Sa2, time slices 4c–5b) in Gotland, Sweden (Górka 1987); the Caradocian (Sandbian stage slices Sa1–Sa2, time slices 5a–5b) in Shropshire, England (Turner 1984) and Indiana, USA (Loeblich and Tappan 1978; Colbath 1979); the Caradocian–Ashgillian (Sandbian–Katian stage slices Sa1–Ka4, time slices 5a–VIId) in Gotland, Sweden (Eiserhardt 1992) and the Labrador Sea, Canada (Legault 1982); and the Ashgillian (Katian stage slices Ka1–Ka4, time slices VIa–VIa) in Anticosti Island, Québec, Canada (Jacobson and Achab 1985) and the Maquoketa Shale, Missouri, USA (Wicander et al. 1999). *Musivum gradzinskii* (Plate 1, figure 3) occurs in the MG-19 to MG-30 interval of the Ghelli Formation, Khoshyeilagh region, Alborz Mountains, Iran (Figure 4; Supplementary data, S4). Initially documented from Devonian samples in the Holy Cross Mountains, Poland (Wood and Turnau 2001), it was later identified in the Upper Ordovician Ghelli Formation, Iran, within the *nigerica* and *merga* chitinozoan biozones (middle–late Katian stage slices Ka3–Ka4, time slices VIc–VIId) (Ghavidel-Syooki 2016). In the present study, its association with *Tanuchitina fistulosa* and *Acanthochitina barbata* suggests an older age (Katian stage slices Ka1–Ka2, time slices VIa–VIb). *Ordoviciidum heteromorphicum* (Plate 5, figures 19, 20) occurs from MG-19 to MG-30 interval in the Ghelli Formation, Khoshyeilagh region, Alborz Mountains, Iran (Figure 4; Supplementary data, S4). It has been recorded from the late Darriwilian stage slice Dw3 (time slice 4c) in Sweden (Kjellström 1971; Rubinstein and Vajda 2023) and the Ashgillian (Katian–Hirnantian stage slices Ka1–Hi2, time slices VIa–VIId) in Libya (Hill and Molyneux 1988; Vecoli 1999). *Orthosphaeridium rectangulare* var. *quadricornis* (Plate 6, figures 2, 6; 3, 4, 7) occurs in the MG-19 to MG-30 interval of the Ghelli Formation, Khoshyeilagh region, Alborz Mountains, Iran (Figure 4; Supplementary data, S4). Researchers have documented it from the Arenig (Floian stage slices FI1–FI3, time slices 2a–2c) in China (Yin 1995); late Arenig (Floian stage slice FI3, time slice 2c) in the Griffelschiefer, Germany (Heuse et al. 1994); late Llanvirn (Darriwilian stage slice Dw3, time slice

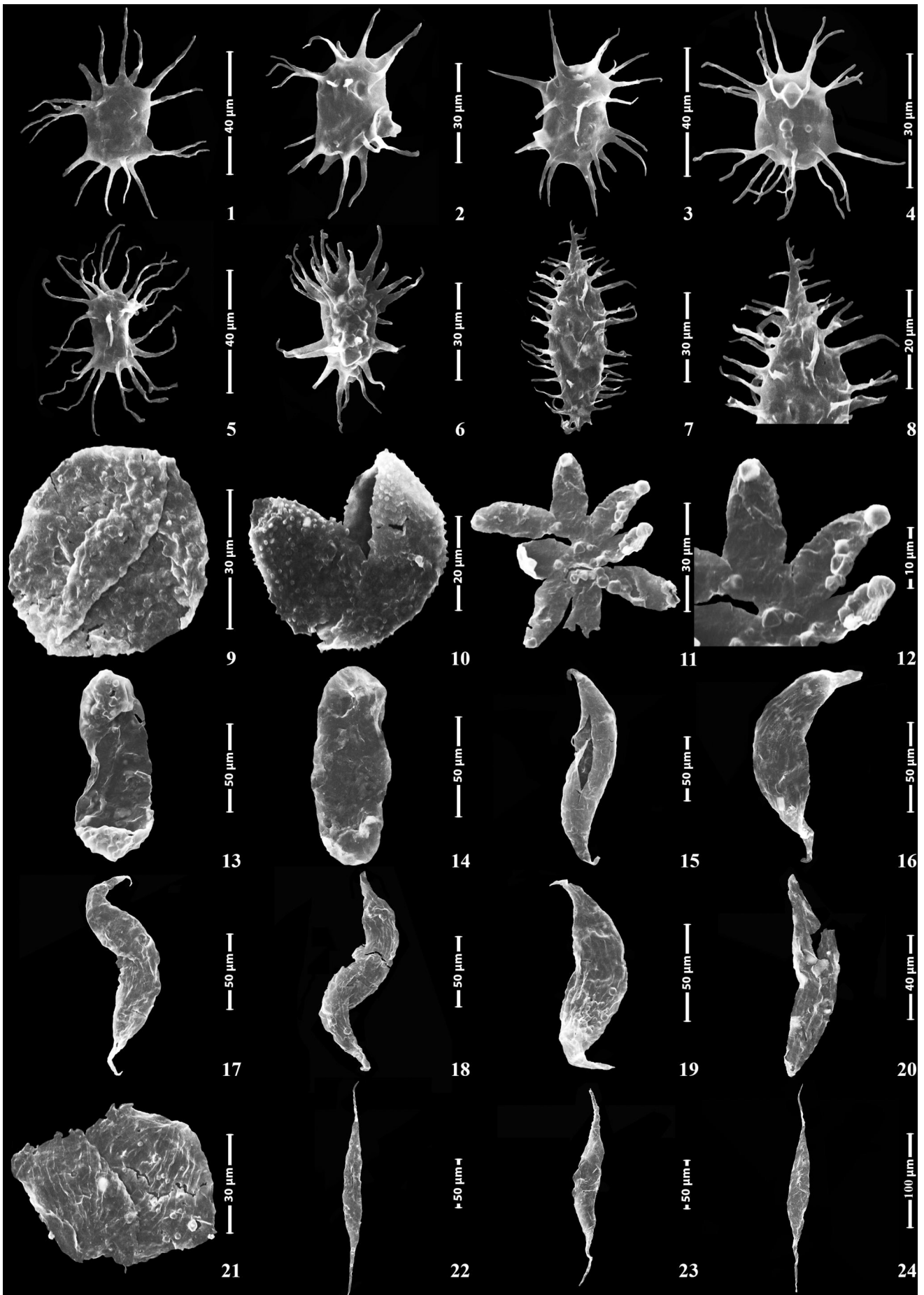
Plate 2. Figures 1, 5; 2, 6; 23. *Baltisphaeridium bramkaense* Górka 1979 (sample MG-6; five specimens); Figures 4b, 8b. *Baltisphaeridium accinctum* Loeblich and Tappan 1978 (sample MG-31; 10 specimens); Figures 4a, 8a, 22. *Baltisphaeridium perclarum* Loeblich and Tappan 1978 (sample MG-31; five specimens); Figures 9, 13, 17. *Baltisphaeridium llanvirnianum* Deunff 1977 (sample MG-6; one specimen); Figures 11, 15. *Baltisphaeridium calicispinae* Górka 1969 (sample MG-6; 3 specimens); Figures 12, 16, 24. *Baltisphaeridium oligopsakium* Loeblich and Tappan 1978 (sample MG-31; one specimen); Figures 10, 14. *Baltisphaeridium bystrentos* Loeblich and Tappan 1978 (sample MG-6; five specimens); Figure 18. *Baltisphaeridium tillabadensis* sp. nov. (sample MG-6; two specimens); Figures 19, 20. *Baltisphaeridium delicatum* (Turner 1984) Eiserhardt 1989 (sample MG-6; nine specimens); Figure 21. *Baltisphaeridium iranensis* sp. nov. (sample MG-6; four specimens).



4c) in Germany (Burmam 1970b, 1976); late Middle Ordovician (Darriwilian stage slices Dw1–Dw3, time slices 4a–4c) in Iran (Ghavidel-Syooki and Piri-Kangarshahi 2023, 2024); early Caradocian (Sandbian stage slice Sa1, time slice 5a) in the Arabian Peninsula (Jachowicz 1995); Caradocian (Sandbian stage slices Sa1–Sa2, time slices 5a–5b) in Iraq (Al-Ameri 2010), England (Downie 1984; Turner 1984), and the Czech Republic (Vavrdová 1974); and Ashgillian (Katian stage slices Ka1–Ka4, time slices VIa–VIc) in Jordan (Keegan et al. 1990) and north-eastern Iran (Ghavidel-Syooki 2017a). *Orthosphaeridium octospinosum* var. *octospinosum* (Plate 6, figures 8, 9) occurs in the MG-19 to MG-30 interval of the Ghelli Formation, Khoshyeilagh region, Alborz Mountains, Iran (Figure 4; Supplementary data, S4). Researchers have documented it from the Middle Ordovician (Dapingian–Darriwilian stage slices Dp1–Dw3, time slices 3a–4c) in Sweden (Kjellström 1971; Górká 1987); the Caradocian (Sandbian stage slices Sa1–Sa2, time slices 5a–5b) in eastern Canada (Martin 1983); the Ashgillian (Katian stage slices Ka1–Ka4, time slices VIa–VIc) in the USA (Loeblich 1970), Morocco (Elaouad-Debbaj 1988), Portugal (Elaouad-Debbaj 1978), and Turkey (Dean and Martin 1978); the Caradocian–Ashgillian (Sandbian–Katian stage slices Sa1–Ka4, time slices 5a–VIc) in Iran (Ghavidel-Syooki 2000, 2003, 2021); the Hirnantian stage slices Hi1–Hi2 (time slice VII) in the Arabian Peninsula (Miller and Al-Ruwaili 2007); the early late Katian stage slice Ka4 (time slice VIc) in south-western Libya (Abuhmida 2013); and the Katian–Hirnantian stage slices Ka1–Hi2 (time slices VIa–VII) in north-eastern Alborz Mountains, Iran (Ghavidel-Syooki 2017c; Ghavidel-Syooki and Borji 2018). *Orthosphaeridium octospinosum* var. *insculptum* (Plate 6, figures 1, 5) occurs in the MG-19 to MG-30 interval of the Ghelli Formation in the Khoshyeilagh region (Figure 4; Supplementary data, S4). Researchers have documented it in the Middle to early Late Ordovician (Darriwilian–Sandbian stage slices Dw3–Sa2, time slices 4c–5b) in Gotland, Sweden (Górká 1987); the Llandeilo–Caradoc (Darriwilian–Sandbian stage slices Dw3–Sa2, time slices 4c–5b) in Ontario, Canada (Martin 1983); the Llanvirn–Ashgillian (Darriwilian–Katian stage slices Dw3–Ka4, time slices 4c–VIc) in Estonia (Uutela and Tynni 1991); the Caradocian (Sandbian stage slices Sa1–Sa2, time slices 5a–5b) in Libya (Deunff and Massa 1975); and the Ashgillian (Katian stage slices Ka1–Ka4, time slices VIa–VIc) in Portugal (Elaouad-Debbaj 1978), Québec, Canada (Jacobson and Achab 1985), Morocco (Elaouad-Debbaj 1988), north-eastern Libya (Hill and Molyneux 1988), south-eastern Turkey (Stemans et al. 1996; Paris et al. 2007), Missouri, USA (Wicander et al. 1999), and Oklahoma, USA (Playford and Wicander 2006). It also appears in the late Ashgillian (Hirnantian stage slices Hi1–Hi2, time slice VII) in southern Norway (Smelror et al.

1997), southern Tunisia (Vecoli et al. 2009), southern Estonia (Delabroye, Vecoli, et al. 2011), Québec, Canada (Delabroye, Munnecke, et al. 2011), south-western Libya (Abuhmida 2013), and Iran (Ghavidel-Syooki 2000, 2001, 2003, 2006, 2008, 2016, 2017a, 2017b, 2017c). In Iran, it has been recorded in the Hirnantian stage slices Hi1–Hi2 (time slice VII) in the Zagros Mountains (Ghavidel-Syooki et al. 2011b), the Katian stage slices Ka1–Ka4 (time slices VIa–VIc) in the Robat-e Gharabil area, Alborz Mountains (Ghavidel-Syooki and Borji 2018), the latest Darriwilian to early Sandbian stage slices Dw3–Sa1 (time slices 4c–5a) in the Gerd-Kuh area, Alborz Mountains (Ghavidel-Syooki and Piri-Kangarshahi 2023), and the Katian stage slices Ka1–Ka4 (time slices VIa–VIc) in the Simeh-Kuh locality, Alborz Mountains (Ghavidel-Syooki and Piri-Kangarshahi 2024). *Polygonium polyacanthum* (Plate 1, figure 11; Plate 3, figures 13–15) is recorded for the first time in the MG-19 to MG-30 interval of the Ghelli Formation, Khoshyeilagh region (Figure 4; Supplementary data, S4). This cosmopolitan taxon spans the Ordovician Period and has been documented in the Caradocian–Ashgillian (Sandbian–Katian stage slices Sa1–Ka4, time slices 5a–VIc) in Kansas, USA (Wright and Meyers 1981), and the Ashgillian (Katian stage slices Ka1–Ka4, time slices VIa–VIc) in Missouri, USA (Wicander et al. 1999). *Polygonium gracile* (Plate 3, figure 12) occurs in the MG-19 to MG-30 interval of the Ghelli Formation in the Khoshyeilagh region (Figure 4; Supplementary data, S4). This cosmopolitan taxon spans from the Upper Cambrian to the Devonian (Sarjeant and Stancliffe 1994) and has been recorded in the Ashgillian (Katian stage slices Ka1–Ka4, time slices VIa–VIc) on Anticosti Island, Québec, Canada (Jacobson and Achab 1985), and in Missouri, USA (Wicander et al. 1999). *Veryhachium oklahomense* (Plate 6, figure 24) appears throughout the MG-19 to MG-30 interval and persists into the succeeding assemblage biozone in the Ghelli Formation, Khoshyeilagh region (Figure 4; Supplementary data, S4). This cosmopolitan taxon ranges from the Ordovician to the Devonian. Previous records include the Arenig–Ashgillian (Floian–Katian stage slices F1–Ka4, time slices 2a–VIc) in Estonia (Uutela and Tynni 1991), Caradocian (Sandbian stage slices Sa1–Sa2, time slices 5a–5b) in Shropshire, England (Turner 1984), and Gotland, Sweden (Eiserhardt 1992), among others, including various locations in the USA, Libya, and Iran. *Veryhachium trispinosum* (Plate 6, figure 23) appears in the MG-19 to MG-30 interval and continues into the succeeding assemblage biozone of the Ghelli Formation in the study area (Figure 4; Supplementary data, S4). This worldwide taxon ranges from the Ordovician through the Permian (Wicander and Wood 1981). *Villoscapsula setosapellucula* (Plate 1, figure 19) appears throughout the MG-19 to MG-30 interval and persists into the succeeding assemblage biozone of the

Plate 3. Figures 1–10. *Multiplicisphaeridium irregulare* Staplin et al. 1965 (sample MG-31; two specimens); Figure 11. *Oppilatala persianense* sp. nov. (sample MG-31; 3 specimens); Figure 12. *Polygonium gracile* Vavrdová 1966 (sample MG-19; 29 specimens); Figures 13–15. *Polygonium polyacanthum* (Eisenack 1963) Sarjeant and Stancliffe 1994 (sample MG-19; two specimens); Figures 16–18. *Stellechinatum helosum* Turner 1984 (sample MG-6; two specimens); Figures 19, 20. *Stellechinatum celestum* (Martin 1969) Turner 1984 (sample MG-6; one specimen); Figures 21–23. *Diexaplophasis denticulata* (Stockmans and Willièrè 1963) Loeblich 1969 (sample MG-61; 3 specimens); Figure 24. *Multiplicisphaeridium bifurcatum* Staplin et al. 1965 (sample MG-31; 10 specimens).



Ghelli Formation in the study area (Figure 4; Supplementary data, S4). Previously recorded regions include the Katian stage slices Ka1–Ka4 (time slices VIa–VI d) in the USA, Algeria, Libya, Canada, Morocco, Jordan, and Iran. As a result, the *Ordoviciidium elegantulum* – *Orthosphaeridium ternatum* assemblage biozone, along with the associated acritarch taxa, suggests that the MG-19 to MG-30 interval of the Ghelli Formation corresponds to the latest Sandbian to earliest Katian stage slice Ka1 (time slice VIa; Videt et al. 2010).

4.2.3. *Baltisphaeridium perclarum*–*Baltisphaeridium oligopsakium* assemblage biozone (time slice VIb)

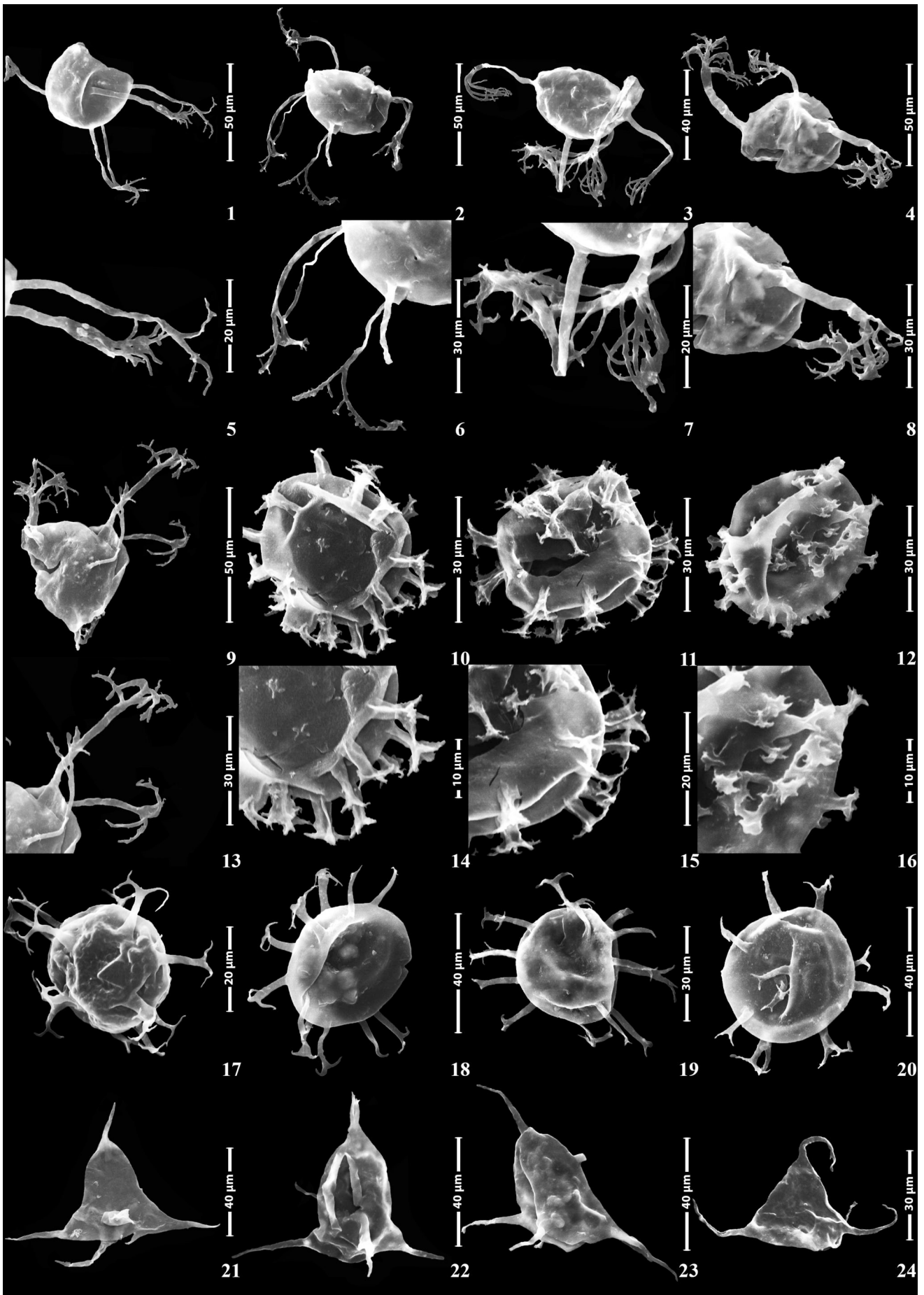
The co-occurrence of *Baltisphaeridium perclarum* and *Baltisphaeridium oligopsakium* Loeblich and Tappan (1978) defines this acritarch assemblage biozone. This biozone succeeds the previous one in the Ghelli Formation at the Khoshyeilagh region, spanning the MG-31 to MG-43 interval over 104 m. *Baltisphaeridium perclarum* (Plate 2, figures 4a, 8a, 22) appears throughout this interval of the study area in the Alborz Mountains, northern Iran (Figure 4; Supplementary data, S4). This microfossil is significant in the Late Ordovician and has been recorded in many regions: the Sandbian stage slices Sa1–Sa2 (time slices 5a–5b) in southern Sweden (Rubinstein and Vajda 2023); the Sandbian–Katian stage slices Sa1–Ka4 (time slices 5a–VI d) in Kansas, USA (Wright and Meyers 1981), Gaspé, Québec, Canada (Martin 1980), north-east Libya (Hill and Molyneux 1988), and Estonia (Uutela and Tynni 1991); the Katian stage slices Ka1–Ka4 (time slices VIa–VI d) in southern Oklahoma, USA (Playford and Wicander 2006); the middle Katian–Hirnantian Ka2–HI2 (time slices VIb–VII) in Oklahoma and Missouri, USA (Wicander et al. 1999); and the Katian stage slices Ka1–Ka4 (time slices VIa–VI d) in Iran (Ghavidel-Syooki 2008, 2016; Ghavidel-Syooki and Piri-Kangarshahi 2021, 2024). *Baltisphaeridium oligopsakium* (Plate 2, figures 12, 16, 24) occurs in the MG-31 to MG-43 interval of the Ghelli Formation in the Khoshyeilagh region within the Alborz Mountains, northern Iran (Figure 4; Supplementary data, S4). Loeblich and Tappan (1978) first documented this species in the Upper Ordovician (Katian) Sylvan Shale of Oklahoma, USA. It has also been recorded in the Arenig–Ashgillian (Floian–Katian stage slices FI1–Ka4, time slices 2a–VI d) in Estonia (Uutela and Tynni 1991); the Richmondian (Katian stage slices Ka1–Ka4, time slices VIa–VI d) of Oklahoma and Missouri, USA (Wicander et al. 1999; Playford and Wicander 2006); and the Katian stage slices Ka1–Ka4 (time slices VIa–VI d) in the Fazel-Abad area, south-eastern Caspian Sea (Ghavidel-Syooki 2017b). This assemblage biozone includes the acritarch taxa *Excultibrachium jahandidehii* sp. nov., *Lohosphaeridium shaveri*, *Lophosphaeridium varum*, *Leiofusa*

litotes, *Multiplicisphaeridium bifurcatum*, *Multiplicisphaeridium irregulare*, *Navifusa ancepsipuncta*, *Oppilatala persianense* sp. nov., and *Peteinosphaeridium accinctulum*.

Excultibrachium jahandidehii sp. nov. (Plate 5, figures 1, 5; 2, 6; 3, 7; 4, 8; 9, 13) and *Oppilatala persianense* sp. nov. (Plate 3, figure 11) appear in the Ghelli Formation in the Khoshyeilagh region for the first time, with detailed descriptions provided in the systematic section. *Leiofusa litotes* (Plate 4, figures 22–24) appears in the MG-31 to MG-43 interval and extends into the next assemblage biozone of the Ghelli Formation in the Khoshyeilagh region (Figure 4; Supplementary data, S4). Loeblich and Tappan (1978) described this taxon in the Katian stage slices Ka1–Ka4 (time slices VIa–VI d) from the Sylvan Shale in Indiana, Ohio, Kentucky, and Oklahoma, USA. It has also been recorded in the Katian stage slices Ka1–Ka3 (time slices VIa–VI c) of the Quwarah Member, Qasim Formation, Arabian Peninsula (Le Hérisse et al. 2015); the Katian stage slices Ka1–Ka4 (time slices VIa–VI d) of the Seyahou Formation, Zagros Mountains (Ghavidel-Syooki 2021); and the Ghelli Formation (Ghavidel-Syooki and Piri-Kangarshahi 2021, 2024). *Lohosphaeridium shaveri* (Plate 1, figure 8) and *Lophosphaeridium varum* (Plate 4, figures 9, 10) occur in the MG-31 to MG-43 interval of the Ghelli Formation in the Khoshyeilagh region (Figure 4; Supplementary data, S4). Loeblich and Tappan (1978) documented *Lohosphaeridium shaveri* in the late Sandbian stage slice Sa2 (time slice 5b) of the Scales Shale, Maquoketa Group, USA. Wicander et al. (1999) described *Lophosphaeridium varum* in the Ashgillian (Katian stage slices Ka1–Ka4, time slices VIa–VI d) of the Maquoketa Shales, north-eastern Missouri, USA. Their presence in the MG-31 to MG-43 interval confirms the Upper Ordovician age.

Multiplicisphaeridium bifurcatum (Plate 3, figure 24) appears in the MG-31 to MG-43 interval of the Ghelli Formation in the Khoshyeilagh region (Figure 4; Supplementary data, S4). This species has been recorded in the Sandbian–Katian stage slices Sa1–Ka4 (time slices 5b–VI d) of Kansas, USA (Wright and Meyers 1981); Gaspé, Quebec, Canada (Martin 1980); the Czech Republic (Vavrdová 1988); and the Moscow Basin, Russia (Umnova 1975). It also occurs in the Ashgillian (Katian–Hirnantian stage slices Ka1–HI2, time slices VIa–VII) of Iran (Ghavidel-Syooki et al. 2011a). *Multiplicisphaeridium irregulare* (Plate 3, figures 1–10) appears in the MG-31 to MG-43 interval of the Ghelli Formation in the study area (Figure 4; Supplementary data, S4). This taxon has been recorded in the lower Floian stage slice FI1 (time slice 2a) of South China (Li 1987; Brocke et al. 2000; Tongiorgi et al. 2003); the Middle Ordovician (Darriwilian stage slice Dw3, time slice 4c) of South China (Brocke et al. 2000) and the Hanadir Member, Qasim Formation, Arabian

Plate 4. Figures 1–6. *Acanthodiacrodiium crassus* (Loeblich and Tappan 1978) comb. nov. Vecoli 1999 (sample MG-6; one specimen); Figures 7, 8. *Cornuferifusa persianense* sp. nov. (sample MG-75; two specimens); Figures 9, 10. *Lophosphaeridium varum* Wicander et al. 1999 (sample MG-31; five specimens); Figures 11, 12. *Speculaforma delicata* Miller et al. 2017 (sample MG-75; five specimens); Figures 13, 14. *Navifusa ancepsipuncta* Loeblich 1970 ex Eisenack et al. 1979 (sample MG-31; one specimen); Figures 15–19. *Dactylofusa platynetrella* (Loeblich and Tappan 1978) Fensome et al. 1990 (sample MG-44; five specimens); Figure 20. *Dactylofusa striata* (Staplin et al. 1965) Fensome et al. 1990 (sample MG-44; one specimen); Figure 21. *Moyeria cabottii* (Cramer 1971) Miller and Eames 1982 (sample MG-61; two specimens); Figures 22–24. *Leiofusa litotes* Loeblich and Tappan 1978 (sample MG-31; 10 specimens).



Peninsula (Le Hérisse et al. 2007); the Sandbian–Katian stage slices Sa1–Ka4 (time slices 5b–Vld) of the Iranian Platform (Ghavidel-Syooki 2008, 2016, 2017a, 2021; Ghavidel-Syooki and Piri-Kangarshahi 2021, 2023, 2024), Kansas, USA (Wright and Meyers 1981), and Gaspé, Québec, Canada (Martin 1980; Achab 1986); the Caradocian (Sandbian stage slices Sa1–Sa2, time slices 5a–5b) of Shropshire, England (Turner 1984); and the Ashgillian (Katian stage slices Ka1–Ka4, time slices VIa–Vld) of Anticosti Island, Québec, Canada (Staplin et al. 1965; Jacobson and Achab 1985) and north-east Libya (Hill and Molyneux 1988). *Navifusa ancepsipuncta* (Plate 4, figures 13, 14) occurs in the MG-31 to MG-43 interval of the Ghelli Formation (Figure 4; Supplementary data, S4). This species has been recorded in the Sandbian stage slices Sa1–Sa2 (time slices 5a–5b) of Shropshire, England (Turner 1984); the Ashgillian (Katian stage slices Ka1–Ka4, time slices VIa–Vld) of Anticosti Island, Québec, Canada (Jacobson and Achab 1985); and the Katian stage slices Ka1–Ka4 (time slices VIa–Vld) in the Sylvan Shale of Indiana, Ohio, Kentucky, and Oklahoma (Loeblich 1970; Loeblich and Tappan 1978), the Arbuckle Mountains, Southern Oklahoma (Playford and Wicander 2006), and Upper Ordovician sediments in Iran (Ghavidel-Syooki 2008, 2016, 2017a, 2017b; Ghavidel-Syooki and Piri-Kangarshahi 2021, 2024). *Peteinosphaeridium accinctulum* (Plate 5, figures 10, 14; 11, 15) is first recorded in the MG-31 to MG-43 interval of the Ghelli Formation in the Khoshyeilagh region (Figure 4; Supplementary data, S4). This taxon has been documented in the Ashgillian (Katian stage slices Ka1–Ka4, time slices VIa–Vld) of the Maquoketa Shale, north-eastern Missouri, USA (Wicander et al. 1999), and the Sylvan Shale, Arbuckle Mountains, Southern Oklahoma (Playford and Wicander 2006). The *Baltisphaeridium perclarum*–*Baltisphaeridium oligopsakium* assemblage biozone, along with associated acritarch taxa, indicates that the MG-31 to MG-43 interval of the Ghelli Formation in the Khoshyeilagh region, northern Iran, corresponds to the Katian stage slices Ka2–Ka3 (time slice VIb).

4.2.4. *Inflatarium trilobatum*–*Dactylofusa platynetrella* assemblage biozone (time slice VIc)

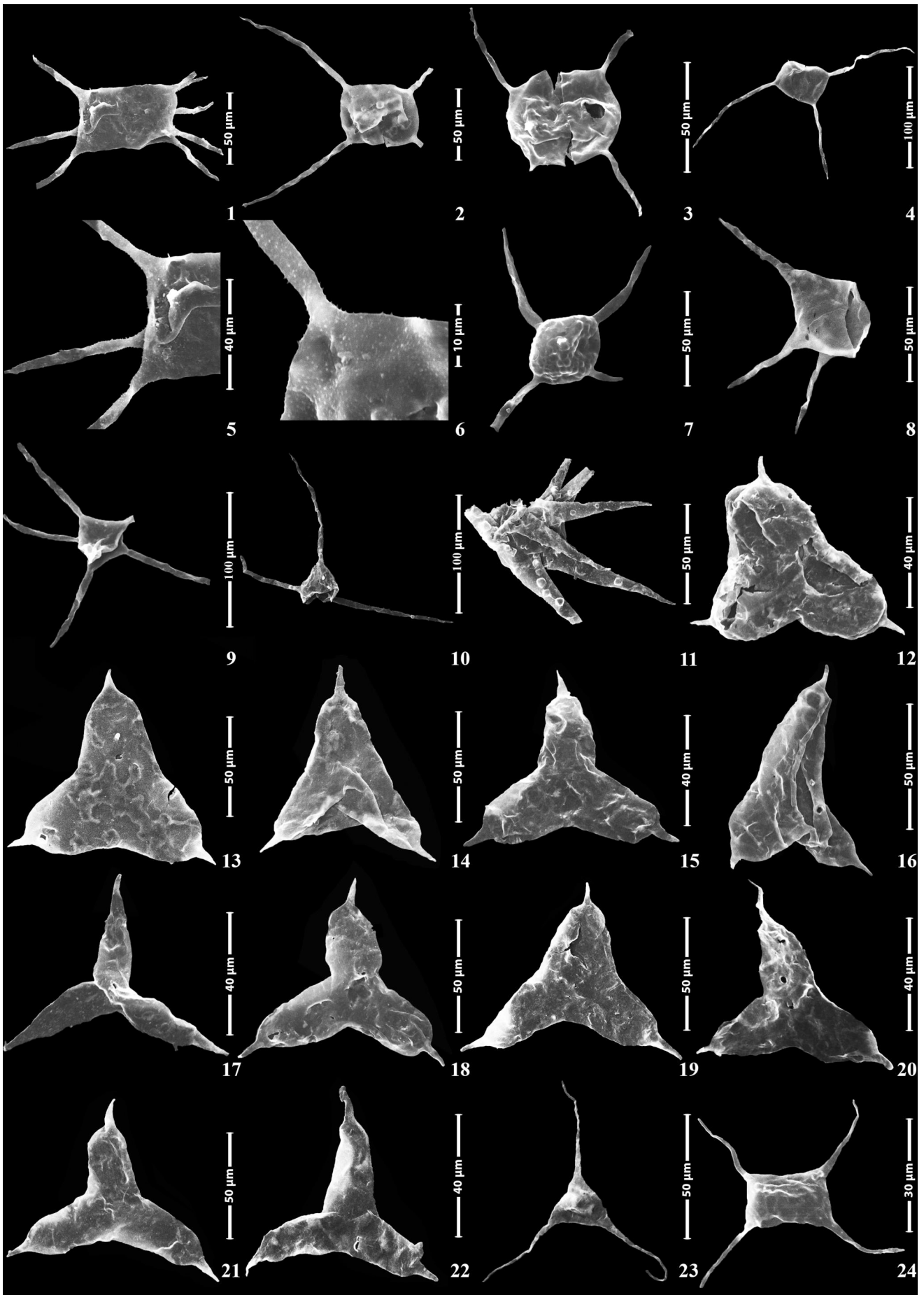
The co-occurrence of *Inflatarium trilobatum* Le Hérisse et al. (2015) and *Dactylofusa platynetrella* (Loeblich and Tappan 1978) Fensome et al. (1990) defines this acritarch assemblage biozone, which directly follows the previous biozone in the Ghelli Formation of the Khoshyeilagh region. This biozone spans the MG-44 to MG-60 interval, covering 136 m in the current study section (Figure 4). *Inflatarium trilobatum* (Plate 6, figures 12, 16, 19) occurs throughout this interval in the Khoshyeilagh area of the Alborz Mountains (Figure 4; Supplementary data, S4).

Previously, researchers documented this taxon in the late Katian–early Hirnantian stage slices Ka4–Hi1 (time slices Vld–lower VII of Videt et al. 2010) within the Quwarah Member of the Qasim Formation, Arabian Peninsula (Le Hérisse et al. 2015), and in the late Katian–Hirnantian stage slices Ka1–Hi2 (time slices VIa–VII) of the Ghelli Formation, Iran (Ghavidel-Syooki et al. 2011a; as *Veryhachium* sp. cf. *V. triangulatum*; Ghavidel-Syooki and Borji 2018; Ghavidel-Syooki and Piri-Kangarshahi 2021, 2024).

Inflatarium trilobatum (Plate 6, figures 12, 16, 19) occurs throughout this interval in the Khoshyeilagh area of the Alborz Mountains (Figure 4; Supplementary data, S4). Previously, researchers documented this taxon in the late Katian–early Hirnantian stage slices Ka4–Hi1 (time slices Vld–lower VII of Videt et al. 2010) within the Quwarah Member of the Qasim Formation, Arabian Peninsula (Le Hérisse et al. 2015), and in the late Katian–Hirnantian stage slices Ka1–Hi2 (time slices VIa–VII) of the Ghelli Formation, Iran (Ghavidel-Syooki et al. 2011a; as *Veryhachium* sp. cf. *V. triangulatum*; Ghavidel-Syooki and Borji 2018; Ghavidel-Syooki and Piri-Kangarshahi 2021, 2024).

Dactylofusa platynetrella (Plate 4, figures 15–19) also appears in the MG-44 to MG-60 interval (Figure 4; Supplementary data, S4). As an index microfossil for the Late Ordovician (Ashgillian), it has been recorded in several regions, including the Katian stage slices Ka1–Ka4 (time slices VIa–Vld) in the Sylvan Shale, Oklahoma, USA (Loeblich and Tappan 1978 as *Eupoikilofusa platynetrella*): the Ashgillian (Katian stage slices Ka1–Ka4, time slices VIa–Vld) in the Hassi-R' Mel area and northern Rhadames Basins, North Africa (Vecoli 1999); the Ashgillian (Katian–Hirnantian stage slices Ka1–Hi2, time slices VIa–VII) in the Quwarah Member, Qasim Formation, Arabian Peninsula (Le Hérisse et al. 2015); the Ashgillian (Katian–Hirnantian stage slices Ka1–Hi2, time slices VIa–VII) at Kuh-Boghrou, Central Iran (Ghavidel-Syooki and Piri-Kangarshahi 2021); the Ashgillian (late Katian–Hirnantian stage slices Ka4–Hi2, time slices Vld–VII) in the Khoshyeilagh area (Ghavidel-Syooki et al. 2011a); the Ashgillian (Katian stage slices Ka1–Ka3, time slices VIa–VIc) at Simeh-Kuh in the Alborz Mountains, northern Iran (Ghavidel-Syooki and Piri-Kangarshahi 2024).

Associated acritarch taxa include *Dactylofusa striata*, *Veryhachium elongatum*, *Inflatarium alborzensis* sp. nov., *Navifusa caspiensis* sp. nov., and *Pirea shahroudensis* sp. nov., each described below. This study records *Inflatarium alborzensis* sp. nov. (Plate 1, figures 4, 5; Plate 6, figures 13–15; 17, 18; 20–22), *Navifusa caspiensis* sp. nov. (Plate 1, figures 6, 7), and *Pirea shahroudensis* sp. nov. (Plate 1, figures 1, 2) from the Ghelli Formation in the Khoshyeilagh region for the first time, with detailed descriptions in the systematic section.



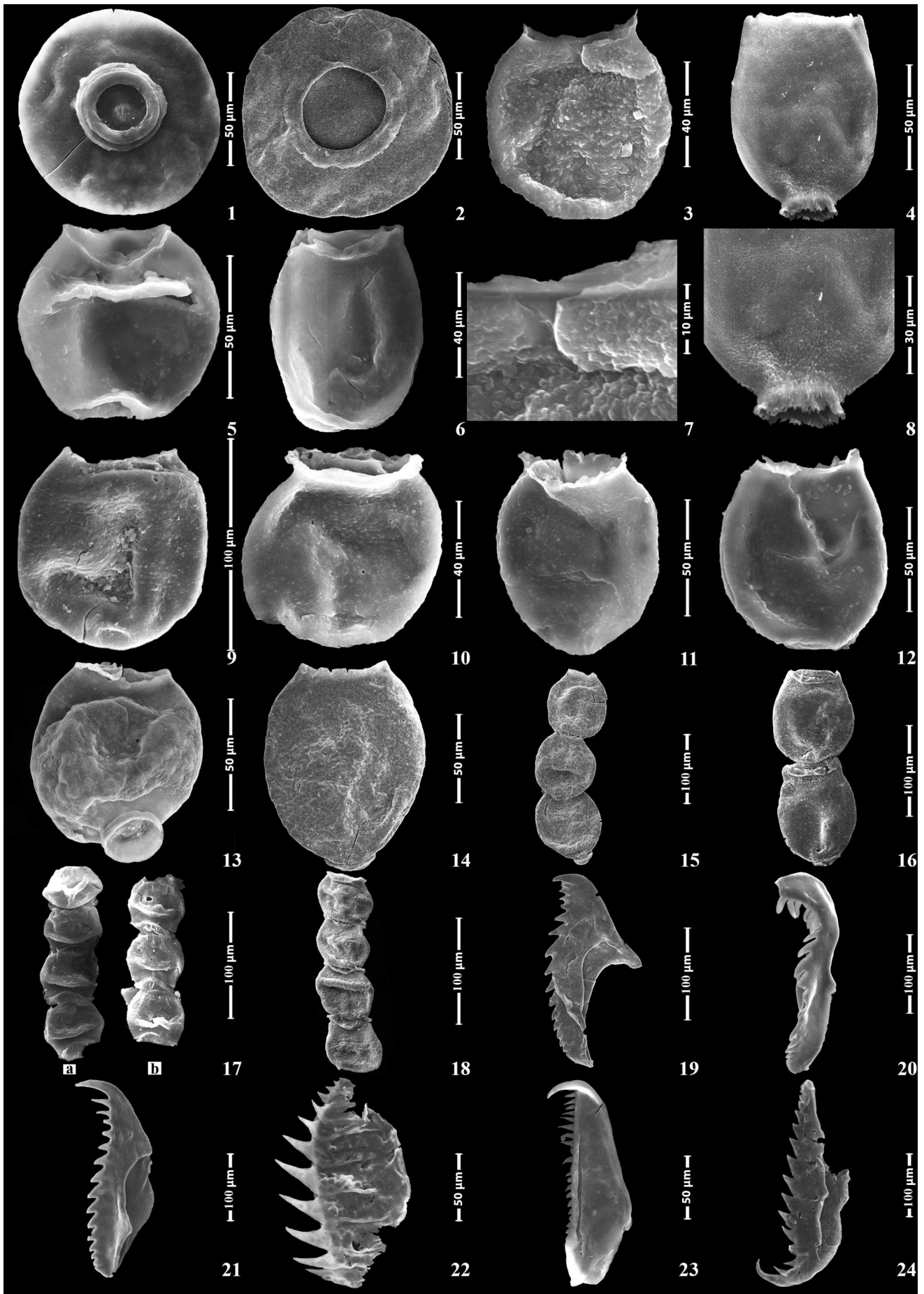
Dactylofusa striata (Plate 1, figures 22, 23; Plate 4, figure 20) appears in the MG-44 to MG-60 interval (Figure 4; Supplementary data, S4) and is an important Upper Ordovician (Ashgillian) microfossil. Previous records include the Upper Ordovician Prague Basins, Czech Republic (Vavrdová 1966); the Late Ordovician (Katian stage slices Ka1–Ka4, time slices VIa–VIId) in *Decellograptus complanatus* of the Vaureal Formation, Anticosti Island, Québec, Canada (Jacobson and Achab 1985, as *Eupoikilofusa striata*); the Ashgillian (Katian stage slices Ka1–Ka4, time slices VIa–VIId) in North Africa (Vecoli 1999, borehole NI2, samples 2813.1–2775.1); the Ashgillian (Katian stage slices Ka1–Ka4, time slices VIa–VIId) in the Gorgan Schists, southern Caspian Sea, northern Iran (Ghavidel-Syooki 2008); the Ashgillian (late Katian–Hirnantian stage slices Ka4–Hi2, time slices VIId–VII) in the Ghelli Formation, Khoshyeilagh area (Ghavidel-Syooki et al. 2011a); the Ashgillian (Katian stage slices Ka1–Ka4, time slices VIa–VIId) in the Ghelli Formation type section (Ghavidel-Syooki 2016); the Ashgillian (Katian stage slices Ka1–Ka4, time slices VIa–VIId) in Fazel-Abad, south-eastern Caspian Sea, northern Iran (Ghavidel-Syooki 2017b) and the Ashgillian (Katian Ka1–Ka4, time slices VIa–VIId) in the Ghelli Formation, Kuh-e Boghou, Central Iran (Ghavidel-Syooki and Piri-Kangarshahi 2021). *Veryhachium elongatum* (Plate 1, figure 20; Plate 6, figure 23) appears in the MG-44 to MG-60 interval (Figure 4; Supplementary data, S4). Previous records include the lower Wenlock Series (Silurian) of the Welsh Borderland, England (Downie 1963), and the latest Caradocian–Ashgillian (latest Sandbian–Katian Sa2–Ka4, time slices 5b–VIId) in the Quwarah Member, Qasim Formation, Arabian Peninsula (Le Hérisse et al. 2015). The *Inflatarium trilobatum*–*Dactylofusa platynetrella* assemblage biozone, along with associated acritarch taxa, confirms that the MG-44 to MG-60 interval of the Ghelli Formation in the Khoshyeilagh region corresponds to the early Ka4 (time slice VIc).

4.2.5. *Poikilofusa spinata*–*Dorsennidium hamii* assemblage biozone (time slice VIId)

The co-occurrence of *Poikilofusa spinata* (Staplin et al. 1965) Loeblich and Tappan (1978) and *Dorsennidium hamii* (Loeblich 1970) Sarjeant and Stancliffe (1994) defines this assemblage biozone, which follows the previous biozone and spans the MG-61 to MG-74 interval of the Ghelli Formation in the Khoshyeilagh region, covering 112 m (Figure 4). *Poikilofusa spinata* (Plate 1, figure 24) occurs in this interval of the Ghelli Formation, northern Iran (Figure 4; Supplementary data, S4). Researchers have recorded it in various regions: the late Middle Ordovician (Darriwilian, Trenton Formation, Anticosti Island, Canada) (Staplin et al. 1965), the Ashgillian (Katian, Vaural Formation, Anticosti

Island, Québec, Canada) (Jacobson and Achab 1985), the Middle–Late Ordovician (Darriwilian–Katian, Central North America) (Loeblich and Tappan 1978), and the Ashgillian (Katian–Hirnantian, Abarsaj Formation, south-eastern Caspian Sea) (Ghavidel-Syooki and Hoseinzadeh-Moghadam 2005, as *Dactylofusa spinata*). *Dorsennidium hamii* (Plate 5, figures 21–24) is restricted to the MG-61 to MG-74 interval of the Ghelli Formation (Figure 4; Supplementary data, S4). Records of this species span the Mohawkian (Caradocian) and Edenian (upper Caradocian) of Québec and south-east Ontario (Martin 1980), the Ashgillian (Katian) of Anticosti Island (Jacobson and Achab 1985), and the Caradocian–Ashgillian of the USA (Wright and Meyers 1981; Wicander et al. 1999), Sweden (Eiserhardt 1992), the Czech Republic (Vavrdová 1988), Morocco (Elaouad-Debbaj 1988), and Iran (Ghavidel-Syooki et al. 2011a; Ghavidel-Syooki 2021; Ghavidel-Syooki and Piri-Kangarshahi 2021). The associated acritarchs in this biozone include *Dorsennidium iranense* sp. nov., *Tunisphaeridium bicaudatum*, *Neoverhachium carminae*, *Diexapallophosis denticulata*, and *Moyeria cabottii*. In this study, *Dorsennidium iranense* sp. nov. (Plate 1, figure 16) is documented for the first time in the MG-61 to MG-74 interval (Figure 4; Supplementary data, S4). *Tunisphaeridium bicaudatum* (Plate 1, figure 12) appears in MG-61 and persists into the succeeding biozone. Previous records place it in the late Katian–early Hirnantian (Quwarah Member, Qasim Formation, Arabian Peninsula) (Le Hérisse et al. 2015). *Neoverhachium carminae* (Plate 1, figures 14, 15) spans MG-61 to MG-88 of the Ghelli Formation and has been recorded in the Middle Silurian of North America (Cramer 1971), the Late Ordovician (Katian–Hirnantian) of the Arabian Peninsula (Le Hérisse et al. 2015), North China (Li et al. 2006), and Iran (Ghelli Formation, Gorgan Schists, and Central Iran) (Ghavidel-Syooki 2008; Ghavidel-Syooki et al. 2011b; Ghavidel-Syooki 2016, 2017a, 2017b; Ghavidel-Syooki and Piri-Kangarshahi 2021). *Diexapallophosis denticulata* (Plate 3, figures 21–23) first appears in MG-61 and persists through MG-88. This long-ranging microfossil has been documented across Sweden (Kjellström 1971; Górká 1987), the UK (Turner 1985), the USA (Loeblich and Tappan 1978; Wicander et al. 1999; Playford and Wicander 2006), the Czech Republic (Vavrdová 1988), the Arabian Peninsula (Jachowicz 1995; Le Hérisse et al. 2015; 2017), and Iran (Ghavidel-Syooki 2008, 2016, 2017a; Ghavidel-Syooki and Piri-Kangarshahi 2021). *Moyeria cabottii* (Plate 1, figures 9, 10; Plate 4, figure 21) occurs from MG-61 to MG-88 in the Ghelli Formation. Previous records span the Middle–Upper Ordovician strata in Sweden (Kjellström 1971; Górká 1987), England (Turner 1985), the USA (Loeblich and Tappan 1978; Colbath 1979), the Czech Republic (Vavrdová 1988), China (Li et al. 2006), and Iran (Ghavidel-Syooki 2017a, 2017b). As a common palynomorph in Ordovician–Silurian

Plate 6. Figures 1, 5. *Orthosphaeridium octospinosum* var. *insculptum* (Loeblich 1970) Navidi-Izad et al. 2020 (sample MG-19; one specimen); Figures 2, 6; 3, 4, 7. *Orthosphaeridium rectangulare* var. *quadricornis* Navidi-Izad et al. 2020 (sample MG-20; five specimens); Figures 8, 9. *Orthosphaeridium octospinosum* var. *octospinosum* Navidi-Izad et al. 2020 (sample MG-19; two specimens); Figure 10. *Orthosphaeridium ternatum* (Burmman 1970) Eisenack et al. 1976 (sample MG-19; three specimens); Figure 11. *Stellechinatum khoshyeilaghensis* sp. nov. (sample MG-6; one specimen); Figures 12, 16, 19. *Inflatarium trilobatum* Le Hérisse et al. 2015 (sample MG-44; 10 specimens); Figures 13–15, 17, 18, 20–22. *Inflatarium alborzensis* (Ghavidel-Syooki and Piri-Kangarshahi 2024) comb. nov. (sample MG-44; 10 specimens); Figure 23. *Veryhachium trispinosum* (Eisenack 1963) Stockmans and Williéri 1963 (sample MG-19; 10 specimens); Figure 24. *Veryhachium oklahomense* Loeblich 1970 (sample MG-19; three specimens).



shallow-water environments (Gray and Boucot 1989), it also appears in non-marine deposits. Recent studies transferred *Moyeria* from incertae sedis Acritarcha to Euglenida, classifying it among the oldest freshwater protozoans (Strother et al. 2020). This assemblage biozone and its acritarch taxa confirm that the MG-61 to MG-74 interval of the Ghelli Formation corresponds to the late Katian stage slice Ka4 (time slice VIId).

4.2.6. *Speculaforma delicata*–*Safirotheca safira* assemblage biozone (time slice VII)

The co-occurrence of *Speculaforma delicata* Miller et al. (2017) and *Safirotheca safira* Vavrdová (1989) defines the acritarch assemblage biozone in this study. This biozone spans the MG-75 to MG-88 interval of the Ghelli Formation in the Khoshyeilagh region, covering 355 m (Figure 4; Supplementary data, S4). *Speculaforma delicata* (Plate 4, figures 11, 12) has been documented in the Grimsby Formation (Silurian) of New York and West Virginia, USA (Miller and Eames 1982); the Sarah Formation (Hirnantian) in the Arabian Peninsula (Miller et al. 2017); and the Upper Ordovician Ghelli Formation at Kuh-e Saluk, northern Iran (Ghavidel-Syooki 2000; as lobate coenobium; see Plate 3, figure 5). In this study, it occurs within the *elongata* and *oulebsiri* chitinozoan biozones, spanning the MG-75 to MG-88 interval. *Safirotheca safira* (Plate 1, figure 25) also appears in this interval and serves as a key marker for the Late Ordovician, confined to the Peri-Gondwanan palaeo-province (Jardiné et al. 1974; Vavrdová 1988, 1989; Vecoli 1999; Le Hérisse et al. 2015; Ghavidel-Syooki 2016, 2017a, 2017b; Ghavidel-Syooki and Piri-Kangarshahi 2021). *Cornuferifusa persianense* sp. nov. (Plate 4, figures 7, 8) is also recorded in this interval (Figure 4; Supplementary data, S4), with previous occurrences restricted to the same stratigraphical level (Ghavidel-Syooki et al. 2011a; as *Cornuferifusa* sp.). The *Speculaforma delicata*–*Safirotheca safira* assemblage biozone, along with associated acritarch taxa, suggests that the MG-75 to MG-88 interval of the Ghelli Formation in northern Iran correlates with the Hirnantian stage slices Hi1–Hi2 (time slice VII) and aligns with the *Tanuchitina elongata* and *Spinachitina oulebsiri* chitinozoan biozones.

4.3. Systematics of new chitinozoan species

Most of the chitinozoan taxa discussed here are assigned to established species; hence, their formal systematic treatment is omitted, and comprehensive descriptions are reserved solely for newly identified taxa. Measurements are provided in μm , with values expressed as minimum (mean) and maximum; 'n' represents the number of specimens measured. The following abbreviations are utilised: L = total vesicle length; Lp = chamber length; Dp = maximum chamber diameter; Ln = oral tube length; dcoll = collarete diameter; tcar = width of carina; ls = spine length.

Group **INCERTAE SEDIS CHITINOZOA** Eisenack 1931
Order **OPERCULATIFERA** Eisenack 1931
Family **DESMOCHITINIDAE** Eisenack 1931 emend. Paris 1981
Subfamily **DESMOCHITININAE** Paris 1981

Genus *Desmochitina* Eisenack 1931

Desmochitina sp. nov. A

Plate 7, figures 4, 8

Holotype. Plate 7, figure 4.

Type locality. Khoshyeilagh region, 70 km north of Shahroud city, south of the Caspian Sea within the Alborz Mountains in northern Iran.

Type stratum. The Upper Ordovician (Katian) Ghelli Formation (MG-19 to MG-23 interval).

Dimensions. L = 95 μm ; dcoll = 55 μm ; the open rounded hole at the basal part of the vesicle has a diameter of 25 μm .

Description. *Desmochitina* sp. nov. A occurs in the Upper Ordovician Ghelli Formation (sample MG-53) at the Khoshyeilagh region within the Alborz Mountains, in the north of Iran. It is a small specimen with a simple conical chamber, lacking a neck and flexure, and has straight to slightly convex flanks. An open, rounded hole is present at the basal part of the vesicle. The chamber is perforated and bears a mucron (possibly a peduncle) with a ragged margin.

Remarks. This species is distinct from other species of *Desmochitina*, typically exhibiting granulous ornamentation rather than actual spines on the flanks. The most unusual characteristic of Iranian specimens is perforated mucron (possible peduncle) with a ragged margin.

Order **PROSOMATIFERA** Eisenack 1972

Family **CONOCHITINIDAE** Eisenack 1931, emend. Paris 1981

Subfamily **BELONECHITININAE** Paris 1981

Genus *Belonechitina* Jansonius 1964

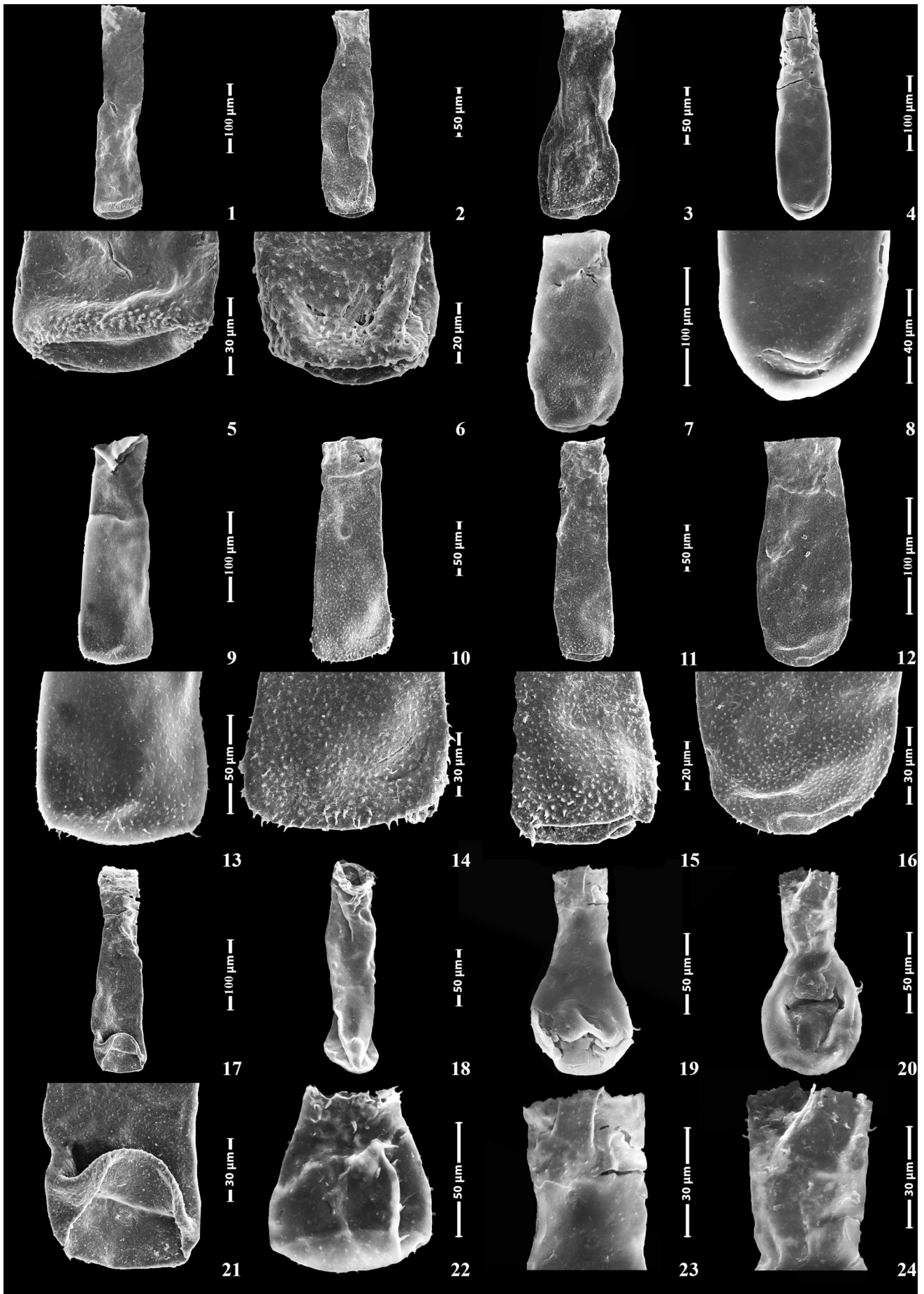
Type species. *Conochitina micracantha* subsp. *robusta* Eisenack 1959

Belonechitina iranense sp. nov.

Plate 8, figures 4, 8

Holotype. Plate 8, figure 4.

← **Plate 7.** Figures 1, 5; 17, 21. *Belonechitina micracantha* (Eisenack 1931) emend. Paris 1981 (sample MG-21; 5 specimens); Figures 2, 6; 3. *Belonechitina robusta* (Eisenack 1959) (sample MG-6; 15 specimens); Figures 4, 8. *Belonechitina iranense* sp. nov. (sample MG-19; 2 specimens); Figures 7, 12, 16. *Belonechitina britannica* Vandenbroucke 2008 (sample MG-8; 7 specimens); Figures 9, 13; 10, 14; 11, 15. *Belonechitina wesenbergensis* (Eisenack 1959) (sample MG-7; 8 specimens); Figure 18. *Pistillachitina iranense* sp. nov. (sample MG-20; 3 specimens); Figures 19, 23; 20, 24. *Angochitina* cf. *communis* Eisenack 1967 (sample MG-23; 6 specimens); Figure 22. *Angochitina communis* Jenkins 1967 (sample MG-20; 3 specimens).



Type locality. Khoshyeilagh region, 70 km north of Shahroud city, south of the Caspian Sea within the Alborz Mountains in northern Iran.

Type stratum. In the Upper Ordovician (Katian) Ghelli Formation, samples of MG-19 to MG-30

Derivation of name. The name refers to Iran, the country where this species was first described.

Dimensions. $L = 270$ (277) $284 \mu\text{m}$; $L_p = 200$ (209) $218 \mu\text{m}$; $L_n = 65$ (67.5) $70 \mu\text{m}$; $d_{\text{coll}} = 32$ (35.5) $39 \mu\text{m}$; $D_p = 69$ (71.5) $74 \mu\text{m}$; $n = 10$

Description. This species is long, slender, and conical, with maximum diameter one-third of the way above the basal margin. The vesicle tapers towards the aperture, and the base varies from flat to invaginated with a rounded basal edge. The vesicle surface is granular, with the granularity decreasing towards the aperture.

Remarks. This species resembles *Conochitina* sp. 2, described by Ghavidel-Syooki and Winchester-Seeto (2002), but it differs in having a granular surface on the vesicle.

Genus *Pistillachitina* Taugourdeau 1966

Pistillachitina iranense sp. nov.

Plate 8, figure 18; Plate 11, figures 1, 5; 2, 6

1995 *Pistillachitina* sp. Al-Hajri, p. 38, pl. III, figs. 2, 3.

2017 *Pistillachitina* sp. Al-Shawareb et al. p. 348, pl. 4, fig. 1.

2023 *Pistillachitina* sp. Ghavidel-Syooki, p. 12, pl. 5, fig. 17.

Holotype. Plate 11, figure 2.

Type locality. Khoshyeilagh region, 70 km north of Shahroud city, south of the Caspian Sea within the Alborz Mountains in northern Iran.

Type stratum. Upper Ordovician (Katian) Ghelli Formation, samples MG-19 to MG-30.

Derivation of name. The name refers to Iran, the country where this species was first described.

Dimensions. $L = 337 \mu\text{m}$; aboral widening = $72 \mu\text{m}$; $d_{\text{coll}} = 49 \mu\text{m}$.

Description. *Pistillachitina iranense* sp. nov. possesses an elongate, slender, cylindrical vesicle with a well-rounded base that terminates aborally. Its basal margin is distinctly

rounded. The cyst's surface is adorned with sparse, simple spines with no observable aperture. While this species bears a resemblance to *Pistillachitina* sp., documented in Ordovician strata of the Arabian Peninsula (Al-Hajri 1995; Al-Shawareb et al. 2017), it can be distinguished from counterparts found in the Lower Ktaoua, Upper Ktaoua, and lower second Bani formations of Morocco (Elaouad-Debbaj 1986) and Iran (Ghavidel-Syooki and Winchester-Seeto 2002).

Remarks. *Pistillachitina iranense* sp. nov. stands apart from other species of *Pistillachitina* due to its distinctive feature of a lengthy, slender, cylindrical vesicle, culminating aborally with a prominent lenticular widening.

Pistillachitina alborzensis sp. nov.

Plate 11, figure 4

Holotype. Plate 11, figure 4.

Type locality. Khoshyeilagh region, 70 km north of Shahroud city, south of the Caspian Sea within the Alborz Mountains in northern Iran.

Type stratum. Upper Ordovician (Katian) Ghelli Formation, samples of MG-19 to MG-30.

Derivation of the name. The name refers to the Alborz Mountains, where this species was first described.

Dimensions. $L = 300$ (332) $364 \mu\text{m}$; $L_p = 49$ (51) $53 \mu\text{m}$; $d_{\text{coll}} = 50$ (57) $64 \mu\text{m}$.

Description. *Pistillachitina alborzensis* sp. nov. features an elongate, slender, cylindrical vesicle that bifurcates approximately two-thirds along its length. The cyst exhibits variable diameter, with its widest point typically near the basal region of the vesicle. The cylindrical branch measures $20 \mu\text{m}$ in length and $37 \mu\text{m}$ in width. The vesicle has a distinctly rounded basal margin. The surface of the vesicle is smooth, showcasing a noticeable flaring aperture.

Remarks. *Pistillachitina alborzensis* sp. nov. can be distinguished from other species of *Pistillachitina* by exhibiting variable thickness along the cyst and the dichotomous branch.

Order **PROSOMATIFERA** Eisenack 1972

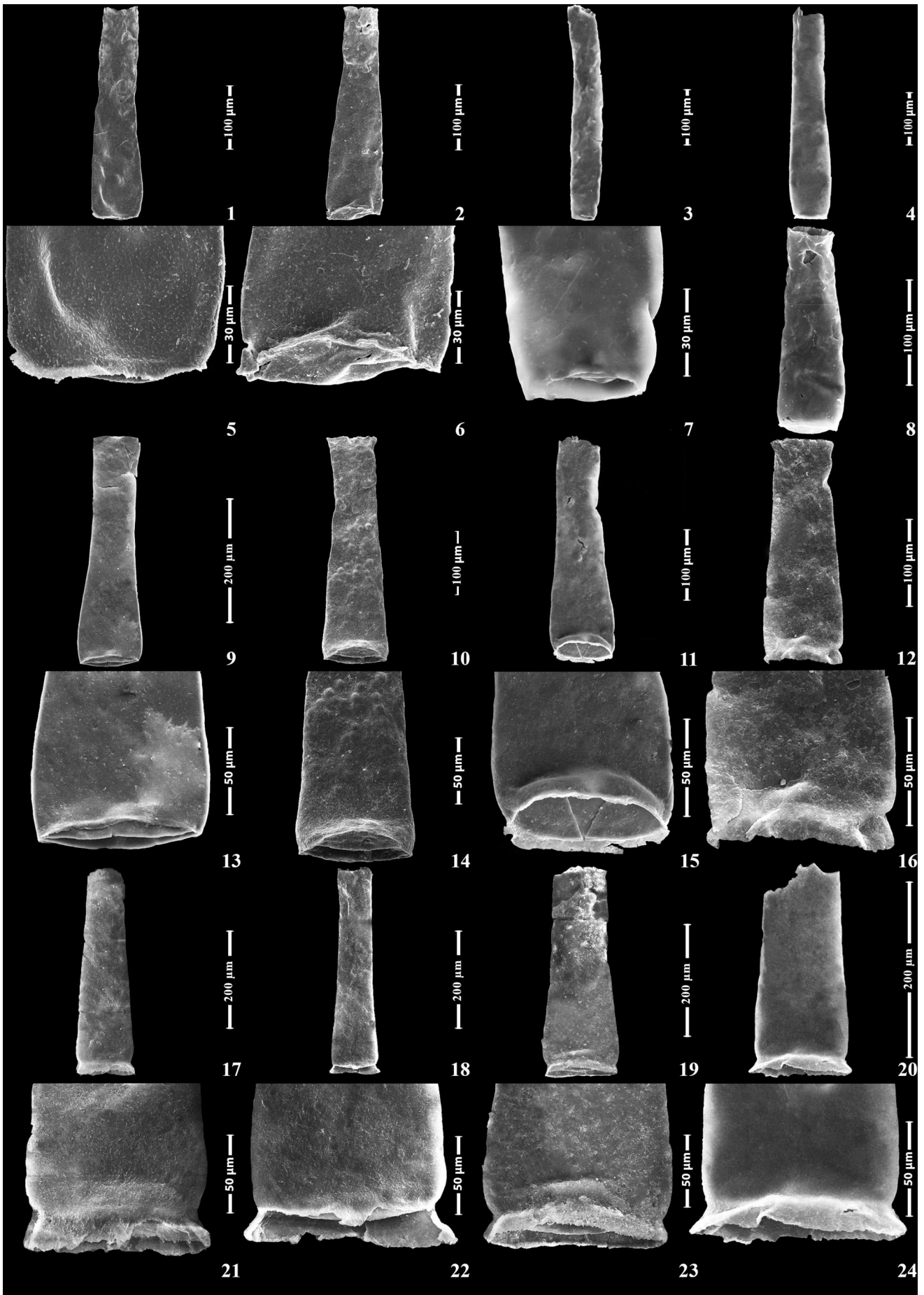
Family **Conochitinidae** Eisenack 1931 emend. Paris 1981

Subfamily **Belonechitininae** Paris 1981

Genus **Acanthochitina** Eisenack 1931 emend. Jenkins 1967

Type species. *Acanthochitina barbata* Eisenack 1931.

← **Plate 8.** Figures 1, 5; 17, 21. *Belonechitina micracantha* (Eisenack 1931) emend. Paris 1981 (sample MG-21; five specimens); Figures 2, 6; 3. *Belonechitina robusta* (Eisenack 1959) (sample MG-6; 15 specimens); Figures 4, 8. *Belonechitina iranense* sp. nov. (sample MG-19; two specimens); Figures 7, 12, 16. *Belonechitina brittanica* Vandenbroucke 2007 (sample MG-8; seven specimens); Figures 9, 13, 10, 14, 11, 15. *Belonechitina wesenbergensis* (Eisenack 1959) (sample MG-7; eight specimens); Figure 18. *Pistillachitina iranense* sp. nov. (sample MG-20; three specimens); Figures 19, 23, 20, 24. *Angochitina* cf. *communis* Eisenack 1967 (sample MG-23; six specimens); Figure 22. *Angochitina communis* Jenkins 1967 (sample MG-20; three specimens).



***Acanthochitina?* sp. nov. A.**

Plate 13, figure 20

Dimensions. $L = 225 \mu\text{m}$; $D_p = 113 \mu\text{m}$; $D_c = 80 \mu\text{m}$; $l_s = 16\text{--}18 \mu\text{m}$.

Type locality. Khoshyeilagh region, 70 km north of Shahrud city, south of the Caspian Sea within the Alborz Mountains in northern Iran.

Type stratum. The middle part of the lower member of the Ghelli Formation (samples of MG-31 to MG-40).

Description. The specimens of this species possess cylindrical vesicles with fragile necks that are easily broken. The flexure is not developed. The flanks are slightly convex, and the maximum width is at the margin. The margin is rounded and carries a reticulated network. *Acanthochitina?* sp. nov. A differs from *Clathrochitina* because its basal margin supports a reticulated network rather than a relatively small number of distinct processes that coalesce distally. The species is kept in open nomenclature due to poor preservation and few available specimens.

Remarks. *Acanthochitina?* sp. A. is characterised by a cylindrical chamber, a reticulated network at the basal margin, and broken processes in the chamber.

4.4. Chitinozoan biostratigraphy

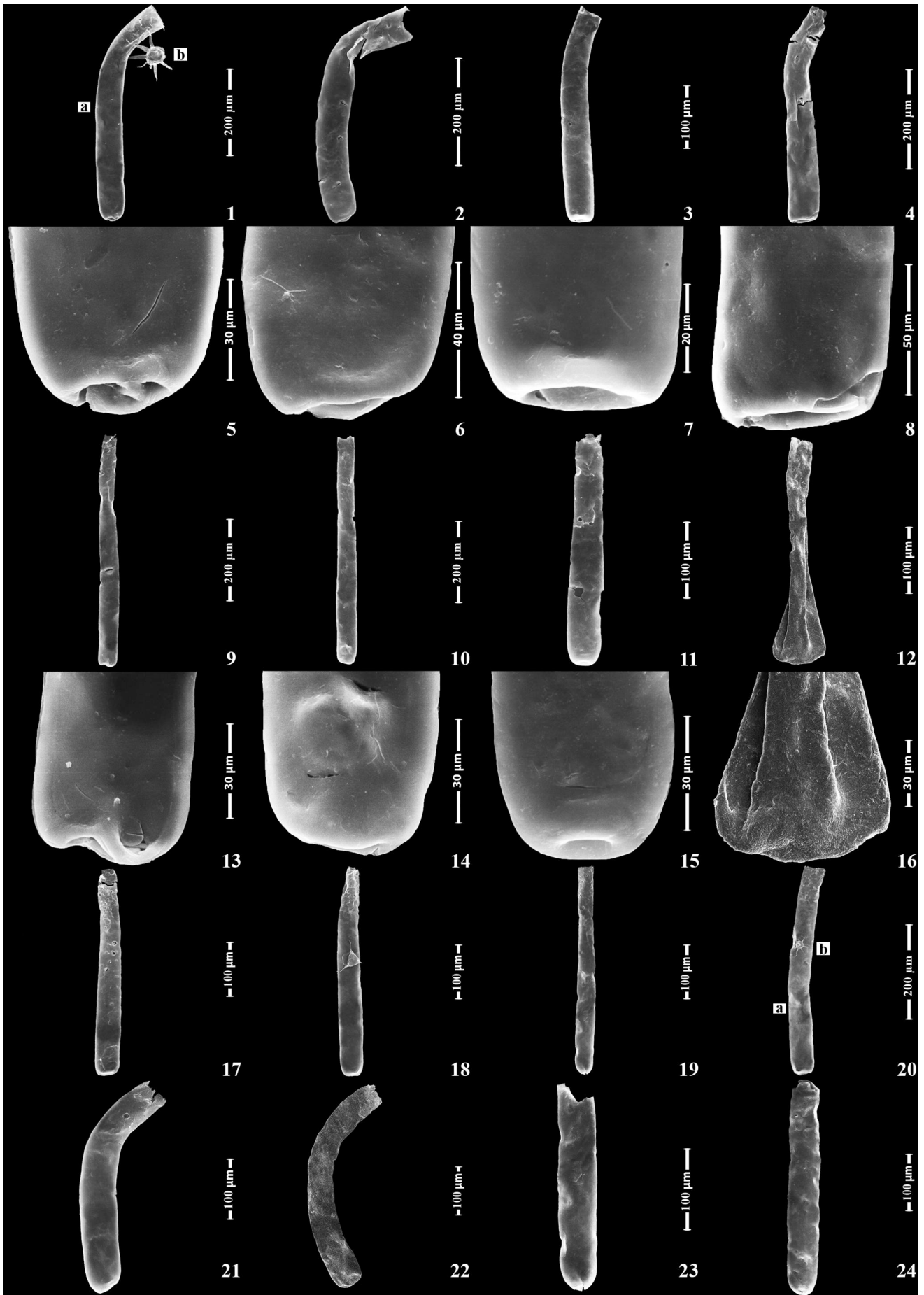
The chitinozoan microfauna represents a group of extinct and enigmatic organic-walled microfossils exclusively of marine origin (Paris 1981; Sutherland 1994). Spanning the Ordovician to the Late Devonian (~488–359 Ma), they have proven instrumental in determining the palaeogeographical affinities of various terranes across continents (Cocks and Verniers 1998). Additionally, they play a significant role in high-resolution biostratigraphy, given their short-ranging nature, facilitating the establishment of biozonations (Paris 1990, 1996). These biozonations, anchored by index species with limited temporal ranges, are observed in sedimentary sections devoid of significant breaks in the deposition. In this investigation, the analysis of the chitinozoan microfauna within the Ghelli Formation from the Khoshyeilagh area revealed the presence of seven chitinozoan biozones in the Upper Ordovician marine siliciclastic succession. This analysis verified the FAD and LAD of several well-known chitinozoan taxa within the Peri-Gondwana palaeo-province. A detailed discussion of these chitinozoan biozones and their corresponding biostratigraphical ages is presented below in ascending stratigraphical order (refer to Figure 5).

4.4.1. *Belonechitina robusta* biozone

The biozone begins with the FAD of *Belonechitina robusta* Eisenack (1959) in the lowermost samples of the lower Ghelli Formation. *Belonechitina robusta* (Plate 8, figures 2, 6; 3) occurs throughout the MG-6 to MG-18 interval, spanning 105 m of micaceous olive-grey shale in the Khoshyeilagh region (Figure 5; Supplementary data, S5). This taxon has been recorded in the Upper Ordovician, including the Sandbian stage slices Sa1–Sa2 of Europe (Portugal, France, Spain, and Bohemia; Paris 1990), from the Balclatchie Group of Scotland in Sandbian stage slice Sa1 (Jansonius 1964), and in England and Baltoscandinavia in the early Katian stage slice Ka1 (Grahn 1981, 1982; Nölvak and Grahn 1993). It also appears in the Viola Springs Formation, Oklahoma (Ross 1982), and the Trenton Group, Canada (Barnes et al. 1981), in the Sandbian Stage. On the Iranian platform, *B. robusta* has been documented in the Sandbian–early Katian of the Ghelli Formation, Gorgan Schists, and Seyahou Formation (Ghavidel-Syooki 2008, 2016, 2017b, 2023; Ghavidel-Syooki and Piri-Kangarshahi 2021, 2024). These occurrences confirm its widespread distribution from the early Sandbian to early Katian across North America, Europe, and Iran. Its distinct morphology and broad geographical range establish *B. robusta* as a key biostratigraphical marker for the Sandbian–early Katian stage slices Sa1–Ka1 (5a1–Vla). The associated chitinozoan taxa in this biozone include *Belonechitina brittanica* Vandenbroucke 2007, *Belonechitina capitata* (Eisenack 1962), *Belonechitina wesenbergensis* (Eisenack 1959), *Calpichitina lenticularis* (Bouché 1965), *Cyathochitina campanulaeformis* (Eisenack 1931) Eisenack 1962, *Cyathochitina kuckersiana* (Eisenack 1934), *Desmochitina minor* Eisenack 1931, *Desmochitina juglandiformis* Laufeld 1967, *Desmochitina erinacea* Eisenack 1931, *Eisenackitina rhenana* (Eisenack 1939), *Pistillachitina pistillifrons* (Eisenack 1939), *Rhabdochitina magna* Eisenack 1931 and *Rhabdochitina usitata* Jenkins 1967; each species is described in detail below.

Belonechitina brittanica (Plate 8, figures 7, 12, 16) occurs in the MG-6 to MG-18 interval of the Ghelli Formation in the Khoshyeilagh region and extends into the basal part of the succeeding biozone (Figure 5; Supplementary data, S5). This marks its first record in the Upper Ordovician strata of the Alborz Mountains, northern Iran. Previously, researchers documented *B. brittanica* in the Upper Ordovician (Sandbian stage slices Sa1–Sa2, time slices 5a–5b; Webby et al. 2004) from the Torrington Shale Formation, UK (Vandenbroucke 2007) and the Seyahou Formation, Zagros Mountains, southern Iran (Ghavidel-Syooki 2023).

Belonechitina capitata (Plate 14, figures 17, 21) first appears at the base of the *B. robusta* biozone and persists through the MG-6 to MG-18 interval of the Ghelli Formation in the Khoshyeilagh area, extending into the basal part of the succeeding biozone (Figure 5; Supplementary data, S5). Researchers have documented this taxon in the Darriwilian



stage slices Dw1–Dw3 (time slices 4a–4c; Webby et al. 2004) in Estonia (Tammekänd et al. 2010); the Darriwilian–late Sandbian (Dw1–Sa2; time slices 4a–5b) in the Baltic (Eisenack 1962, 1968b); and the Darriwilian–early Sandbian (Dw1–Sa1; time slices 4a–5a) in the Arabian Peninsula (Al-Hajri 1995) and Canada (Achab and Asselin 1995). Further records include the early Sandbian–early Katian (Sa1–Ka1; time slices 5a–Vlb) in Sweden (Laufeld 1967; Grahn 1981, 1982); the Sandbian–early Katian (Sa1–Ka1; time slices 5a–Vla) in Scandinavia (Grahn and Nölvak 2007); the Katian (Ka1–Ka3; time slices Vla–Vlb) in England (Vandenbroucke et al. 2008); the middle Katian (Ka2–Ka3; time slices Vlb–Vld) in Libya (Molyneux and Paris 1985; Abuhmida 2013); and the early Katian (Ka1; time slice Vla) in the Simeh-Kuh locality within the Alborz Mountains, northern Iran (Ghavidel-Syooki and Piri-Kangarshahi 2024).

Belonechitina wesenbergensis (Plate 8, figures 9, 13; Plate 10, figures 14, 15) first appears in the MG-6 to MG-18 interval of the Ghelli Formation and extends into the basal part of the succeeding biozone in the Khoshyeilagh area (Figure 5; Supplementary data, S5). It has been documented in the Darriwilian–Hirnantian (Dw1–Hi2; time slices 4a–VII) of Sweden, Finland, Estonia (Grahn 1981, 1982; Nölvak et al. 1995), and the UK (Vandenbroucke 2007). Jenkins (1969) recorded it in the Sandbian (Sa1–Sa2; time slices 5a–5b) of the Viola Limestone, USA. Ghavidel-Syooki and Winchester-Seeto (2002) and Ghavidel-Syooki (2017a) reported it in the Sandbian–early Katian (Sa1–Ka1; time slices 5a–Vla) of the Ghelli Formation at Kuh-e Saluk, Alborz Mountains, northern Iran.

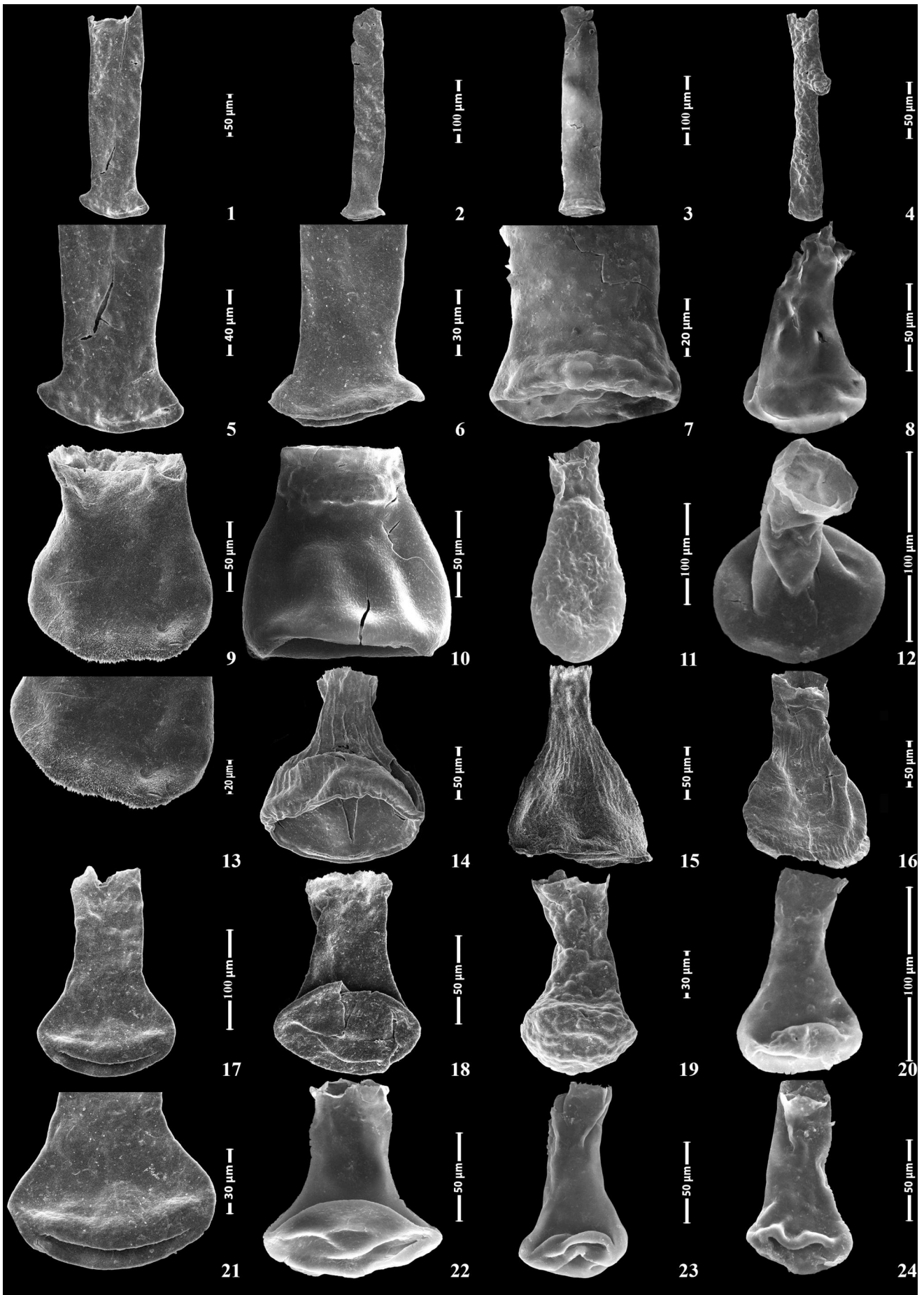
Calpichitina lenticularis (Plate 7, figures 1, 2) first emerges at the base of the *robusta* biozone, persists through the MG-6 to MG-18 interval, and extends into the basal part of the succeeding biozone in the Khoshyeilagh region (Figure 5; Supplementary data, S5). It has been recorded in the Darriwilian (Dw1–Dw3; time slices 4a–4c) of the *Calymene* to *Marrolothus* Shale, France (Rauscher and Doubinger 1967; Rauscher 1970); the late Darriwilian–early Sandbian (Dw3–Sa1; time slices 4c–5a) of Dalby, Öland, Sweden (Grahn 1981); the Sandbian (Sa1–Sa2; time slices 5a–5b) of the Louredo Formation, Portugal (Paris 1979); and the Sandbian–Katian (Sa1–Ka4; time slices 5a–Vld) of Morocco (Elaouad-Debbaj 1984; Bourahrouh et al. 2004) and Algeria (Oulebsir and Paris 1995). On the Iranian Platform, this species appears in the Sandbian–early Katian (Sa1–Ka1; time slices 5a–Vla) of the Seyahou Formation, High Zagros Mountains (Ghavidel-Syooki 2000, 2021, 2023), and the Ghelli Formation, Alborz Mountains (Ghavidel-Syooki and Winchester-Seeto 2002; Ghavidel-Syooki 2008, 2016, 2017a, 2017b, 2017c; Ghavidel-Syooki and Borji 2018; Ghavidel-Syooki and Piri-Kangarshahi 2024), as well as in the Katian (Ka1–Ka4; time slices Vla–Vld) of Kuh-e Boghoh, Central Iran (Ghavidel-Syooki and Piri-

Kangarshahi 2021). In the Arabian Peninsula, it has been identified in the late Sandbian–middle Katian (Sa2–Ka3; time slices 5b–Vlb) of the Quwarah Member, Qasim Formation, southern Persian Gulf (Al-Hajri 1995; Al-Shawareb et al. 2017); and in the latest Katian–Hirnantian (Ka4–Hi2; time slices Vld–VII) of Libya (Abuhmida 2013). Scandinavian records include the Sandbian–early Katian (Sa1–Ka1; time slices 5a–Vla) (Grahn and Nölvak 2007) and the Greenscoe section, Southern Lake District, UK (Van Nieuwenhove et al. 2006). In the Arabian Peninsula, this species defines the *Calpichitina lenticularis* biozone (Al-Hajri 1995), spanning from its FAD to the FAD of the *Tanuchitina fistulosa* biozone.

Cyathochitina campanulaeformis (Plate 11, figure 15) first appears at the onset of the *robusta* biozone and persists through the succeeding biozones in the Khoshyeilagh area (Figure 5; Supplementary data, S5). This taxon spans the Ordovician–Silurian (Paris 1990; Butcher 2009). *Cyathochitina kuckersiana* (Plate 11, figure 16) emerges at the base of the *robusta* biozone and extends into the succeeding biozones (Figure 5; Supplementary data, S5). This cosmopolitan species ranges from the Early Ordovician (Floian) to the Early Silurian (Telychian) and has been recorded in various regions, including late Floian–late Darriwilian (Fl3–Dw3; time slices 2c–4c) in the USA (Grahn and Bergström 1984) and Estonia (Tammekänd et al. 2010); late Darriwilian (Dw3; time slice 4c) in Sweden (Laufeld 1967; Grahn 1981); late Darriwilian–late Katian (Dw3–Ka4; time slices 4c–Vld) in Morocco (Soufiane and Achab 1993); Sandbian–early Katian (Sa1–Ka1; time slices 5a–Vla) in the USA (Siesser et al. 1998); Katian (Ka2–Ka3; time slice Vlb) in Sweden (Grahn 1981), Estonia (Eisenack 1962); Katian (Ka1–Ka3; time slices Vla–Vlb) and Russia (Laufeld 1971); Upper Ordovician (Sa1–Hi2; time slices 5a1–VII) in the Iranian Platform (Ghavidel-Syooki 2023; Ghavidel-Syooki and Piri-Kangarshahi 2024); Middle–Late Ordovician in South China (Liang et al. 2023); Katian (Ka4; time slice Vld) in Morocco (Le Heron and Craig 2008) and Argentina (de la Puente and Rubinstein 2013); late Hirnantian (Hi2; time slice VII) to Early Silurian (Rhuddanian) in northern Chad and south-eastern Libya (Le Hérisse et al. 2013); and Llandovery (Rhuddanian–Telychian) in north-east Libya (Hill et al. 1985), Wales (Mullins and Loydell 2002), Latvia (Loydell et al. 2003), Jordan (Butcher 2009), and Canada (Soufiane and Achab 2000).

Desmochitina minor (Plate 7, figures 5, 6, 17a, 17b) occurs in the MG-6 to MG-18 interval of the Ghelli Formation in the Khoshyeilagh area (Figure 5; Supplementary data, S5) and ranges from the Early Ordovician to Silurian (Paris 1990; Butcher 2009). *Desmochitina erinacea* (Plate 7, figures 3, 7; Plate 9, figures 10–12) first appears at the base of the *robusta* biozone and extends into the succeeding biozone (Figure 5; Supplementary data, S5). This cosmopolitan species has been reported from the latest Darriwilian to late

←
Plate 10. Figures 1, 5. *Rhabdochitina gracilis* Eisenack 1962 (1a) (sample MG-42; three specimens); and *Baltisphaeridium llanvirianum* Deunff 1977 (1b) (sample MG-9; five specimens); Figures 2, 6; 3, 7; 4, 8; 11, 15. *Rhabdochitina gracilis* Eisenack 1962 (sample MG-50; three specimens); Figures 12, 16. *Pistillachitina comma* (Eisenack 1959) (sample MG-23; nine specimens); Figures 9, 13, 10, 14; 17–19. *Rhabdochitina magna* Eisenack 1931 (sample MG-14; eight specimens); Figure 20. *Rhabdochitina magna* Eisenack 1931 (a) (sample MG-14; eight specimens) and *Multiplicisphaeridium bifurcatum* Staplin et al. 1965 (b) (sample MG-14; eight specimens); Figures 21, 22. *Rhabdochitina curvata* Al-Shawareb et al. 2017-Eisenack 1931 (sample MG-61; three specimens); Figures 23, 24. *Rhabdochitina usitata* Jenkins 1967 (sample MG-9; six specimens).



Sandbian (time slices 4c–5b) in South China (Liang et al. 2017); Darriwilian–late Sandbian (time slices 4a–5b) in Baltoscandia (Nölvak and Grahn 1993; Nölvak et al. 2019, 2022), early Sandbian to late Katian (time slices 5a–VId) in England (Vandenbroucke 2007); and Sandbian (time slices 5a–5b) in the Alborz Mountains and Central Iranian basins (Ghavidel-Syooki and Piri-Kangarshahi 2021, 2024). In Baltoscandia, it does not extend beyond Sandbian stage slice Sa2 (time slice 5b; see Nölvak and Grahn 1993). *Desmochitina juglandiformis* (Plate 7, figures 13–16) first appears at the base of the *robusta* biozone and extends into the succeeding biozone (Figure 5; Supplementary data, S5). It has been recorded from Sandbian (time slices 5a–5b) in Sweden (Laufeld 1967) and Belgium (Vanmeirhaeghe 2006); the *robusta* biozone in northern Gondwana (southern Spain, Vanmeirhaeghe 2006), and Iran (Ghavidel-Syooki 2017b, 2017c; Ghavidel-Syooki and Piri-Kangarshahi 2024); and the early Katian (time slice VIa) in the *clingani* graptolite zone in Europe (Verschaeve 2004; Zalasiewicz et al. 2004). *Eisenackitina rhenana* (Plate 11, figures 9, 13) appears in two samples from the basal part of the *robusta* biozone in the Khoshyeilagh area (Figure 5; Supplementary data, S5). It has been reported from the early Sandbian (time slice 5a) in the Louredo Formation, Portugal (Paris 1981); the lower Wood Brook and Spy Wood Brook sections in the Shelve Inlier, Welsh Borderland, England (Vandenbroucke 2007); and the early Sandbian (time slice 5a) at the Simeh-Kuh locality in the Alborz Mountains of northern Iran (Ghavidel-Syooki and Piri-Kangarshahi 2024).

Pistillachitina pistillifrons (Plate 11, figures 3, 7) first appears at the base of the *robusta* biozone in the Khoshyeilagh region and extends into the succeeding biozones (Figure 5; Supplementary data, S5). It has been documented in the Sandbian stage slice Sa1 (time slice 5a) in Cardigan, England (Vandenbroucke 2007); Katian stage slices Ka2–Ka4 (time slices VIb–VId) in the Upper Ktaoua Formation, Morocco (Elaouad-Debbaj 1984); and late Katian stage slice Ka4 (time slice VId) in the Ghelli Formation, Alborz Mountains, northern Iran (Ghavidel-Syooki and Winchester-Seeto 2002; Ghavidel-Syooki and Piri-Kangarshahi 2024), as well as in the Seyahou Formation, High Zagros Mountains, southern Iran (Ghavidel-Syooki 2023). Paris (1990) reported its range from the *Lagenochitina deunffii* to *Lagenochitina dalbyensis* biozones in Sandbian stage slices Sa1–Sa2 (time slices 5a–5b; Webby et al. 2004). Based on the age assigned to *Belonechitina robusta* and associated taxa, 105 m of the basal part of the Ghelli Formation at Khoshyeilagh corresponds to Sandbian–middle Katian stage slices Sa1–Ka2 (time slices 5a–VIb).

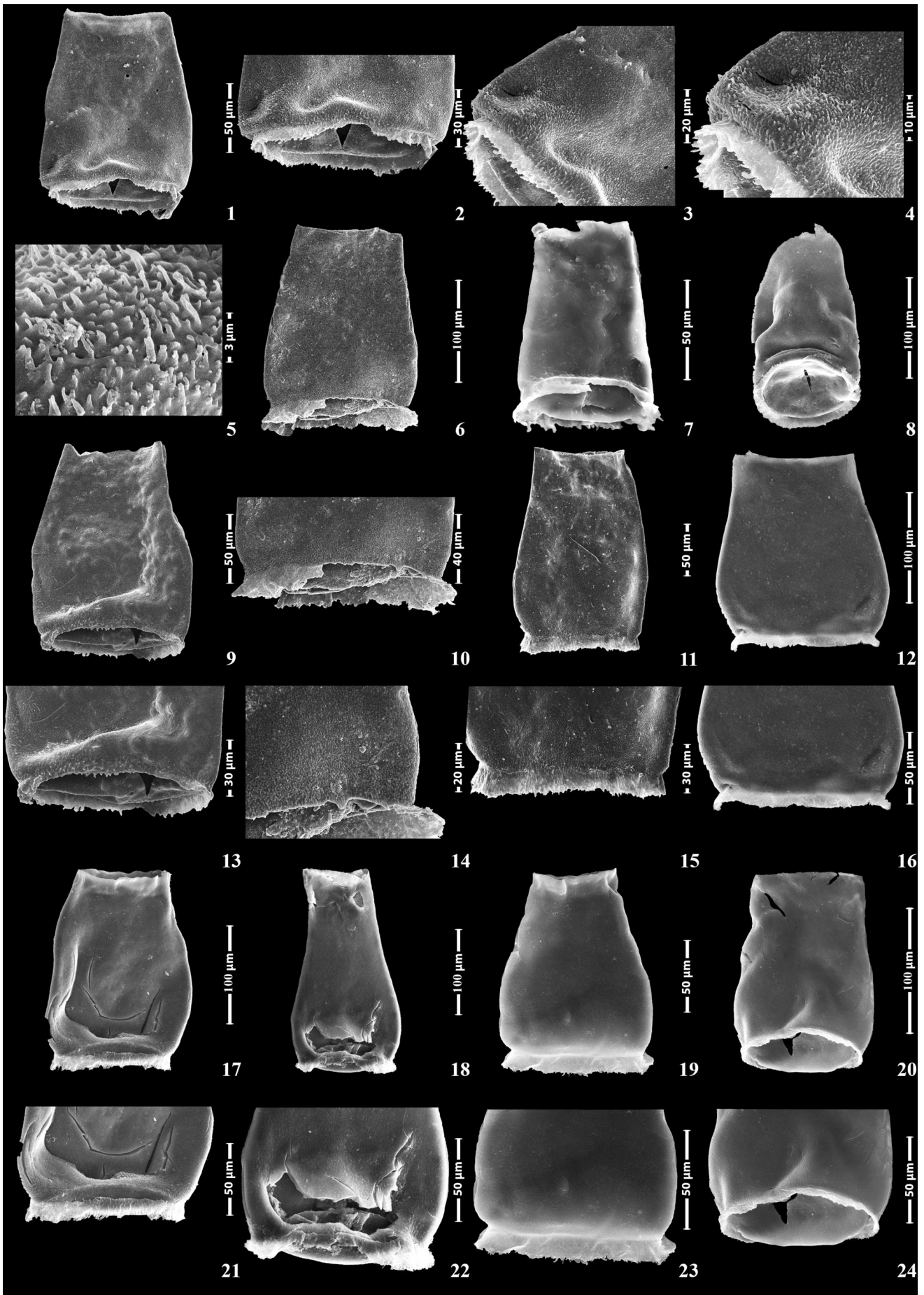
Rhabdochitina magna (Plate 10, figures 9, 13, 14, 17–20) first appears at the base of the *robusta* biozone and extends into the succeeding biozone (Figure 5; Supplementary data,

S5). It has been recorded from late Floian–early Darriwilian stage slices FI3–Dw1 (time slices 2c–4a) in Öland, Sweden (Grahn 1980, 1981); early Darriwilian–middle Katian Dw1–Ka3 (time slice 4a–VIb) in Estonia (Eisenack 1962, 1965, 1968a, 1968b); and late Darriwilian stage slice Dw3 (upper time slice 4c) in the Meadowtown Beds, Welsh Borderland, England (Jenkins 1967). In Iran, it has been reported from late Darriwilian–early Sandbian stage slices Dw3–Sa1 (time slices 4c–5a) in the uppermost Laskarak and lower Ghelli Formation at Simeh-Kuh, Alborz Mountains (Ghavidel-Syooki and Piri-Kangarshahi 2024). *Rhabdochitina usitata* (Plate 10, figures 23, 24) emerges in the basal *robusta* biozone and extends into the succeeding biozone in the Khoshyeilagh area (Figure 5; Supplementary data, S5). It has been recorded from the Darriwilian stage slices Dw1–Dw3 (time slices 4a–4c) in western Newfoundland, Canada (Albani et al. 2001); late Darriwilian stage slice Dw3 (time slice 4c) in the Lashkarak Formation at GerdKuh (Ghavidel-Syooki and Piri-Kangarshahi 2023); and the late Darriwilian–early Sandbian stage slices Dw3–Sa1 (time slices 4c–5a; Videt et al. 2010) in the Ghelli Formation at Simeh-Kuh, Alborz Mountains (Ghavidel-Syooki and Piri-Kangarshahi 2024). Additional records include Darriwilian–Sandbian stage slices Dw1–Sa2 (time slices 4a–5b) in Shropshire, England (Jenkins 1967); Sandbian stage slices Sa1–Sa2 (time slices 5a–5b) on Anticosti Island, Québec, Canada (Achab 1984); Darriwilian stage slices Dw1–Dw3 (time slices 4a–4c) in western Newfoundland, Canada (Albani et al. 2001); late Sandbian stage slice Sa2 (time slice 5b) in England (Vandenbroucke 2007); Sandbian stage slices Sa1–Sa2 (time slices 5a–5b) in the Viola limestones, Arbuckle Mountains, Oklahoma, USA (Jenkins 1969); and Sandbian–Katian stage slices Sa1–Ka4 (time slices 5a–VId) in Iran (Ghavidel-Syooki 2001). In northern Iran, it has been recently reported from Sandbian stage slices Sa1–Sa2 (time slices 5a–5b) in the uppermost Laskarak and lower Ghelli Formation at Simeh-Kuh, Alborz Mountains (Ghavidel-Syooki and Piri-Kangarshahi 2024).

4.4.2. *Tanuchitina fistulosa* biozone

This biozone represents the partial range of *Tanuchitina fistulosa* from its FAD to the FAD of *Acanthochitina barbata* (Taugourdeau and de Jekhowsky 1960; Paris et al. 2000b). Researchers have documented *T. fistulosa* in the upper Caradocian (early Katian) of the Algerian Sahara (Taugourdeau and de Jekhowsky 1960), Morocco (Bourahrouh et al. 2004), the Arabian Peninsula (Al-Hajri 1995; Paris et al. 2000b; Al-Shawareb et al. 2017), Turkey (Paris et al. 2007), and Iran (Ghavidel-Syooki 2001, 2017b, 2017c, 2023; Ghavidel-Syooki and Winchester-Seeto 2002; Ghavidel-Syooki and Piri-Kangarshahi 2021, 2024). Additionally, it appears in the Hirnantian stage slices Hi1–Hi2

Plate 11. Figures 1, 5; 2, 6. *Pistillachitina iranense* sp. nov. (sample MG-22; 7 specimens); Figures 3, 7. *Pistillachitina pistillifrons* (Eisenack 1939) (sample MG-11; 11 specimens); Figure 4. *Pistillachitina alborzensis* sp. nov. (sample MG-21; 9 specimens); Figures 8, 12. *Euconochitina lepta* (Jenkins 1970) emend. Paris et al. 1999 (sample MG-32; 8 specimens); Figures 9, 13. *Eisenackitina rhenana* Eisenack 1939 (sample MG-7; 5 specimens); Figure 10. *Lagenochitina prussica* Eisenack 1931 (sample MG-23; 35 specimens); Figure 11. *Lagenochitina baltica* Eisenack 1931 (sample MG-21; 3 specimens); Figure 14. *Cyathochitina costata* Grahn 1982 (sample MG-34; 9 specimens); Figure 15. *Cyathochitina campanulaeformis* (Eisenack 1931) (sample MG-8; 15 specimens); Figure 16. *Cyathochitina kuckersiana* (Eisenack 1934) (sample MG-17; 10 specimens); Figures 17, 21; 18, 24. *Fungochitina spinifera* (Eisenack 1962) (sample MG-21; 5 specimens).



(time slice VII) of the Baq'a Shale Member, Sarah Formation, Arabian Peninsula (Paris et al. 2015). In this study, *T. fistulosa* (Plate 9, figures 12, 16; 17, 21; 18, 22; 19, 22; 20, 24) occurs in the MG-19 to MG-30 interval, spanning 96.7 m of micaceous dark shales in the Ghelli Formation, Khoshyeilagh region (Figure 5; Supplementary data, S5), and follows the preceding one. It features a diverse assemblage, including *Angochitina dicranum* Jenkins (1967), *A. communis* Jenkins (1967), *A. cf. communis* Jenkins (1967), *Ancyrochitina onniensis* Jenkins (1967), *Belonechitina iranense* sp. nov., *B. micracantha* (Eisenack) Paris 1931, *Desmochitina* sp. A, *D. minor typica* Eisenack (1931), *Fungochitina spinifera* Eisenack (1962) *Lagenochitina baltica* Eisenack (1931), *L. prussica* Eisenack (1931), *Pistillachitina iranense* sp. nov., *P. alborzensis* sp. nov., *P. comma* Eisenack (1959), *Spinachitina bulmani* (Jansonius) Jenkins (1967), and *Tanuchitina alborzensis* Ghavidel-Syooki (2017c), each described below. In the current study, *Angochitina communis* (Plate 8, figure 22) and *A. cf. communis* (Plate 8, figures 19, 23; 20, 24) occur in the MG-19 to MG-30 interval of the Ghelli Formation, Khoshyeilagh region (Figure 5; Supplementary data, S5). Researchers have documented *A. communis* in the late Sandbian stage slice Sa2 (time slice 5b) of the upper Dalby Limestone, Sweden (Grahn 1981; the Katian stage slices Ka1–Ka3 (time slices VIa–VIb) in the Onnia beds, Welsh Borderland, England (Jenkins 1967; Vandenbroucke 2007); and the Katian stage slices Ka1–Ka4 (time slices VIa–VIId) in the Quwarah Member, Qasim Formation, Arabian Peninsula (Paris et al. 2015) and the Iranian Platform (Ghavidel-Syooki 2021; Ghavidel-Syooki and Piri-Kangarshahi 2021, 2024).

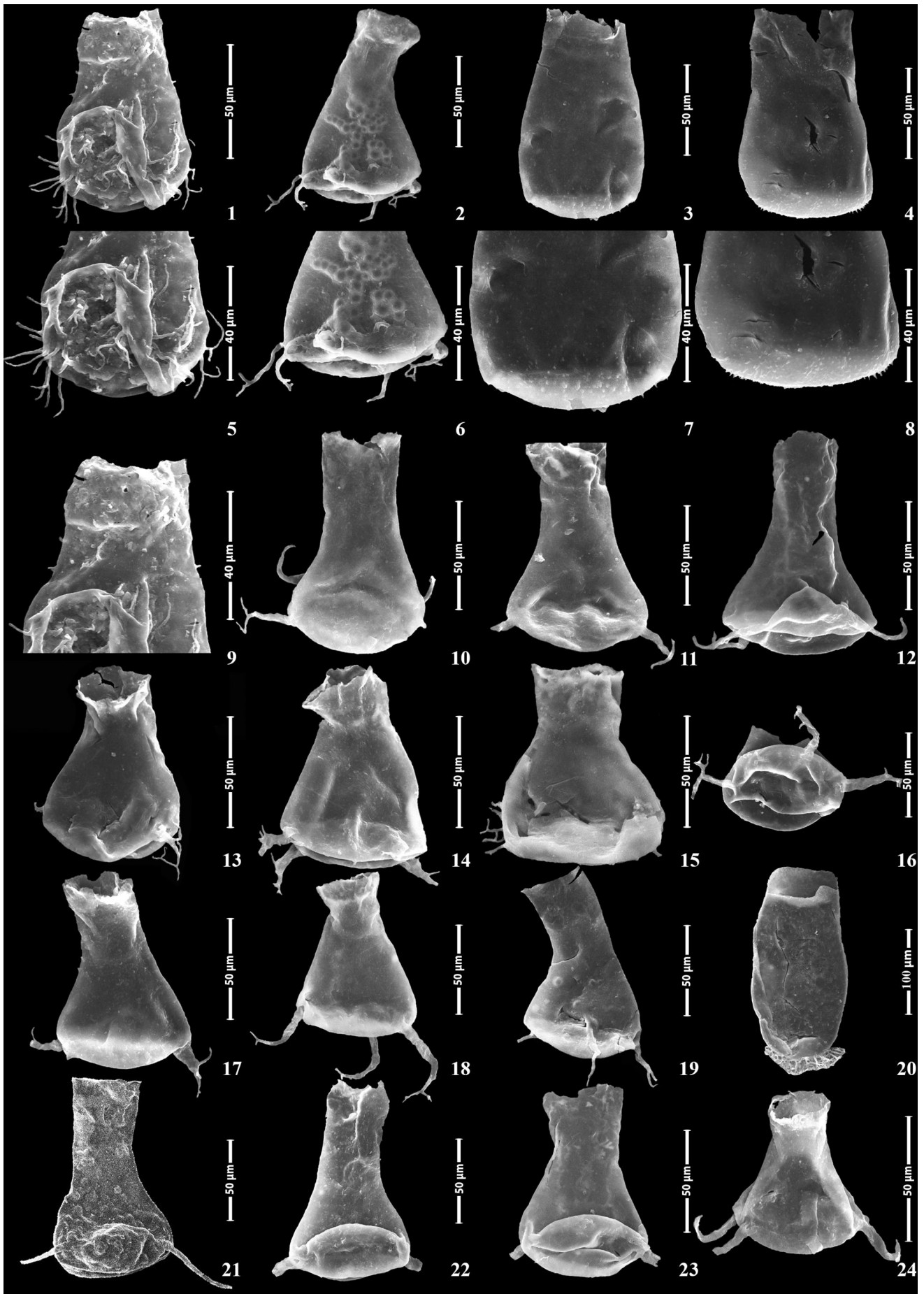
Angochitina dicranum (Plate 13, figures 1, 5; 9) occurs throughout the *fistulosa* biozone in the Khoshyeilagh locality (Figure 5; Supplementary data, S5). Jenkins (1967) documented this taxon in the early Katian stage slice Ka1 (time slice VIa) of the Onnia beds, Welsh Borderland, England. Additionally, *A. cf. dicranum* appears in the *fistulosa* biozone of the Ghelli Formation at the Simeh-Kuh locality, Alborz Mountains (Ghavidel-Syooki and Piri-Kangarshahi 2024).

Ancyrochitina onniensis (Plate 13, figures 13–16) occurs in the MG-19 to MG-30 interval of the Ghelli Formation in the Khoshyeilagh area (Figure 5; Supplementary data, S5). Researchers have documented this taxon in the early Katian stage slice Ka1 (time slice VIa) of the Onnia Beds, Shropshire, England (Jenkins 1967; Vandenbroucke 2007); and the late Katian stage slice Ka4 (time slices VIc–VIId) of the Upper Ktaoua Formation, Anti-Atlas, Morocco (Elaouad-Debbaj 1984), and the *fistulosa* biozone of the Ghelli Formation at the Simeh-Kuh locality, Alborz Mountains, northern Iran (Ghavidel-Syooki and Piri-Kangarshahi 2024). *Belonechitina micracantha* (Plate 8, figures 1, 5; 17, 21) first appears at the base of the *fistulosa* biozone and spans the MG-19 to MG-30 interval of the Ghelli Formation (Figure 5; Supplementary data, S5). This taxon has a broad distribution, recorded from Sweden (Darrivilian–Dapingian stage slices Dp1–Dw3; time

slices 3a–4c) (Vandenbroucke 2004); Arabian Peninsula (Dapingian–early Katian stage slices Dp1–Ka1; time slices 3a–VIa) (Al-Hajri 1995; Al-Shawareb et al. 2017); Turkey (Paris et al. 2007); UK and Australia (Darrivilian stage slices Dw1–Dw3; time slices 4a–4c) (Winchester-Seeto et al. 2000; Vanmeirhaeghe 2006; Paris et al. 2007); Canada and Scandinavia (Darrivilian–early Katian stage slices Dw1–Ka1; time slices 4a–VIa) (Achab and Asselin 1995; Grahn and Nölvak 2007); Libya (Sandbian–Katian stage slices Sa1–Ka4; time slices 5a–VIId) (Molyneux and Paris 1985; Abuhmida 2013); Morocco and UK (middle Katian stage slices Ka2–Ka4; time slices VIb–VIId) (Elaouad-Debbaj 1984; Bourahrouh et al. 2004; Van Nieuwenhove et al. 2006; Le Heron and Craig 2008); UK (Sandbian–middle Katian stage slices Sa1–Ka3; time slices 5a–VIb) (Vandenbroucke et al. 2008); China (Darrivilian–Hirnantian stage slices Dw1–Hi2; time slices 4a–VII) (Xiaofeng and Xiaohong 2004); and the Iranian Platform (Sandbian–Hirnantian stage slices Sa1–Hi2; time slices Sa–VII) (Ghavidel-Syooki 2008, 2021, 2023; Ghavidel-Syooki and Borji 2018; Ghavidel-Syooki and Piri-Kangarshahi 2021, 2024).

Belonechitina iranense sp. nov. (Plate 8, figures 4, 8) appears in the MG-19 to MG-30 interval of the Ghelli Formation in the Khoshyeilagh region (Figure 5; Supplementary data, S5). *Desmochitina* sp. A (Plate 7, figures 4, 8) occurs in the MG-19 to MG-30 interval of the Ghelli Formation in the Khoshyeilagh region (Figure 5; Supplementary data, S5). Due to its distinct features, it is recognised as a new species. *Desmochitina minor typica* (Plate 7, figure 18) first appears at the base of the *fistulosa* biozone and extends into the succeeding biozone. This taxon has been recorded in England (Sandbian–Katian stage slices Sa1–Ka4; time slices 5a1–VIId) Vandenbroucke (2007); Arabian Peninsula (Katian: Ka1–Ka4; time slices VIa–VIId), Quwarah Member, Qasim Formation (Paris et al. 2015) and Iranian Platform (Ghavidel-Syooki et al. 2011b; Ghavidel-Syooki et al. 2011a; Ghavidel-Syooki et al. 2023; Ghavidel-Syooki and Piri-Kangarshahi 2021, 2024).

Fungochitina spinifera (Plate 11, figures 17, 21; 18–24) occurs throughout the MG-19 to MG-30 interval of the *fistulosa* biozone and extends into the succeeding biozone of the Ghelli Formation in the Khoshyeilagh area (Figure 5; Supplementary data, S5). This taxon has been documented in England (late Sandbian–early Katian stage slices Sa2–Ka1; time slices 5b–VIa), Greenscoe section, southern Lake District, and historical type areas (Van Nieuwenhove et al. 2006; Vandenbroucke 2007); Arabian Peninsula (Hirnantian stage slices Hi1–Hi2; time slice VII) (Paris et al. 2015; Al-Shawareb et al. 2017); Iran (Katian stage slices Ka1–Ka4; time slices VIa–VIId) (Ghavidel-Syooki 2017c, 2023; Ghavidel-Syooki and Borji 2018; Ghavidel-Syooki and Piri-Kangarshahi 2021, 2024); and Libya (late Hirnantian stage slice Hi2; time slice VII) Abuhmida (2013). Van Nieuwenhove et al. (2006) correlated the *F. spinifera* biozone with the upper part of the *Euconochitina tanvillensis*, *Belonechitina robusta*, and



Tanuchitina fistulosa biozone, and the lower part of the *Acanthochitina barbata* biozone.

Lagenochitina baltica (Plate 11, figure 10) appears in the MG-19 to MG-30 interval of the Ghelli Formation in the Khoshyeilagh area, Alborz Mountains, northern Iran (Figure 5; Supplementary data, S5). This taxon has been recorded in China (Darriwilian–Hirnantian stage slices Dw1–Hi2; time slices 4a–VII) (Wang and Chen 2004); England and Portugal (Sandbian–early Katian stage slices Sa1–Ka1; time slices 5a–VIa) (Jenkins 1967; Paris 1979; Vandenbroucke 2004, 2005; Vandenbroucke et al. 2008); Northern Gondwanan Domain, Scandinavia, Belgium and Morocco (Sandbian–Hirnantian stage slices Sa1–Hi2; time slices 5a–VII) (Paris 1990; Bourahrouh et al. 2004; Vanmeirhaeghe 2006; Grahn and Nölvak 2007); Libya (early–middle Katian stage slices Ka1–Ka3; time slices VIa–VIb; Molyneux and Paris 1985); Iran, England and Belgium (Katian–Hirnantian stage slices Ka1–Hi2; time slices VIa–VII) (Vanmeirhaeghe et al. 2005; Ghavidel-Syooki 2008, 2011b, 2017b, 2017c, 2023; Ghavidel-Syooki and Piri-Kangarshahi 2021, 2024); Estonia (late Katian stage slice Ka4; time slice VIId) (Eisenack 1959, 1965; Nölvak 1980); Turkey (Katian–Hirnantian stage slices Ka1–Hi2; time slices VIa–VII) Paris et al. (2007); Canada (middle Katian stage slices Ka2–Ka3; time slice VIb) (Achab 1977); England (middle Katian–Hirnantian stage slices Ka2–Hi2; time slices VIb–VII) (Van Nieuwenhove et al. 2006) and Morocco (Hirnantian stage slices Hi1–Hi2; time slice VII) (Le Heron and Craig 2008).

Lagenochitina prussica (Plate 11, figure 11) first appears at the base of the *fistulosa* biozone and extends into subsequent biozones (Figure 5; Supplementary data, S5). This taxon has been recorded in Sweden and Russia (Sandbian–Hirnantian stage slices Sa1–Hi2; time slices Sa1–VII) (Laufeld 1971; Grahn 1982); Sweden (early Katian stage slice Ka1; time slice VIa) (Laufeld 1967); England (early–mid Katian stage slices Ka1–Ka3; time slices VIa–VIb) (Vandenbroucke 2005); Belgium and Morocco (late Katian stage slice Ka4; time slices VIc–VIId) (Vanmeirhaeghe 2006; Le Heron and Craig 2008); Turkey and Libya (Late Katian–Hirnantian stage slices Ka4–Hi2; time slices VIId–VII) (Paris 1988, 2007); Iran, Baltica, and Morocco (Katian–Hirnantian stage slices Ka1–Hi2; time slices VIa–VII) (Nölvak 1980; Elaouad-Debbaj 1984; Ghavidel-Syooki 2008, 2017b; Ghavidel-Syooki and Piri-Kangarshahi 2021, 2024); and North Gondwana Domain (mid-Katian–late Hirnantian stage slices Ka2–Hi2; time slices VIb–VII) (Paris 1990; Paris et al. 2000a; Bourahrouh et al. 2004; Abuhmida 2013).

Pistillachitina comma (Plate 10, figures 12, 16) occurs in the MG-19 to MG-30 interval of the Ghelli Formation in the Khoshyeilagh region (Figure 5; Supplementary data, S5). This taxon has been recorded in the Darriwilian–Sandbian stage slices Dw3–Sa2 (time slices 4c–5b) (Webby et al. 2004) in Öland, Sweden (Grahn 1981); the upper Caradocian (late

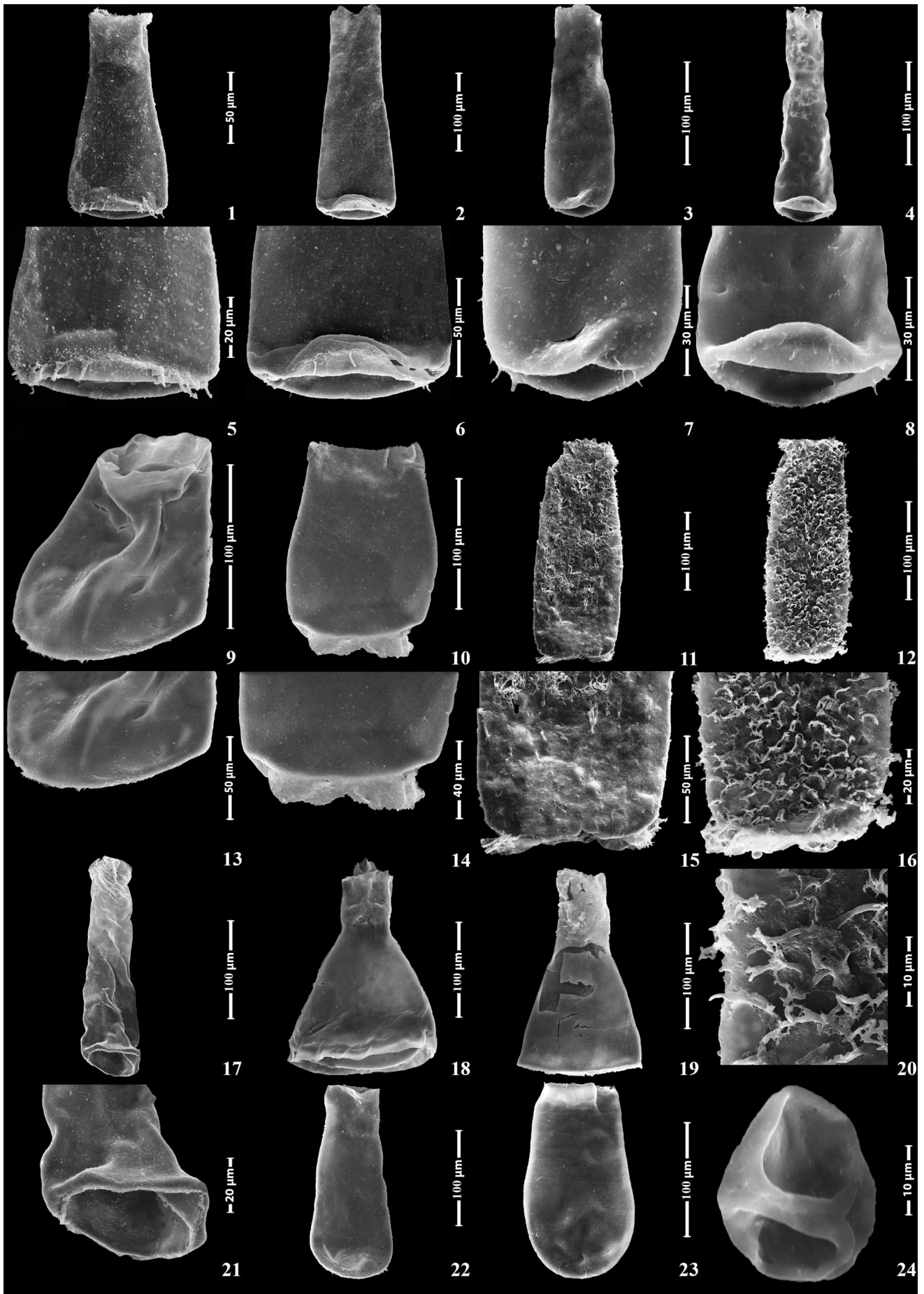
Sandbian, slice Sa2; time slice 5b) in Estonia (Eisenack 1959, 1965); the Katian stage slices Ka1–Ka4 (time slices VIa–VIId) in the Quwarah Member of the Qasim Formation, Arabian Peninsula (Paris et al. 2015); and the Iranian Platform (middle Katian–Hirnantian stage slices Ka3–Hi2; time slices VIc–VII) (Ghavidel-Syooki 2017c, 2023; Ghavidel-Syooki and Piri-Kangarshahi 2021).

Pistillachitina iranense sp. nov. (Plate 8, figure 18; Plate 11, figures 1, 5; 2, 6) and *Pistillachitina alborzensis* sp. nov. (Plate 11, figure 4) occur throughout the *fistulosa* biozone (MG-19 to MG-30) of the Ghelli Formation in the Khoshyeilagh area (Figure 5; Supplementary data, S5). These taxa differ from other species of *Pistillachitina*, as detailed in the chitinozoan systematics section (4.3). *Spinachitina bulmani* (Plate 13, figures 3, 7; 4, 8; Plate 14, figures 9, 13) occurs in the MG-19 to MG-30 interval of the Ghelli Formation at the Khoshyeilagh section (Figure 5; Supplementary data, S5). This species has been documented in the late Sandbian stage slice Sa2 (time slice 5b; Webby et al. 2004) in Scotland and Shropshire, England (Jansonius 1964; Jenkins 1967); Sandbian–Katian stage slices Sa1–Ka4 (time slices 5a–VIId) in Belgium (Vanmeirhaeghe 2006); and Katian stage slices Ka1–Ka4 (time slices VIa–VIId) in Morocco (Elaouad-Debbaj 1984), Anticosti Island, Canada (Achab 1978), Norway (Grahn et al. 1994), Libya (Molyneux and Paris 1985), England (Vandenbroucke 2005), and Iran (Ghavidel-Syooki and Winchester-Seeto 2002). It also appears in Katian–Hirnantian stage slices Ka1–Hi2 (time slices VIa–VII) on the Iranian Platform (Ghavidel-Syooki 2008, 2017b, 2017c, 2023; Ghavidel-Syooki et al. 2011a; Ghavidel-Syooki and Borji 2018; Ghavidel-Syooki and Piri-Kangarshahi 2021, 2024); the early Hirnantian stage slice Hi1 (lower time slice VII) in the Memouniat Formation, Libya (Abuhmida 2013). Additionally, it has been reported in Sandbian–Katian stage slices Sa1–Ka4 (time slices 5a–VIId) across Avalonia, Laurentia, Gondwana, and South China (Liang et al. 2023).

Tanuchitina alborzensis (Plate 9, figures 1, 5; 2, 5) occurs in the MG-19 to MG-30 interval of the Ghelli Formation at the Khoshyeilagh section. It was first recorded from the Katian stage slices Ka1–Ka4 (time slices VIa–VIId) in the Ghelli Formation at its type locality, Kuh-e Saluk, Alborz Mountains (Ghavidel-Syooki 2017b, 2017c), and similar occurrences were reported at the Simeh-Kuh locality (Ghavidel-Syooki and Piri-Kangarshahi 2024). The *Tanuchitina fistulosa* biozone and associated chitinozoan taxa in the MG-19 to MG-30 interval suggest an upper Caradocian (upper Streffordian) or early Katian Ka1 stage (upper time slice VIa).

4.4.3. *Acanthochitina barbata* biozone

This biozone represents part of the range of *Acanthochitina barbata* Eisenack (1931), spanning from its FAD to the FAD of *Armoricochitina nigerica* (Bouché 1965). Researchers consider *Acanthochitina barbata* a key index microfossil for the



early Ashgillian (middle Katian stage slices Ka2–Ka3; time slice VIb; Videt et al. 2010) in the North Gondwana Domain, following the *Tanuchitina fistulosa* biozone (Paris 1999; Paris et al. 2000a; Webby et al. 2004; Videt et al. 2010). In this dataset, *Acanthochitina barbata* (Plate 14, figures 11, 15; 12, 16, 20) occurs in the MG-31 to MG-40 interval of the Ghelli Formation, spanning 80.6 m of alternating black micaceous papery shales and grey thin-bedded sandstones of the Upper Ordovician (Figure 5; Supplementary data, S5) in the Khoshyeilagh region. This biozone also includes *Acanthochitina* sp. A, *Cyathochitina costata* Grahn (1982), *Euconochitina lepta* (Jenkins 1970) Paris et al. (1999), and *Tanuchitina ontariensis* Jansonius (1964), each described below. *Acanthochitina?* sp. nov. A (Plate 13, figure 20) occurs in the MG-31 to MG-40 interval of the Ghelli Formation in the Khoshyeilagh section, Alborz Mountains, northern Iran (Figure 5; Supplementary data, S5). Its classification remains open due to insufficient specimens, preventing confirmation of vesicle ornamentation and potential designation as a new species. *Cyathochitina costata* (Plate 11, figure 14) occurs through the MG-31 to MG-40 interval of the Ghelli Formation in the Khoshyeilagh section (Figure 5; Supplementary data, S5). This species has been recorded in the Katian stage slices Ka1–Ka3 (time slices VIa–VIb) in Götland, Sweden (Grahn 1982); the early Katian stage slice Ka1 (time slice VIa) in Estonia (Nölvak 1980); the Katian stage slices Ka2–Ka3 (time slice VIb; Videt et al. 2010) in the Ghelli Formation at Kuh-e Saluk and Simeh-Kuh, Alborz Mountains, northern Iran (Ghavidel-Syooki and Winchester-Seeto 2002; Ghavidel-Syooki and Piri-Kangarshahi 2024); the late Hirnantian stage slice Hi2 (upper time slice VII) in Latvia (Hints et al. 2010); and the Bir Tlacin Formation, Libya (Abuhmida 2013). *Euconochitina lepta* (Plate 11, figures 8, 12) spans the *barbata* biozone in the Khoshyeilagh section (Figure 5; Supplementary data, S5). This taxon has been recorded in the Katian stage slices Ka1–Ka4 (time slices VIa–VIId) in the Sylvan Shale, Oklahoma, USA (Jenkins 1970); the late Katian stage slice Ka4 (time slices VIc–VIId) in England (Vandenbroucke 2007); the mid–late Katian stage slices Ka2–Ka4 (time slices VIb–VIId) in Morocco (Elaouad-Debbaj 1984) and Algeria (Oulebsir and Paris 1995; Paris et al. 2000a); and the Katian stage slices Ka1–Ka4 (time slices VIa–VIId) in the Arabian Peninsula (Al-Shawareb et al. 2017), south-eastern Turkey (Paris et al. 2007), and the Iranian Platform (Ghavidel-Syooki and Winchester-Seeto 2002; Ghavidel-Syooki 2008, 2016, 2017a, 2017b, 2017c, 2021, 2023; Ghavidel-Syooki and Borji 2018; Ghavidel-Syooki and Piri-Kangarshahi 2021, 2024).

Tanuchitina ontariensis (Plate 9, figures 9, 13; 8, 10, 14) occurs throughout the *barbata* biozone (Figure 5; Supplementary data, S5) and is a distinctive Late Ordovician species. It has been recorded in the Katian stage slices Ka1–Ka4 (time slices VIa–VIId) in the Sylvan Shale, Oklahoma, USA

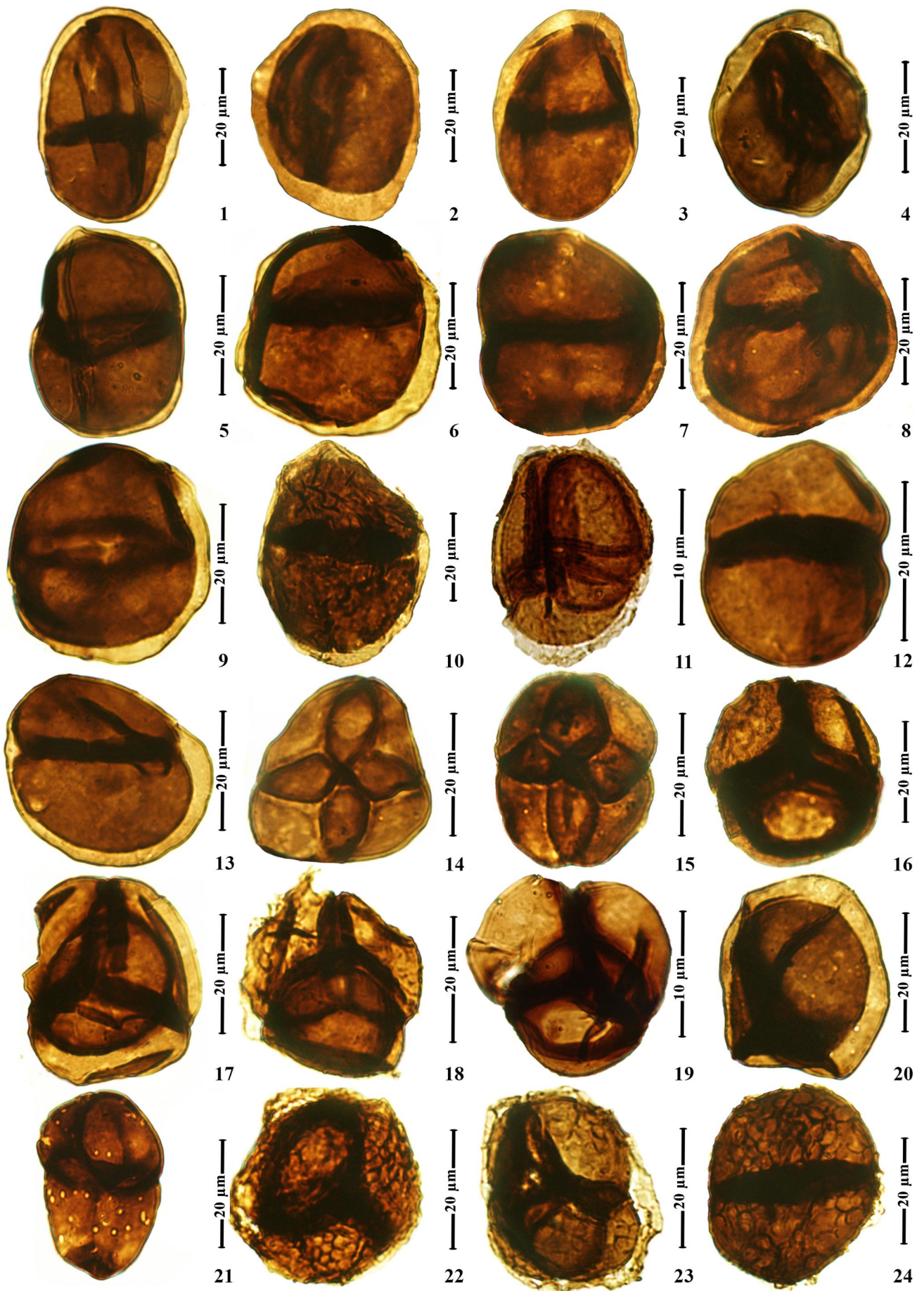
(Jenkins 1970); the Vaureal Formation, Canada (Achab 1983); the Arabian Peninsula (Al-Hajri 1995); Turkey (Paris et al. 2007); and the Upper Ordovician Ghelli and Seyahou formations on the Iranian Platform (Ghavidel-Syooki 2017b, 2017c, 2023; Ghavidel-Syooki and Borji 2018; Ghavidel-Syooki and Piri-Kangarshahi 2021, 2024). These chitinozoan species characterise the Katian Stage (Jenkins 1969; Elaouad-Debbaj 1984, 1988; Ghavidel-Syooki and Winchester-Seeto 2002; Van Nieuwenhove et al. 2006; Ghavidel-Syooki 2008, 2016, 2017a, 2017b, 2017c, 2023; Vandenbroucke et al. 2009; Abuhmida 2013; Ghavidel-Syooki and Piri-Kangarshahi 2024). Chronostratigraphical comparisons with Paris et al. (2000a), Bergström et al. (2009), Webby et al. (2004), and Videt et al. (2010) indicate that the MG-30 to MG-40 interval of the Ghelli Formation in the Khoshyeilagh section corresponds to the middle Katian stage slices Ka2–Ka3 (time slice VIb).

4.4.4. *Armoricochitina nigerica* biozone

This biozone represents the partial range of *Armoricochitina nigerica* (Bouché 1965), from its FAD to the FAD of *Ancyrochitina merga* in the North Gondwana Domain. In the current dataset, *A. nigerica* (Plate 12, figures 6, 10, 14; 9, 13; 12, 16; 18, 22; 19, 23; Plate 14, figures 10, 14) appears in the MG-41 to MG-60 interval of the Ghelli Formation, spanning 161 m of alternating black shale and grey sandstone beds at the Khoshyeilagh (Figure 5; Supplementary data, S5). This species is documented in the Late Ordovician (Ashgillian) of the North Gondwana Domain (Bouché 1965; Molyneux and Paris 1985; Al-Hajri 1995; Oulebsir and Paris 1995; Paris et al. 2000a; Ghavidel-Syooki 2008, 2023). *Armoricochitina nigerica* is a key chitinozoan microfossil that defines the northern Gondwanan high palaeolatitude during the Late Ordovician. Its absence in the United Kingdom and Belgium suggests it did not extend northward across the Rheic Ocean margin (Paris et al. 2015). This biozone is notable for the presence of several key species, including *Armoricochitina alborzensis* Ghavidel-Syooki and Winchester-Seeto (2002), *Armoricochitina iranica* Ghavidel-Syooki and Winchester-Seeto (2002), *Armoricochitina persianense* Ghavidel-Syooki (2017c), and *Rhabdochitina gracilis* Eisenack (1962), each described below.

Armoricochitina alborzensis (Plate 12, figures 8, 11, 15, 17, 21; 20, 24) and *A. iranica* (Plate 12, figure 7) were first described from the Upper Ordovician Ghelli Formation at Kuh-e Saluk, Alborz Mountains. These taxa, along with *A. nigerica*, have been recorded from the uppermost Katian (Ka3–Ka4) in northern Iran (Ghavidel-Syooki and Winchester-Seeto 2002; Ghavidel-Syooki 2016, 2017b, 2017c; Ghavidel-Syooki and Borji 2018), and from Kuh-e Boghou and the Seyahou Formation (Ghavidel-Syooki and Piri-Kangarshahi 2021; Ghavidel-Syooki 2023). *Armoricochitina persianense* (Plate 12, figures 1–5) also occurs in the MG-41 to MG-60

Plate 14. Figures 1, 5; 2, 6; 3, 7; 4, 8; 22. *Spinachitina oulebsiri* Paris et al. 2000b (sample MG-83; 20 specimens); Figures 9, 13. *Spinachitina bulmani* Jansonius 1964 (sample MG-20; eight specimens); Figures 10, 14. *Armoricochitina nigerica* (Bouché 1965) (sample MG-44; 35 specimens); Figures 11, 15; 12, 16, 20. *Acanthochitina barbata* Eisenack 1931 (sample MG-36; 20 specimens); Figures 17, 21. *Belonechitina capitata* (Eisenack 1962) (sample MG-9; 20 specimens); Figure 18. *Cyathochitina campanulaeformis* (Eisenack 1931) (sample MG-8; 15 specimens); Figure 19. *Cyathochitina kuckersiana* (Eisenack 1934) (sample MG-18; 15 specimens); Figure 23. *Conochitina* sp. (sample MG-75; two specimens); Figure 24. *Cheilotetras caledonica* Wellman and Richardson 1993 (sample MG-49; eight specimens).



interval at the Khoshyeilagh region, as documented by Ghavidel-Syooki (2017b, 2017c). *Rhabdochitina gracilis* (Plate 10, figures 1, 5; 2, 6; 3, 7; 4, 8; 11, 15) first appears in the MG-41 to MG-60 interval at Khoshyeilagh (Figure 5; Supplementary data, S5) and has been recorded in the Late Ordovician (Katian) of the Arabian Peninsula (Al-Shawareb et al. 2017). These findings suggest a late middle Katian age for this interval, correlating with the early Ka4 stage slice (time slice VIc).

4.4.5. *Ancyrochitina merga* biozone

This biozone spans the total range of *Ancyrochitina merga* Jenkins (1970), from its FAD to the FAD of *Tanuchitina elongata* (Bouché 1965), the succeeding index species in the North Gondwana Domain. In the present dataset, *A. merga* (Plate 13, figures 2, 6; 10, 11, 12, 17, 18, 19) appears through the MG-61 to MG-74 interval of the Ghelli Formation at the Khoshyeilagh section, covering 112.8 m of black to olive-grey shales. This microfossil is well documented from the Upper Ordovician, particularly the late Katian stage slice Ka4 (time slice VIc), in various regions such as the United States (Jenkins 1970), Libya (Molyneux and Paris 1985; Paris 1988; Abuhmida 2013), Morocco (Elaouad-Debbaj 1984; Bourahrouh et al. 2004), Algerian Sahara (Oulebsir and Paris 1995), the Arabian Peninsula (Al-Hajri 1995; Paris et al. 2000a; Paris et al. 2015; Al-Shawareb et al. 2017), Turkey (Oktay and Wellman 2019), and Iran (Ghavidel-Syooki 2001, 2008, 2016, 2017c, 2023; Ghavidel-Syooki and Winchester-Seeto 2002; Ghavidel-Syooki et al. 2011b; Ghavidel-Syooki et al. 2011a; Ghavidel-Syooki and Piri-Kangarshahi 2021). The biozone includes notable taxa such as *Plectochitina sylvanica* Jenkins (1970), *Rhabdochitina curvata* Al-Shawareb et al. (2017), and *Tanuchitina anticostiensis* (Achab 1977), each described below.

Plectochitina sylvanica (Plate 13, figures 21–24) appears from MG-61 to MG-74 in the Ghelli Formation at the Khoshyeilagh region (Figure 5; Supplementary data, S5). Researchers have recorded this taxon in the Katian stage slice Ka4 (time slice VIc) in the Sylvan Shale, Oklahoma, USA (Jenkins 1970), Morocco (Elaouad-Debbaj 1984, 1986; Bourahrouh et al. 2004), Libya (Molyneux and Paris 1985), the Arabian Peninsula (Al-Hajri 1995), and Iran (Ghavidel-Syooki 2000, 2023; Ghavidel-Syooki and Winchester-Seeto 2002). *Rhabdochitina curvata* (Plate 10, figures 21, 22) spans MG-61 to MG-74 in the Ghelli Formation at the Khoshyeilagh region, Alborz Mountains, northern Iran (Figure 5; Supplementary data, S5). Researchers first described this taxon from the late middle Katian–early Hirnantian stage slices Ka2–Hi1 (time slices VIb–VII) in the Quwarah Member of the Qasim Formation, Arabian Peninsula (Al-Shawareb et al. 2017), and later reported it from the late middle Katian stage

slices Ka3–early Ka4 (time slices VIb–VIc) in the Ghelli Formation at Simeh-Kuh, Alborz Mountains, northern Iran (Ghavidel-Syooki and Piri-Kangarshahi 2024).

Tanuchitina anticostiensis (Plate 9, figures 11, 15) occurs throughout MG-61 to MG-74 in the Ghelli Formation at the Khoshyeilagh region (Figure 5). This taxon, an important Upper Ordovician (Caradocian to Ashgillian) microfossil, appears in the Sandbian–Hirnantian stage slices Sa1–Hi2 (time slices 5a–VII) in Canada (Achab 1977) and north-eastern Libya (Molyneux and Paris 1985); the late Katian–early Hirnantian stage slices Ka4–Hi1 (time slices VIc–VII) in Libya (Abuhmida 2013); and the Katian stage slices Ka1–Ka4 (time slices VIa–VIc) on the Iranian Platform (Ghavidel-Syooki 2017c, 2023; Ghavidel-Syooki and Borji 2018; Ghavidel-Syooki and Piri-Kangarshahi 2024). Comparison with chronostratigraphical charts (Paris et al. 2000a; Webby et al. 2004; Bergström et al. 2009; Videt et al. 2010) confirms that the MG-61 to MG-74 interval of the Ghelli Formation at Khoshyeilagh corresponds to the late Katian stage slice Ka4 (time slice VIc).

4.4.6. *Tanuchitina elongata* biozone

Paris (1990, 1996) and Paris et al. (2000b) defined this biozone as the partial-range biozone of *Tanuchitina elongata* (Bouché 1965), extending from its FAD to the FAD of *Spinachitina oulebsiri* (Paris et al. 2000b), the succeeding index species in the North Gondwana Domain (Paris 1990; Webby et al. 2004; Videt et al. 2010). Paris et al. (2000b) originally defined the *T. elongata* biozone in the Late Ordovician of the Algerian Sahara, setting its upper boundary at the FAD of *S. oulebsiri*. In this study, *T. elongata* (Plate 9, figures 3, 7; 4) first appears in the MG-75 to MG-79 interval of the Ghelli Formation at the Khoshyeilagh section (Figure 5; Supplementary data, S5), covering 109.2 m of conglomerate, olive-grey shale, and mottled medium-bedded sandstone. The basal 20 m of metamorphic heterogeneous conglomerate lacks palynomorphs, while the remaining sections contain poorly preserved specimens. Researchers have extensively documented this biozone in the Late Ordovician (early Hirnantian) across northern Africa, including Morocco, Tunisia, Libya, and Algeria (Bouché 1965; Elaouad-Debbaj 1988; Paris 1990; Oulebsir and Paris 1995; Paris et al. 2000b; Bourahrouh et al. 2004; Abuhmida 2013), as well as in the Middle East, including Iran (Ghavidel-Syooki and Winchester-Seeto 2002; Ghavidel-Syooki 2008, 2016, 2017c, 2023; Ghavidel-Syooki and Piri-Kangarshahi 2021), Turkey (Stemans et al. 1996; Paris et al. 2007; Oktay and Wellman 2019), and the Arabian Peninsula (McClure 1988; Al-Hajri 1995; Paris et al. 2000a; Paris et al. 2015; Al-Shawareb et al. 2017). This study identified co-occurring chitinozoan species within this biozone, including *Conochitina* sp. (Plate 14,

←
Plate 15. Figures 1–8; 13, 20. *Abditusdyadus laevigatus* Wellman and Richardson 1996 (sample MG-45; 15 specimens); Figures 10, 24. *Segestrespora membranifera* (Johnson 1985) Burgess 1991 (sample MG-82; nine specimens); Figures 11, 22, 23. *Velatitetras retimembrana* (Miller and Eames) Stemans et al. 1996 (sample MG-47; nine specimens); Figure 12. *Dyadospora asymmetrica* Ghavidel-Syooki 2017a (sample MG-85; four specimens); Figures 14, 15. *Tetrahdraletes medinensis* (Strother and Traverse 1979) emend. Wellman and Richardson 1993 (sample MG-11; five specimens); Figures 16, 17. *Tetrahdraletes grayae* Strother 1991 (sample MG-11; seven specimens); Figures 18, 19. *Imperfectotriletes patinatus* Stemans et al. 2000 (sample MG-83; seven specimens); Figure 21. *Dyadospora ferdowsii* Ghavidel-Syooki and Piri-Kangarshahi 2021 (sample MG-79; three specimens).

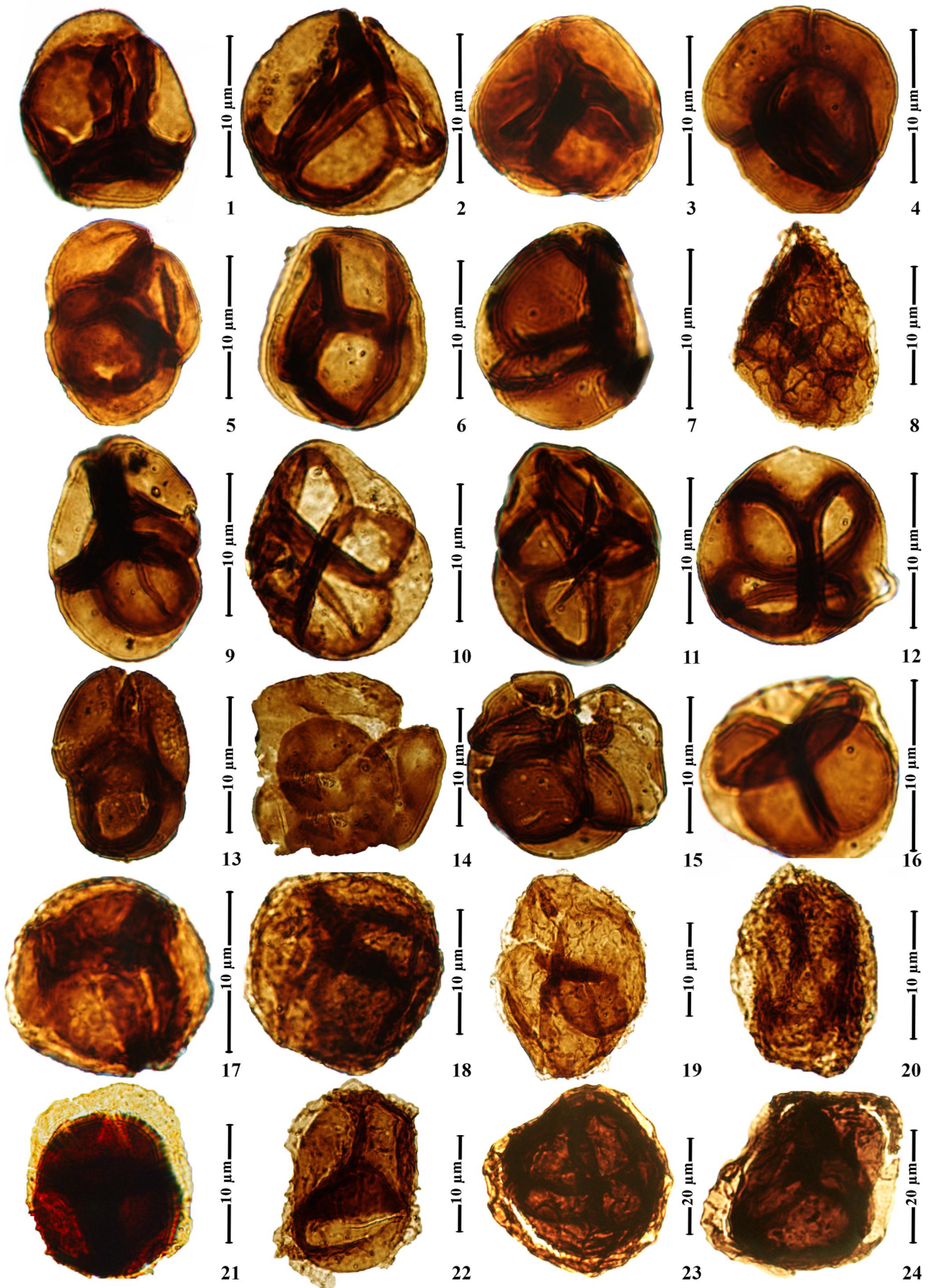


figure 23). *Rhabdochitina curvata* and *Tanuchitina anticostiensis* extend from the preceding biozone into the *elongata* biozone (Figure 5; Supplementary data, S5). Comparison with the chronostratigraphical charts of Paris (1990) and Webby et al. (2004) indicates that this biozone corresponds to the early Hirnantian stage slice Hi1 (lower level of time slice VII), aligning with the lower part of the upper member of the Ghelli Formation in the Khoshyeilagh region.

4.4.7. *Spinachitina oulebsiri* biozone

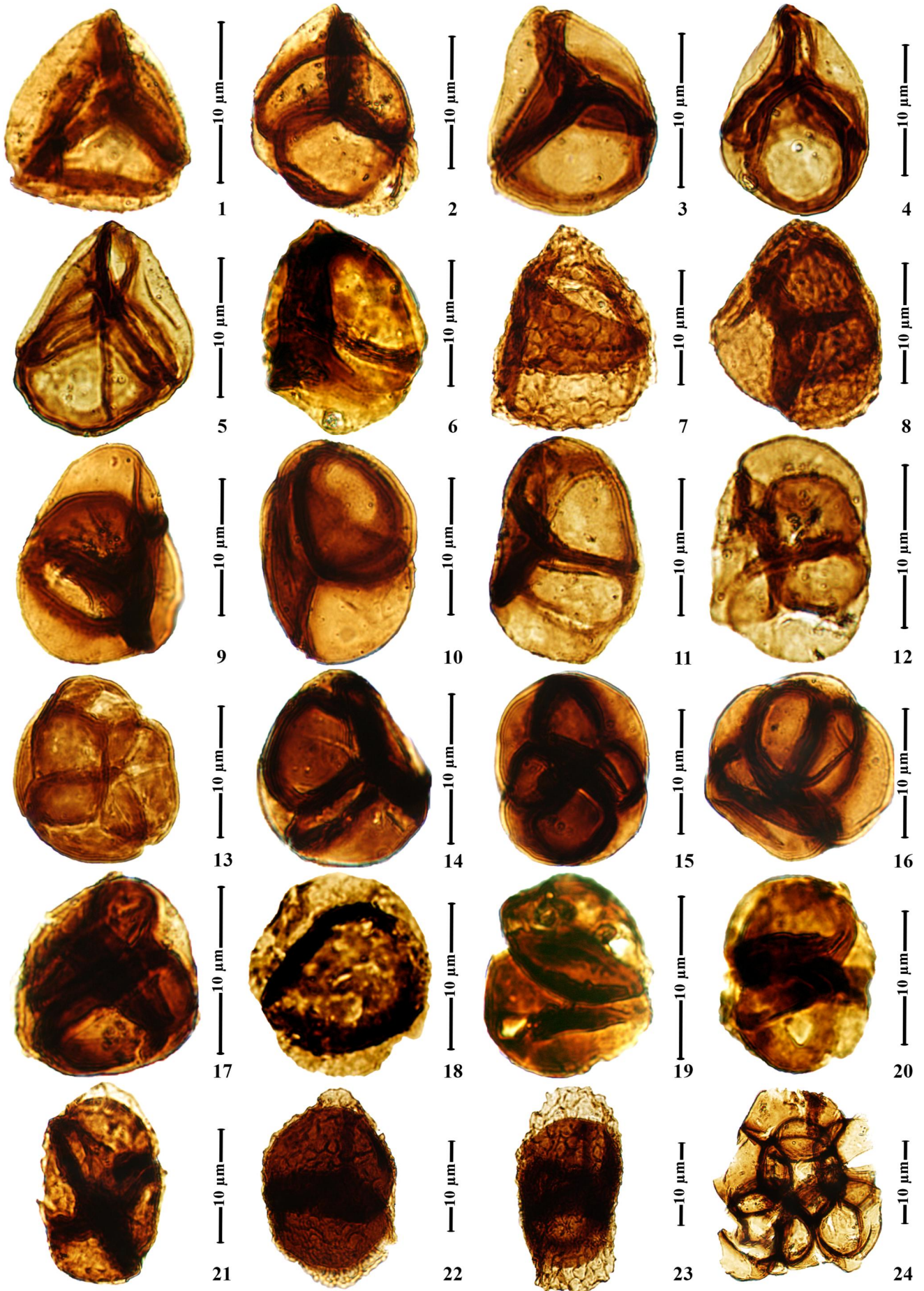
This biozone spans the entire range of *Spinachitina oulebsiri* (Paris et al. 2000b), from its FAD to the FAD of *Spinachitina fragilis* (Nestor 1980), the succeeding index species in the North Gondwana Domain (Paris 1990; Webby et al. 2004; Videt et al. 2010). In this study, *S. oulebsiri* (Plate 14, figures 1, 5; 2, 6; 3, 7; 4, 8) occurs throughout the MG-80 to MG-88 interval of the Ghelli Formation, spanning 246 m of alternating olive-grey shale and silty sandstone in the study area (Figure 5; Supplementary data, S5). Researchers first identified the *Spinachitina oulebsiri* biozone in the Upper Member of the M'Kratta Formation, north-east Algerian Sahara, Borj Nili area (Paris et al. 2000b), correlating it indirectly with the *Normalograptus persculptus* graptolite zone of the latest Hirnantian (Paris 1990 in Webby et al. 2004; Bergström et al. 2009). Subsequent records include the Late Ordovician–Early Silurian of northern Chad (Le Hérisse et al. 2013), the Hirnantian Sahara ice sheet (Le Heron and Craig 2008), Libya (Abuhmida 2013), Turkey (Steevens et al. 1996; Paris et al. 2007), and Iran (Ghavidel-Syooki 2008; Ghavidel-Syooki et al. 2011b; Ghavidel-Syooki 2017c, 2023; Ghavidel-Syooki and Borji 2018; Ghavidel-Syooki and Piri-Kangarshahi 2021). Co-occurring chitinozoan taxa in this biozone include *Rhabdochitina curvata* and *Tanuchitina anticostiensis*, which persisted from the preceding biozone into the *oulebsiri* biozone (Figure 5; Supplementary data, S5). *Spinachitina oulebsiri* has also been recorded from the latest Hirnantian to possibly the earliest Rhuddanian in the Soom Shale Member of the Cedarberg Formation, South Africa (Vandenbroucke et al. 2009); Hirnantian in the M'Kratta Formation (Well N1-2), north-east Algerian Sahara (Paris et al. 2000b); and the Hirnantian in the lower and upper members of the Second Bani Formation, Morocco (Bourahrouh et al. 2004). It also appears in the Zapla Formation, north-western Argentina (de la Puente 2009; de la Puente and Rubinstein 2013), and the Upper Member of the Salar del Rincon Formation, north-western Argentina (de la Puente et al. 2020). This biozone is crucial for defining the uppermost Ordovician and early Silurian in the Northern Gondwana Domain. However, Butcher (2009) questioned the taxonomic validity of *Spinachitina oulebsiri* and the biozone's utility, suggesting that *S. oulebsiri* might be a senior synonym of *Spinachitina fragilis* (Nestor 1980). Paris et al. (2000b) proposed that *S.*

oulebsiri could represent an early developmental stage of the *S. fragilis* lineage, with increased vesicle length, progressive differentiation of the flexure, and the development of a crown of spines, while the diameter remains stable. Vandenbroucke et al. (2009) acknowledged challenges in distinguishing the two species, particularly with poorly preserved specimens, but maintained the distinction based on subtle morphological differences. The presence of *Spinachitina oulebsiri* in the MG-80 to MG-88 interval of the Ghelli Formation suggests a latest Hirnantian age for the upper part of the formation, aligning with records from the Algerian Sahara (Paris et al. 2000b; Webby et al. 2004), Turkey (Steevens et al. 1996; Paris et al. 2007), South Africa (Vandenbroucke et al. 2009), and the Zapla Formation of Argentina (de la Puente 2009; de la Puente and Rubinstein 2013). Comparison with the chronostratigraphical chart of Videt et al. (2010) indicates that this biozone corresponds to the late Hirnantian stage slice Hi2 and the upper level of time slice VII in the Ghelli Formation at the Khoshyeilagh region, Alborz Mountains, northern Iran.

4.5. Biostratigraphy of cryptospores

Researchers widely acknowledge that bryophyte-like land plants appeared in parts of Gondwana by the mid-Ordovician period (Strother et al. 1996; Le Hérisse et al. 2007; Rubinstein et al. 2010, 2011). Discoveries of cryptospores in the Middle Ordovician Hanadir Shale Member of the Qasim Formation and the Dapingian section of the Sajir Member of the Saq Formation in the Arabian Peninsula (Vecoli and Cesari 2019) provide the earliest evidence of land plants. These cryptospores display morphological features similar to spores produced by some living liverworts (Gray 1985; Taylor 1995; Strother et al. 1996; Richardson 1996b; Steevens 2000; Wellman and Gray 2000; Wellman et al. 2003). Slightly older, though less diverse and poorly preserved, cryptospores with comparable morphologies were identified in north-west Argentina (Rubinstein et al. 2010). Vavrdová (1990) also found isolated specimens of smooth permanent tetrads and dyads from the Klabava Formation in Bohemia (Arenig–Llanvirn). Richardson (1996a, 1996b) thoroughly reviewed all major cryptospore morphological types, including monads, permanent dyads, and tetrads, and explored their stratigraphical importance. He outlined the evolutionary stages of early land vegetation based on morphological changes in terrestrial palynomorphs from the Ordovician to the Early Devonian periods. Richardson (1996b) introduced the 'pre-cryptospore' phase to describe the earliest Ordovician spore-like palynomorphs, such as *Virgatasporites* and *Attritasporites*, which might have come from freshwater algae or early terrestrial vegetation. Combaz (1967) initially classified these palynomorphs as 'spores'. Vecoli (2000, 2004) also explored

Plate 16. Figures 1–3; 5–7. *Rimosotetras problematica* Burgess 1991 (sample MG-55; seven specimens); Figures 4, 9, 14, 15. *Imperfectotrilletes patinatus* Steevens et al. 2000 (sample MG-83; seven specimens); Figures 10–12. *Tetraedraletes medinensis* (Strother and Traverse 1979) emend Wellman and Richardson 1993 (sample MG-40; five specimens); Figure 13. *Cryptotetras erugata* Strother et al. 2015 (sample MG-15; five specimens); Figure 16. *Segestrespora burgessii* Steevens et al. 1996 (sample MG-83; 1 three specimens). Figures 8, 17–20, 22–24. *Velatitetras retimembrana* (Miller and Eames) Steevens et al. 1996 (sample MG-47; nine specimens); Figure 21. *Velatitetras rugosa* (Strother and Traverse 1979) Steevens et al. 1996 (sample MG-70; four specimens).



the connection between Tremadocian sporomorph assemblages and palynofacies, indicating nearshore depositional environments with potential terrestrial sediment input. The presence of primitive land plants during the earliest Ordovician (Tremadocian) supports recent findings that suggest terrestrial flora may have been widespread since the Cambrian (Strother et al. 2004; Taylor and Strother 2008, 2009; Tomescu et al. 2009). Cryptospores preserved within sporangia have been reported from Caradoc-age sediments in the Hasirah Member of the Safiq Formation, Haima Supergroup of Oman (Wellman et al. 2003). In Iran, cryptospore records date back to the Late Cambrian (Furongian), with *Virgatasporites rudii* first recorded in the Ilebeyk Formation, High Zagros Mountains (Ghavidel-Syooki 2019). Later, researchers documented cryptospores from the Lower Ordovician Lashkarak Formation (Tremadocian–early Floian) in the eastern Alborz Mountains (Navidi-Izad et al. 2022), along with well-preserved cryptospores and trilete spores from the Upper Ordovician Ghelli Formation in the Alborz Mountains (Ghavidel-Syooki 2016) and Central Iran (Ghavidel-Syooki and Piri-Kangarshahi 2021). This study reports 15 species of cryptospores (in 10 genera), listed below.

4.5.1. *Tetraedraletes medinensis*–*Tetraedraletes grayae* assemblage biozone

The co-occurrence of *Tetraedraletes medinensis* (Strother and Traverse), Wellman and Richardson (1993), and *Tetraedraletes grayae* Strother (1991) defines this terrestrial assemblage biozone. This biozone appears in the basal part of the Ghelli Formation in the Khoshyeilagh region. It extends through the MG-6 to MG-44 interval, covering the study section's thickness of 314 m (Figure 6; Supplementary data, S6). *Tetraedraletes medinensis* (Plate 15, figures 14, 15; Plate 16, figures 10–12; Plate 17, figures 12, 13 and 15–17) occurs in the MG-6 to MG-44 interval of the Ghelli Formation in the study section of the Khoshyeilagh area. Researchers have recorded this species in various localities, including the Caradoc type section (Sandbian stage slices Sa1–Sa2 and time slices 5a–5b), Shropshire, England (Wellman and Richardson 1996); the Upper Ordovician at Hlásná Třebaň, Czechoslovakia (Vavrdová 1988); the Upper Ordovician (late Katian–Hirnantian stage slices Ka4–Hi2 and time slices VI–VII) in the Bedinan Formation, south-eastern Turkey (Stemans et al. 1996); the Ordovician/Silurian boundary in the upper member of the Salar del Rincon Formation, Puna region, north-west Argentina (Rubinstein and Vaccari 2004); the Hirnantian–Llandovery (*persculptus* graptolite biozone–*turriculatus* graptolite biozone) of south-west Wales (Burgess 1991); the latest Ashgillian or earliest Llandovery (Rhuddanian) in the Cedaberg Formation, South Africa; the

Upper Ordovician (Katian–Hirnantian stage slices Ka1–Hi2 and time slices VIa–VII) deposits of Anticosti Island, Québec, Canada, and Estonia (Vecoli et al. 2011); the Upper Ordovician (Hirnantian stage slices Hi1–Hi2 and time slice VII of Videt et al. 2010); the Upper Ordovician (Katian–Hirnantian stage slices Ka1–Hi2 and time slices VIa–VII) the Ghelli Formation at the type section of Kuh-e Saluk (Ghavidel-Syooki 2016) and Kuh-e Boghou, Central Iran (Ghavidel-Syooki and Piri-Kangarshahi 2021); the latest Ordovician (Hirnantian stage slices Hi1–Hi2 and time slice VII) the Qusaiba-1 borehole, Sarah Formation, the Arabian Peninsula (Wellman et al. 2015); and the late Middle Ordovician (Darriwilian stage slices Dw1–Dw3 and time slices 4a–4c) Hanadir Shale Member of the Qasim Formation, the Arabian Peninsula (Strother et al. 2015).

Tetraedraletes grayae (Plate 15, figures 16, 17; Plate 17, figure 24) also occurs in the MG-6 to MG-44 interval of the Ghelli Formation in the study section of the Khoshyeilagh area (Figure 6; Supplementary data, S6). Researchers have documented this taxon in various regions, including the Ashgillian (Katian–Hirnantian stage slices Ka1–Hi2 and time slices VIa–VII) Couches Fort Atkinson Dolomite, Maquoketa Group, Illinois, USA (Strother 1991); the Oostduinkerke borehole, Brabant Massif, Belgium (Stemans 2001); the Kosov Formation, Central Bohemia, Czech Republic; the Upper Ordovician (Katian–Hirnantian stage slices Ka1–Hi2 and time slices VIa–VII) strata of Anticosti Island, Québec, Canada (Vecoli et al. 2011); the late Middle Ordovician (Darriwilian stage slices Dw1–Dw3 and time slices 4a–4c) Hanadir Shale Member of the Qasim Formation, the Arabian Peninsula (Strother et al. 2015); and the Late Ordovician (Hirnantian stage slices Hi1–Hi2 and time slice VII) Ghelli Formation of the Khoshyeilagh area, the Alborz Mountains, northern Iran (Mahmoudi et al. 2014). *Cryptotetras erugata* (Plate 16, figure 13; Plate 17, figure 9) also occurs in MG-6 and continues into the subsequent biozones (Figure 6; Supplementary data, S6). Strother et al. (2015) initially documented this species from the Hanadir Shale Member of the Qasim Formation, the late Middle Ordovician (Darriwilian stage slices Dw1–Dw3 and time slices 4a–4b of Webby et al. 2004) on the Arabian Peninsula. Researchers have also recorded this taxon from the Upper Ordovician (Katian–Hirnantian stage slices Ka1–Hi2 and time slices VIa–VII) in the Ghelli Formation at its type locality in Kuh-e Saluk, the Alborz Mountains of northern Iran (Ghavidel-Syooki 2016), and from the same formation in Kuh-e Boghou, Central Iran (Ghavidel-Syooki and Piri-Kangarshahi 2021). In the current study, this cryptospore assemblage corresponds to the *Belonechitina robusta*, *Tanuchitina fistulosa*, and *Acanthochitina barbata* chitinozoan biozones, spanning Sandbian–Katian stage slices Sa1–Ka3 and time slices 5a–VIb.

←
Plate 17. Figures 1–5. *Tetraedraletes grayae* Strother 1991 (sample MG-11; seven specimens); Figure 6. *Velatitetras rugosa* (Strother and Traverse) Stemans et al. 1996 (sample MG-58; four specimens); Figures 7, 8. *Velatitetras retimembrana* (Miller and Eames) Stemans et al. 1996 sample MG-65; five specimens); Figure 9. *Cryptotetras erugata* Strother et al. 2015 (sample MG-29; five specimens); Figures 10, 11, 14. *Cheilotetras caledonica* Wellman and Richardson 1993 (sample MG-62; five specimens). Figure 18. *Segestrespora laevigata* Burgess 1991 (sample MG-87; three specimens); Figures 12–13, 15–17. *Tetraedraletes medinensis* (Strother and Traverse 1979) Wellman and Richardson 1993 (sample MG-22; five specimens); Figures 19–20. *Pseudodyadospora laevigata* Johnson 1985 (sample MG-45; 10 specimens); Figures 21–23. *Segestrespora membranifera* (Johnson) Burgess 1991 sample MG-82; nine specimens); Figure 24. Cluster of *Tetraedraletes grayae* Strother 1991 sample MG-38; five specimens).

4.5.2. *Rimosotetras problematica*–*Cheilotetras caledonica* assemblage biozone

The co-occurrence of *Rimosotetras problematica* Burgess (1991) and *Cheilotetras caledonica* Wellman (1993) defines this terrestrial assemblage biozone. This biozone immediately follows the preceding one and spans the MG-45 to MG-74 interval of the Ghelli Formation in the Khoshyeilagh region, covering a thickness of 242 m (Figure 6; Supplementary data, S6). *Rimosotetras problematica* (Plate 16, figures 1–3 and 5–7) occurs within the MG-45 to MG-74 interval of the Ghelli Formation. This taxon exhibits a long stratigraphical range from the Late Ordovician to Silurian (Richardson 1988; Burgess and Richardson 1991; Steemans et al. 1996; Wellman and Richardson 1996; Wellman and Gray 2000; Le Hérisse et al. 2001; Rubinstein and Vaccari 2004; Spina and Vecoli 2009; Vecoli et al. 2011). Additionally, records of this species span from the late Middle Ordovician (Darrivilian stage slices Dw1–Dw3 and time slices 4a–4c) in the Hanadir Shale Member of the Qasim Formation, the Arabian Peninsula (Strother et al. 2015), to the Early Devonian (Lochkovian) Tawil Formation in the Arabian Peninsula (Steenmans et al. 2007). Furthermore, *Rimosotetras problematica* has been documented in the Upper Ordovician (Hirnantian stage slices Hi1–Hi2 and time slice VII of Videt et al. 2010) from the Ghelli Formation in the Khoshyeilagh area, northern Iran (Mahmoudi et al. 2014); the Upper Ordovician (Katian–Hirnantian stage slices Ka1–Hi2 and time slices VIa–VII) in the Ghelli Formation at its type locality of Kuh-e Saluk (Ghavidel-Syooki 2016); and the Upper Ordovician (Katian–Hirnantian stage slices Ka1–Hi2 and time slices VIa–VII) from the Ghelli Formation of Kuh-e Boghou, Central Iran (Ghavidel-Syooki and Piri-Kangarshahi 2021). *Cheilotetras caledonica* (Plate 17, figures 10, 11, 14) is confined to the MG-45 to MG-74 interval of the Ghelli Formation in the Khoshyeilagh area (Figure 6; Supplementary data, S6). This species has been reported from post-Ordovician strata worldwide, ranging from Early–Late Silurian (Burgess and Richardson 1991; Wellman 1993; Molyneux et al. 1996; Wellman and Richardson 1996; Hagstrom 1997; Molyneux et al. 2007, 2008) to Early Devonian deposits (Burden et al. 2002; Steemans et al. 2007). Additionally, *Cheilotetras caledonica* has been documented in Upper Ordovician (Katian–Hirnantian stage slices Ka1–Hi2 and time slices VIa–VII) deposits in Canada and Estonia (Vecoli et al. 2011); the Upper Ordovician (Hirnantian stage slices Hi1–Hi2 and time slice VII) from the Ghelli Formation in the Khoshyeilagh area, northern Iran (Mahmoudi et al. 2014); and the Upper Ordovician (Katian–Hirnantian stage slices Ka1–Hi2 and time slices VIa–VII) from both the Ghelli Formation in Kuh-e Saluk (Ghavidel-Syooki 2016) and Kuh-e Boghou, Central Iran (Ghavidel-Syooki and Piri-Kangarshahi 2021). The associated cryptospore taxa in this biozone include *Velatitetras rugosa* (Strother and Traverse) Steemans et al. (1996), *Velatitetras retimembrana* (Miller and Eames) Steemans et al. (1996), *Abditusdyadus laevigatus* Wellman and Richardson (1996), and *Pseudodyadospora laevigata* Johnson (1985), each described below.

In the current study, *Velatitetras rugosa* (Plate 16, figure 21; Plate 17, figure 6) occurs within the MG-45 to MG-74

interval of the Ghelli Formation in the Khoshyeilagh area. Researchers have previously documented this taxon in various regions, including the Ashgillian (Hirnantian stage slices Hi1–Hi2 and time slice VII of Videt et al. 2010) in the Velleda Member of the Ellis Bay Formation, Anticosti Island, Québec, Canada (Richardson and Ausich 2007); the Caradocian–Ashgillian (Sandbian–Hirnantian stage slices Sa1–Hi2 and time slices 5a–VII) in the Bedinan Formation, Turkey (Steenmans et al. 1996); the Ashgillian (Katian–Hirnantian stage slices Ka1–Hi2 and time slices VIa–VII) in the Oostduinkerke borehole, Brabant Massif, Belgium (Steenmans 2001); the Ashgillian–Early Llandovery in Hlásná Třebaň, Czechoslovakia (Vavrdová 1988, 1989); the Early Llandovery (Rhuddanian) in Bronydd (Steenmans et al. 2000; Wellman et al. 2000); the Late Silurian–Early Devonian (Ludlow–Lochkovian) in the Tadrart Formation, Ghadamis basin, Tunisia (Spina and Vecoli 2009); Upper Ordovician (Katian–Hirnantian) strata of Canada and Estonia (Vecoli et al. 2011); and the Upper Ordovician (Sandbian–Hirnantian stage slices Sa1–Hi2 and time slices 5a–VII) in the Ghelli Formation of both North and Central Iranian basins (Ghavidel-Syooki 2016; Ghavidel-Syooki and Piri-Kangarshahi 2021).

Velatitetras retimembrana (Plate 15, figures 11, 22, 23; Plate 16, figures 8, 17, 18, 19, 20, 22, 23, 24; Plate 17, figures 7, 8) occurs throughout the MG-45 to MG-74 interval and extends into the succeeding cryptospore assemblage of the Ghelli Formation in the study section (Figure 6; Supplementary data, S6). Researchers have recorded this species in various locations, including the Late Ordovician (Sandbian–Hirnantian stage slices Sa1–Hi2 and time slices 5a–VII) in the Bedinan Formation, south-eastern Turkey (Steenmans et al. 1996); the Ashgillian–Llandovery in Wales, UK (Burgess 1991); the Llandovery (Rhuddanian–Aeronian) in Niagara Gorge, Lewiston, New York, USA (Miller and Eames 1982); the Llandovery (Rhuddanian) in Tuscarora, Central Pennsylvania, USA (Johnson 1985); the Ashgillian (Sandbian–Hirnantian stage slices Sa1–Hi2 and time slices 5a–VII) in the Drakes Formation, Ohio, USA (Gray 1988); the late Llandovery in the Jupiter Formation, Anticosti Island, Québec, Canada (Duffield 1985); the Llandovery (Rhuddanian–Aeronian) in north-east Libya (Richardson 1988); the Late Ordovician in the Kosov Formation, Hlásná Třebaň, Czech Republic (Vavrdová 1988, 1989); and the Late Ordovician (Sandbian–Hirnantian stage slices Sa1–Hi2 and time slices 5a–VII) in the Ghelli Formation of both North and Central Iranian basins (Ghavidel-Syooki 2016; Ghavidel-Syooki and Piri-Kangarshahi 2021).

Abditusdyadus laevigatus Wellman and Richardson (1996) (Plate 15, figures 1–8, 13, 20) occurs in the MG-45 to MG-74 interval of the Ghelli Formation and continues into the succeeding cryptospore assemblage (Figure 6; Supplementary data, S6). Researchers have recorded this taxon from various regions, including the Ashgillian (late Katian–Hirnantian stage slices Ka4–Hi2 and time slices VI d–VII) in the Oostduinkerke borehole, Brabant Massif, Belgium (Steenmans 2001); the Early Llandovery (Rhuddanian) in the Qusaiba Member of the Qalibah Formation, the Arabian Peninsula (Steenmans et al. 2000; Wellman and Gray 2000); the Upper Ordovician

(Katian–Hirnantian stage slices Ka1–Hi2 and Vla–VII) strata of Canada and Estonia (Vecoli et al. 2011); and the Upper Ordovician (Katian–Hirnantian stage slices Ka1–Hi2 and Vla–VII) in the Ghelli Formation of both North and Central Iranian basins (Ghavidel-Syooki 2016; Ghavidel-Syooki and Piri-Kangarshahi 2021).

Pseudodyadospora laevigata Johnson (1985) (Plate 17, figures 19, 20) occurs within the MG-45 to MG-74 interval of the Ghelli Formation and persists into the succeeding cryptospore assemblage (Figure 6; Supplementary data, S6). Researchers have recorded *Pseudodyadospora laevigata* from various locations, including the Ashgillian–early Llandovery in the Kosov Formation, Hlásná Třebaň, Czech Republic (Vavrdová 1974, 1988, 1989); the Ashgillian in the Kalpintag Formation, Southern Xinjiang, China (Wang et al. 1997); the early Llandovery (Rhuddanian) in the Qusaiba Member of the Qalibah Formation, Arabian Peninsula (Stemans et al. 2000; Wellman and Gray 2000); the Ordovician and Silurian in the Bedinan Formation, south-eastern Turkey (Stemans et al. 1996); the Hirnantian stage slices Hi1–Hi2 (time slice VII) in the Velleda Member of the Ellis Bay Formation, Anticosti Island, Québec, Canada (Richardson and Ausich 2007); the Upper Ordovician–Early Silurian in the Arabian Peninsula (Wellman et al. 2015); and the Upper Ordovician (Katian–Hirnantian stage slices Ka1–Hi2 and time slices Vla–VII) in the Ghelli Formation of both North and Central Iranian basins (Ghavidel-Syooki 2016; Ghavidel-Syooki and Piri-Kangarshahi 2021). In the present material, this cryptospore assemblage corresponds to the *Armoricochitina nigerica* and *Ancyrochitina merga* chitinozoan biozones, spanning Katian stage slice Ka4 and time slices VIc–VIId.

4.5.3. *Segestrespora burgessii*–*Segestrespora laevigata* assemblage biozone

Segestrespora burgessii Stemans et al. (1996) and *Segestrespora laevigata* Burgess (1991) define this terrestrial assemblage biozone. This biozone occurs in the upper part of the Ghelli Formation in the Khoshyeilagh region, spanning the MG-75 to MG-88 interval and covering 355 m of the study section (Figure 6; Supplementary data, S6). *Segestrespora burgessii* (Plate 16, figure 16) occurs between the MG-75 and MG-88 intervals of the Ghelli Formation in the Khoshyeilagh region (Figure 6; Supplementary data, S6). Other records of this taxon include the latest Ashgillian (Hirnantian) to earliest Silurian (Rhuddanian) in the Scach to Bronydd Formation, type Llandovery area, south-western Wales, UK (Burgess 1991); the Late Ordovician (Sandbian–Hirnantian stage slices Sa1–Hi2 and time slices 5a1 to VII) in the Bedinan Formation, south-eastern Turkey (Stemans et al. 1996); and the Upper Ordovician (Hirnantian stage slices Hi1–Hi2 and time slice VII) in the Ghelli Formation of both North and Central Iranian basins (Ghavidel-Syooki 2016; Ghavidel-Syooki and Piri-Kangarshahi 2021). This study identifies *Segestrespora laevigata* Burgess (Plate 17, figure 18) within the MG-75 to MG-88 interval of the Ghelli Formation in the study area (Figure 6; Supplementary data, S6). Researchers have reported this species from several regions, including the Late Ordovician (Sandbian–Hirnantian stage

slices Sa1–VII and time slices 5a–VII) of the Bedinan Formation, south-eastern Turkey (Stemans et al. 1996); the Ashgillian (Katian–Hirnantian stage slices Ka1–Hi2 and time slices Vla–VII) from the Oostduinkerke borehole, Brabant Massif, Belgium (Stemans 2001); the latest Ashgillian (Hirnantian) to earliest Silurian (Rhuddanian) in the Scach to Bronydd Formation, Llandovery area, south-western Wales, UK (Burgess 1991); the Early Silurian (Llandovery) of the Qusaiba Member, Qalibah Formation, the Arabian Peninsula (Stemans et al. 2000; Wellman et al. 2000); the Upper Ordovician to lowermost Silurian from Qusaiba-1, Qasim region, Central Arabian Peninsula (Wellman et al. 2015); in the Upper Ordovician (Katian–Hirnantian) on Anticosti Island, Québec, Canada, and in Estonia (Vecoli et al. 2011); and the Upper Ordovician (Hirnantian stage slices Hi1–Hi2 and time slice VII) from the Ghelli Formation in both North and Central Iranian basins (Ghavidel-Syooki 2016; Ghavidel-Syooki and Piri-Kangarshahi 2021). Along with some cryptospore taxa that extend from the preceding assemblage biozones, the associated cryptospore taxa include *Segestrespora membranifera* (Johnson 1985) Burgess (1991), *Dyadospora asymmetrica* Ghavidel-Syooki (2017a), *Dyadospora ferdowsii* Ghavidel-Syooki and Piri-Kangarshahi (2021), and *Imperfectotriletes patinatus* Stemans et al. (2000), each described below.

Segestrespora membranifera (Plate 15, figures 10, 24; Plate 17, figures 21–23) occurs in the MG-75 to MG-88 interval of the Ghelli Formation in the study area (Figure 6; Supplementary data, S6). This taxon is widely distributed geographically and ranges from the Upper Ordovician to the Lower Silurian (Llandovery). Records of *Segestrespora membranifera* include its occurrence in the Late Ordovician (Sandbian–Hirnantian stage slices Sa1–Hi2 and time slices 5a–VII) of the Bedinan Formation, south-eastern Turkey (Stemans et al. 1996) and the Ashgillian (Katian–Hirnantian stage slices Ka1–Hi2 and time slices Vla–VII) of the Oostduinkerke borehole, Brabant Massif, Belgium (Stemans 2001). It also appears in the latest Ashgillian (Hirnantian)–earliest Silurian (Rhuddanian) in the Scach to Bronydd Formation, Ashgillian–Early Silurian (Rhuddanian) type Llandovery area, south-western Wales, UK, within the *persculptus–acinaces* graptolite biozone (Burgess 1991). Additional records include the Ashgillian (Katian–Hirnantian stage slices Ka1–Hi2 and time slices Vla–VII) in the Kosov Formation, bohemicus graptolite biozone, Czechoslovakia (Vavrdová 1989), the Early Silurian (Llandovery) in the Qusaiba Member of the Qalibah Formation, Arabian Peninsula (Stemans et al. 2000; Wellman et al. 2000), and the Upper Ordovician to lowermost Silurian of Qusaiba-1, Qasim region, Central Arabian Peninsula (Wellman et al. 2015). Further occurrences are documented in the Upper Ordovician (Katian–Hirnantian stage slices Ka1–Hi2 and time slices Vla–VII) in Libya (Abuhmida 2013) and the Salar del Rincón Formation, Puna Region, Argentina (Rubinstein and Vaccari 2004). Additionally, records exist from the Upper Ordovician (Katian–Hirnantian stage slices Ka1–Hi2 and time slices Vla–VII) on Anticosti Island, Québec, Canada, and Estonia (Vecoli et al. 2011), as well as from the Ghelli

Formation at its type locality in Kuh-e Saluk, Alborz Mountains (Ghavidel-Syooki 2016) and at Kuh-e Boghou, Central Iranian basin (Ghavidel-Syooki and Piri-Kangarshahi 2021).

Dyadospora asymmetrica (Plate 15, figure 12) also occurs within MG-75 to MG-88 of the Ghelli Formation in the Khoshyeilagh region (Figure 6; Supplementary data, S6). Ghavidel-Syooki (2016) primarily documented this taxon from the Upper Ordovician (Sandbian–Hirnantian stage slices Sa1–Hi2 and time slices 5a–VII) in the Ghelli Formation at Kuh-e Saluk within the Alborz Mountains of north-eastern Iran and at Kuh-e Boghou in the central Iranian basin (Ghavidel-Syooki and Piri-Kangarshahi 2021). *Dyadospora ferdowsii* (Plate 15, figure 21) appears within the MG-75 to MG-88 interval of the Ghelli Formation in the study area (Figure 6; Supplementary data, S6). Ghavidel-Syooki and Piri-Kangarshahi (2021) primarily described this species from the Upper Ordovician (Katian–Hirnantian stage slices Ka1–Hi2 and time slices VIa–VII) in the Ghelli Formation at Kuh-e Boghou in the central Iranian basin.

Imperfectotriletes patinatus (Plate 15, figures 18, 19; Plate 16, figures 4, 9, 14, 15) occurs within the MG-75 to MG-88 interval of the Ghelli Formation in the Khoshyeilagh area (Figure 6; Supplementary data, S6). Various studies have recorded this species, including from the Ashgillian (Katian–Hirnantian stage slices Ka1–Hi2, and time slices VIa–VII) in the Oostduinkerke borehole, Brabant Massif, Belgium (Stemans 2001); the Upper Ordovician and Lowermost Silurian of the Qusaiba-1 shallow-core hole in the Qasim region, Central Arabian Peninsula (Wellman et al. 2015); and the Ashgillian (Katian–Hirnantian stage slices Ka1–Hi2, and time slices VIa–VII) in the Ghelli Formation at Kuh-e Saluk in the Alborz Mountains of north-eastern Iran and Kuh-e Boghou in the central Iranian basin (Ghavidel-Syooki and Piri-Kangarshahi 2021). In the current study, this cryptospore assemblage biozone corresponds to the *Tanuchitina elongata* and *Spinachitina oulebsiri* chitinozoan biozones, spanning the Hirnantian stage slices Hi1–Hi2 and time slice VII of Videt et al. (2010).

5. Palaeobiogeography

Early–Late Ordovician acritarch and chitinozoan taxa exhibit distinct provincialism globally, defined by two major microfloral and microfaunal realms, including the Peri-Gondwana (Peri-Antarctica) and Baltic palaeo-provinces (Vavrdová 1972; Colbath 1990; Ghavidel-Syooki 1990, 1995, 1997; Molyneux et al. 2013). Various palaeoenvironmental factors, such as water temperature and oceanic currents, likely influenced this provincialism (Tongiorgi et al. 1995; Molyneux et al. 2013; Servais et al. 2014). As a result, chronostratigraphical divisions for the Mediterranean and North Gondwana regions follow the framework of Bergström et al. (2009). Servais et al. (2018) clarified that ‘North Gondwana’ refers to parts of the Palaeozoic Gondwana continent that are now in the most northerly positions. However, these areas lay at high southern palaeolatitudes along Gondwana’s subpolar margin during the early Palaeozoic Era. According to Ordovician

palaeogeography reconstructions by Torsvik and Cocks (2017) and the terminology of Servais et al. (2018), the term ‘southern Gondwana’ refers to regions between approximately 60°S and the Ordovician South Pole. These regions mainly include North Africa and parts of the Armorican Terrane Assemblage, such as Bohemia, Saxothuringia, and Iberia. In contrast, the term ‘western Gondwana’ applies to the Arabian Peninsula, Iran, Pakistan, and Western Australia (Figure 7). Meanwhile, ‘eastern Gondwana’ encompasses areas on the opposite margin of the palaeocontinent, with data primarily available from north-western Argentina and Colombia. Additionally, during the Early and Middle Ordovician, South China was a distinct entity located next to the western margin of Gondwana, as depicted in Torsvik and Cocks’ reconstructions (2016, fig. 6.1). This study focuses on the Lower Palaeozoic rock units, including the Lalun, Mila, Lashkarak, and Ghelli formations in the Khoshyeilagh region within the Alborz Mountains, northern Iran. Due to their lithologies, the Lalun, Mila, and Lashkarak formations lack organic-wall microfossils, while the Ghelli Formation contains well-preserved and abundant palynomorphs. The current analysis identified 55 acritarch taxa, which define six acritarch assemblage biozones. In ascending stratigraphical order, these are: *Acanthodiacrodium crassus*–*Baltisphaeridium accinctum* (*A. crassus*–*B. accinctum*), *Ordoviciidium elegantulum*–*Orthosphaeridium ternatum* (*O. elegantulum*–*O. ternatum*), *Baltisphaeridium perclarum*–*Baltisphaeridium oligopsakium* (*B. perclarum*–*B. oligopsakium*), *Inflatarium trilobatum*–*Dactylofusa platynetrella* (*I. trilobatum*–*D. platynetrella*), *Poikilofusa pinata*–*Dorsennidium hamii* (*P. pinata*–*D. hamii*) and *Speculaforma delicata*–*Safirotheca safira* (*S. delicata*–*S. safira*). The *A. crassus*–*B. accinctum* biozone appears in the lowermost part of the Ghelli Formation. Its acritarch taxa have been recorded in Laurentia, Baltica, and Peri-Gondwana (Loeblich and Tappan 1978; Playford and Wicander 2006; Ghavidel-Syooki 2017c; Ghavidel-Syooki and Piri-Kangarshahi 2021, 2024; Rubinstein and Vajda 2023). This biozone corresponds to the Sandbian stage slices Sa1–Sa2 and time slices 5a–5b, marking the first interval of the Ghelli Formation in the Khoshyeilagh area. The *O. elegantulum*–*O. ternatum* biozone immediately follows the preceding biozone. Its acritarch taxa have been recorded in Laurentia, Baltica, and Peri-Gondwana (Loeblich and Tappan 1978; Miller 1991; Vecoli 1999; Le Hérisse et al. 2015; Ghavidel-Syooki 2016, 2017c; Ghavidel-Syooki and Piri-Kangarshahi 2021, 2024; Rubinstein and Vajda 2023). This biozone corresponds to the early Katian stage slice Ka1 (time slice VIa), marking the second interval of the Ghelli Formation in the study area. After the *O. elegantulum*–*O. ternatum* biozone, the *B. perclarum*–*B. oligopsakium* biozone appears in the Ghelli Formation. Its acritarch species have been recorded in Laurentia, Baltica, Avalonia, China, and Peri-Gondwana (Tappan and Loeblich 1971; Loeblich and Tappan 1978; Turner 1984; Jacobson and Achab 1985; Jachowicz 1995; Vecoli 1999, 2000; Le Hérisse et al. 2013; Ghavidel-Syooki and Piri-Kangarshahi 2021, 2024; Rubinstein and Vajda 2023). This biozone corresponds to the mid-Katian stage slices Ka2–Ka3 (time slice VIb of Videt et al. 2010), marking the third interval of the Ghelli Formation.

Following the *B. perclarum*-*B. oligopsakium* biozone, the *I. trilobatum*-*D. platynetrella* biozone and associated acritarch taxa emerge in the Ghelli Formation. Its acritarch taxa have been recorded in Laurentia, Baltica, Avalonia, and Peri-Gondwana (Loeblich and Tappan 1978; Jacobson and Achab 1985; Vecoli 1999; Le Hérisse et al. 2015; Ghavidel-Syooki and Piri-Kangarshahi 2021, 2024). This biozone corresponds to the late Katian stage slice Ka4 (time slice VIc), marking the fourth interval of the Ghelli Formation in the Khoshyeilagh region. After the *I. trilobatum*-*D. platynetrella* biozone in the Ghelli Formation, the *P. spinata*-*D. hamii* biozone and associated acritarch species appear. Its acritarch taxa have been recorded in Laurentia, Baltica, and Peri-Gondwana (Wright and Meyers 1981; Jacobson and Achab 1985; Elaouad-Debbaj 1988; Vavrdová 1988; Eiserhardt 1992; Wicander et al. 1999; Ghavidel-Syooki and Hoseinzadeh-Moghadam 2005; Playford and Wicander 2006; Le Hérisse et al. 2015; Ghavidel-Syooki and Piri-Kangarshahi 2021). This biozone corresponds to the late Katian stage slice Ka4 (time slice VIId), marking the fifth interval of the Ghelli Formation in the current dataset. Following the *P. spinata*-*D. hamii* biozone, the *S. delicata*-*S. safira* biozone appears in the upper part of the Ghelli Formation. This biozone and associated acritarch taxa have been recorded in Laurentia and Peri-Gondwana (Vavrdová 1988, 1989; Ghavidel-Syooki 2000; Le Hérisse et al. 2015; Miller et al. 2017; Ghavidel-Syooki 2017c; Ghavidel-Syooki and Piri-Kangarshahi 2021). This biozone correlates with the Hirnantian stage slices Hi1-Hi2 and time slice VII, marking the final interval of the Ghelli Formation in the Khoshyeilagh area.

Also, 48 chitinozoan taxa were identified and helped to delineate seven chitinozoan biozones, spanning *Belonechitina robusta*, *Tanuchitina fistulosa*, *Acanthochitina barbata*, *Armoricochitina nigerica*, *Ancyrochitina merga*, *Tanuchitina elongata*, and *Spinachitina oulebsiri*, each described below in ascending stratigraphical order. *Belonechitina robusta* appears in the lowermost part of the Ghelli Formation in the Khoshyeilagh region. The *robusta* biozone corresponds to the partial range of this taxon from its FAD to the FAD of *Tanuchitina fistulosa*. The *robusta* biozone indicates the Sandbian stage slices Sa1-Sa2 (time slices 5a-5b) in the North Gondwana Terrane. Following *B. robusta* in the Ghelli Formation at the Khoshyeilagh locality, *Tanuchitina fistulosa* emerges. This biozone corresponds to the partial range of *Tanuchitina fistulosa*, spanning from its FAD to the FAD of *Acanthochitina barbata*. *Tanuchitina fistulosa* has been documented in the early Katian stage slice Ka1 (time slice VIa). After *T. fistulosa* in the Ghelli Formation at the Khoshyeilagh site, *Acanthochitina barbata* appears. This biozone corresponds to the total range of *Acanthochitina barbata*. It spans from its FAD to the FAD of *Armoricochitina nigerica* (Bouché 1965), the succeeding index species in the North Gondwana Domain. *Acanthochitina barbata* is an index microfossil for the early Ashgillian (Pusgillian), or the middle Katian stage slices Ka2-Ka3 (time slice of VIb) in the North Gondwana Domain. Following *A. barbata* in the Ghelli Formation at the Khoshyeilagh area, *Armoricochitina nigerica* emerges. This biozone corresponds to the partial range biozone of

Armoricochitina nigerica, extending from its FAD to the FAD of *Ancyrochitina merga*, the succeeding index species in the North Gondwana. The *A. nigerica* biozone has been documented within the late Katian stage slice Ka4 (time slice VIc). *Armoricochitina nigerica* is a pivotal chitinozoan species, delineating the northern Gondwanan high palaeoplate during the Late Ordovician. Its absence from records in the UK and Belgium suggests that it did not spread to the north of the margin of the Rheic Ocean (Paris et al. 2015). After *A. nigerica* in the Ghelli Formation at the Khoshyeilagh locality, *Ancyrochitina merga* appears. This biozone corresponds to the total range biozone of *Ancyrochitina merga*, extending from its FAD to the FAD of *Tanuchitina elongata*, the succeeding index species in the North Gondwana Domain. The *A. merga* biozone has been documented within the late Katian stage slice Ka4 (time slice VIId). Following *A. merga* in the Ghelli Formation in the Khoshyeilagh site, *Tanuchitina elongata* appears. This biozone corresponds to the partial range biozone *Tanuchitina elongata*, extending from its FAD to the FAD of *Spinachitina oulebsiri*, the succeeding index taxon in the North Gondwana Domain. The *T. elongata* biozone has been documented within the early Hirnantian stage slice Hi1 (lower level of time slice VII). After *T. elongata* in the Ghelli Formation at the Khoshyeilagh region, *Spinachitina oulebsiri* appears. This biozone corresponds to the total range of *Spinachitina oulebsiri* extending from its FAD to the FAD of *Spinachitina fragilis*, the index species succeeding biozone in the North Gondwana Domain. The *S. oulebsiri* biozone has been documented within the late Hirnantian stage slice Hi2 (upper level of time slice VII).

In the current study, I also identified 15 cryptospore taxa and delineated three associated assemblage biozones. These are, in ascending stratigraphical order, *Tetraedraletes medinensis*-*Tetraedraletes grayae* (*T. medinensis*-*T. grayae*), *Rimosotetras problematica*-*Cheilotetras caledonica* (*R. problematica*-*C. caledonica*), and *Segestrespora burgessii*-*Segestrespora laevigata* (*S. burgessii*-*S. laevigata*).

The *T. medinensis*-*T. grayae* biozone emerges at the base of the Ghelli Formation, extending over 314 m. Researchers have recorded cryptospore taxa of this biozone in Laurentia, Baltica, Avalonia, and Peri-Gondwana (Burgess 1991; Strother 1991; Wellman and Richardson 1996; Rubinstein and Vaccari 2004; Vecoli et al. 2011; Strother et al. 2015; Ghavidel-Syooki 2016, 2017c; Ghavidel-Syooki and Piri-Kangarshahi 2021). This terrestrial cryptospore biozone correlates with the *B. robusta* and *T. fistulosa* biozones, and with the lower part of the *A. barbata* biozone, corresponding to the Sandbian-Katian stage slices 5a-Ka3 and time slices 5a-VIb for this thickness of the study section in the Khoshyeilagh area.

Following the *T. medinensis*-*T. grayae* biozone in the Ghelli Formation, the *R. problematica*-*C. caledonica* biozone appears, covering 242 m. Researchers have documented the terrestrial cryptospores of this biozone in Laurentia, Avalonia, Baltica, and Peri-Gondwana (Richardson 1988; Burgess and Richardson 1991; Strother 1991; Steemans et al. 1996; Wellman and Richardson 1996; Wellman et al. 2000; Le Hérisse et al. 2001; Rubinstein and Vaccari 2004; Spina and Vecoli 2009; Vecoli et al. 2011; Strother et al. 2015; Ghavidel-

Syooki 2016, 2017c; Ghavidel-Syooki and Piri-Kangarshahi 2021). In this study, the cryptospore assemblage biozone corresponds to the *Armoricochitina nigerica* and *Ancyrochitina merga* chitinozoan biozones, spanning Katian stage slice Ka4 and time slices VIc–VIId for this thickness of the Ghelli Formation.

After the *R. problematica*–*C. caledonica* biozone in the Ghelli Formation, the *S. burgessii*–*S. laevigata* biozone emerges, covering 355 m. Cryptospore elements of this biozone have been recorded in the Laurentia, Avalonia, Baltica, and Peri-Gondwana (Burgess 1991; Steemans et al. 1996; Vavrdová 1997; Vecoli et al. 2011; Strother et al. 2015; Ghavidel-Syooki 2017c; Ghavidel-Syooki and Piri-Kangarshahi 2021). This cryptospore assemblage biozone correlates with the *Tanuchitina elongata* and *Spinachitina oulebsiri* chitinozoan biozones, including the Hirnantian stage slices Hi1–Hi2 and time slice VII for this interval of the Ghelli Formation in the study section of the Khoshyeilagh area.

6. Conclusions

Palynological analysis of the Lower Palaeozoic rock units (Lalun, Mila, Lashkarak, and Ghelli formations) in the Khoshyeilagh region of the Alborz Mountains, northern Iran, provided valuable insights into the geological and palaeontological characteristics of the study section. This analysis encountered acritarchs, chitinozoans, cryptospores, scolecodonts, and graptolite remains. I identified 118 distinct taxa, including 55 species of acritarchs (28 genera), 48 species of chitinozoans (18 genera), and 15 cryptospores (10 genera). Although scolecodonts and graptolite remains were observed, they were not studied in detail.

The analysis revealed no palynomorphs in the Lalun, Mila, and Lashkarak formations, likely due to red sediments, while the Ghelli Formation contained well-preserved and abundant organic-walled microfossils. Strata older than the upper part of the Ghelli Formation have not been reported from the Khoshyeilagh anticline. Consequently, this study records the lower and middle parts of the Ghelli Formation and the Lalun, Mila (top quartzite member), and Lashkarak formations for the first time in the Khoshyeilagh locality. Precise dating of the section was achieved by identifying acritarchs, chitinozoans, and cryptospores. This study established six acritarch assemblage biozones, seven chitinozoan biozones, and three cryptospore assemblage biozones. Acritarch biozones 1–6 (as numbered in Figure 4) span the siliciclastics of members 1 and 3 of the Ghelli Formation, corresponding to the Sandbian–Hirnantian stage slices Sa1–Hi2 (time slices 5a–VII). Similarly, chitinozoan biozones 1–7 are present in these members, covering the same stages and time slices. Cryptospore biozones 1–3 also occur within these members, aligning with the acritarch and chitinozoan biozones. The study documented 10 new acritarch taxa and five new chitinozoan species, which were discussed in the systematic sections of the article. The identification of well-known chitinozoan taxa, such as *Belonechitina robusta*, *Tanuchitina fistulosa*, *Acanthochitina barbata*, *Armoricochitina nigerica*, *Ancyrochitina merga*, *Tanuchitina elongata*, and *Spinachitina*

oulebsiri, led to the establishment of seven chitinozoan biozones. These taxa are classical components of the Northern Gondwana Domain/Peri-Gondwana palaeoprovince. The presence of these chitinozoan biozones in the Ghelli Formation confirms that the study area was located at a high southern latitude (50–60°S) along the subpolar margin of the Northern Gondwana Domain during the Late Ordovician. Likewise, the dominance of *Dactylofusa* species (e.g. *D. cucurbita* and *D. striata*), *Safirotheca safira*, and *Neoveryhachium* species in the Ghelli Formation confirm the attribution of the Khoshyeilagh region to the Peri-Gondwana province. Two distinct hiatuses occur within the Lower Palaeozoic strata in the Khoshyeilagh area. The first hiatus is between the top quartzite Member of the Mila Formation and the Lashkarak Formation, corresponding to the absence of four other carbonate members of the Mila Formation, spanning the Middle to Late Cambrian. The second hiatus lies between the Ghelli Formation and the Soltan Meidan Basalt Complex (SMBC), covering the Early to Middle Silurian.

Acknowledgements

I express my sincere gratitude to Dr Jim Riding, Chief Editor of *Palynology*, Dr Anthony Butcher (University of Portsmouth, UK), and the anonymous reviewers for their invaluable comments and suggestions, greatly enhancing this manuscript. Special thanks to Dr Roohollah Memarzadeh for his assistance during the fieldwork. I also appreciate the unwavering encouragement of my wife, Fahimeh Ghaemi-Nejad, and my daughters, Hedieh and Mona Ghavidel-Syooki, whose support was pivotal in completing this work. It is important to note that no specific grant from any public, commercial, or not-for-profit funding agencies supported this research.

Disclosure statement

No potential conflict of interest was reported by the author.

References

- Abuhmida F. 2013. Palynological analysis of the Ordovician to Lower Silurian sediments from the Murzuq Basin, southwest Libya [PhD thesis]. Sheffield (UK): University of Sheffield.
- Achab A. 1977. Les chitinozoaires de la zone à *Dicellograptus complanatus* Formation de Vauréal, Ordovicien supérieur, Ile d'Anticosti, Québec. *Canadian Journal of Earth Sciences*. 14(3):413–425.
- Achab A. 1978. Les chitinozoaires de l'Ordovicien supérieur, Formations de Vauréal et d'Ellis Bay de l'Ile d'Anticosti, Québec. *Palinologia*. 1:1–19.
- Achab A. 1983. Chitinozoaires du Llanvirn (Formation de Table Head) de la partie occidentale de Terre-Neuve, Canada. *Canadian Journal of Earth Sciences*. 20(6):918–931.
- Achab A. 1984. Chitinozoaires de l'Ordovicien moyen de subsurface de l'Ile d'Anticosti. Review of Palaeobotany and Palynology. 43(1-3): 123–143.
- Achab A. 1986. Succession des assemblages de chitinozoaires dans l'Ordovicien moyen du Québec et de l'est du Canada. Review of Palaeobotany and Palynology. 48(1-3):269–294.
- Achab A, Asselin E. 1995. Ordovician chitinozoans from the Arctic Platform and the Franklinian miogeosyncline in northern Canada. Review of Palaeobotany and Palynology. 86(1-2):69–90.
- Afshar-Harb A. 1975. The stratigraphy, tectonic, and petroleum geology of Kopet-Dagh region, northern Iran [PhD thesis]. Imperial College London: Petroleum Geology Section of Royal School of Mines.

- Afshar-Harb A. 1994. Geology of the Kopet Dagh region. In: Treatise on the geology of Iran. Tehran: Geological Survey of Iran; Vol. 11; p. 275.
- Al-Ameri TK. 2010. Palynostratigraphy and the assessment of gas and oil generation and accumulations in the Lower Paleozoic, Western Iraq. *Arabian Journal of Geosciences*. 3(2):155–179.
- Albani R, Bagnoli G, Maletz J, Stouge S. 2001. Integrated chitinozoan, conodont, and graptolite biostratigraphy from the upper part of the Cape Cormorant Formation (Middle Ordovician), western Newfoundland. *Canadian Journal of Earth Sciences*. 38(3):387–409.
- Al-Hajri S. 1995. Biostratigraphy of the Ordovician chitinozoa of north-western Saudi Arabia. *Review of Palaeobotany and Palynology*. 89(1-2):27–48.
- Al-Shawareb A, Vecoli M, Miller M. 2017. Late Ordovician (Katian) chitinozoans from Northwest Saudi Arabia: biostratigraphic and paleoenvironmental implications. *Revue de Micropaléontologie*. 60(3):333–369.
- Barnes CR, Norford BS, Skevington D. 1981. The Ordovician System in Canada. Correlation Chart and Explanatory Notes. Vol. 8. China: IUGS, International Union of Geological Sciences; p. 1–27.
- Batten DJ. 1982. Palynofacies, palaeoenvironments, and petroleum. *Journal of Micropalaeontology*. 1(1):107–114.
- Bergström ST, Chen X, Gutiérrez-Marco JC, Dronov A. 2009. The new chronostratigraphic classification of the Ordovician System and its relations to major regional series and stages and $\delta^{13}\text{C}$ chemostratigraphy. *Lethaia*. 42(1):97–107.
- Booth GA. 1979. Lower Ordovician acritarchs from successions in England and North Wales [PhD thesis]. Sheffield (UK): The University of Sheffield; p. 1–469.
- Bouché PM. 1965. Chitinozoaires du Silurien s.1 du Djado (Sahara Nigérien). *Revue de Micropaléontologie*. 8:151–164.
- Bourahrouh A, Paris F, Elaouad-Debbaj Z. 2004. Biostratigraphy, biodiversity, and palaeoenvironments of the chitinozoa and associated palynomorphs from the Upper Ordovician of the Central Anti-Atlas, Morocco. *Review of Palaeobotany and Palynology*. 130(1-4):17–40.
- Bozorgnia F. 1973. Paleozoic foraminiferal biostratigraphy of Central and Eastern Alborz Mountain, Iran. Vol. 4. Iran, Tehran: National Iranian Oil Company, Geological Laboratories Publication; p. 185.
- Brocke R, Li J, Wang Y. 2000. Upper Arenigian to lower Llanvirnian acritarch assemblages from South China: a preliminary evaluation. *Review of Palaeobotany and Palynology*. 113(1-3):27–40.
- Burden ET, Quinn L, Nowlan GS, Bailey-Nill LA. 2002. Palynology and micropaleontology of the Clam Bank Formation (Lower Devonian) of Western Newfoundland, Canada. *Palynology*. 26(1):185–215.
- Burgess ND. 1991. Silurian cryptospores and miospores from the type Llandovery area, Southwest Wales. *Palaeontology*. 34:575–599.
- Burgess ND, Richardson JB. 1991. Silurian cryptospores and miospores from type Wenlock area Shropshire, England. *Palaeontology*. 34(part. 3):601–628 (2 pls.).
- Burmann G. 1970a. Weitere organische Mikrofossilien aus dem unteren Ordovizium. *Paläontologische Abhandlungen, Abteilung B*. 3:289–332.
- Burmann G. 1970b. New, revised, and reassigned species. *Palaeontographica Italica*. 86:117–153.
- Burmann G. 1976. *Äbersicht über das ordovizische Mikroplankton im Südteil der DDR (Vogtland, Wildenfelser Zwischengebirge)*. *Geologisches Jahrbuch*. 7-8:47–62.
- Butcher A. 2009. Early Llandovery chitinozoa from Jordan. *Palaeontology*. 52(3):593–629.
- Cocks LRM, Torsvik TH. 2002. Earth geology from 500 to 400 million years ago: a faunal and palaeomagnetic review. *Journal of the Geological Society*. 159(6):631–644.
- Cocks MRL, Verniers J. 1998. Applicability of planktonic and nektonic fossils to palaeogeographic reconstructions. *Acta Universitatis Carolinae, Geologica*. 42(3-4):399–400.
- Colbath GK. 1979. Organic-walled microphytoplankton from the Eden Shale (Upper Ordovician), Indiana, U.S.A. *Palaeontographica Abteilung B*. 171(1-3):1–38.
- Colbath GK. 1990. Devonian (Givetian-Frasnian) organic-walled phytoplankton from the Limestone Billy Hills reef complex, Canning Basin, Western Australia. *Palaeontographica Abteilung B*. 217(4-6):87–145.
- Combaz A. 1967. Une microbio du Trémadocien dans un sondage d' Hassi-Massaoud. *Acta de la Société, Linnéenne de Bordeaux*. 104: 1–26.
- Combaz A, Lange FW, Pansart J. 1967. Les “Leiofusidae” Eisenack, 1938. *Review of Palaeobotany and Palynology*. 1(1-4):291–307.
- Cramer FH. 1971. Distribution of selected Silurian acritarchs. *Revista Española de Micropaleontología: Número Extraordinario*. 1:1–203.
- Cramer FH, Díez MdCR. 1977. Late Arenigian (Ordovician) acritarchs from Cis-Saharan Morocco. *Micropaleontology*. 23(3):339–360.
- de la Puente GS. 2009. *Quitinozoos del Ordovícico de la Cuenca Andina central (Noroeste Argentino) y su aplicación a la bioestratigrafía, paleobiogeografía paleoambientes* [doctoral thesis]. University of Córdoba; p. 246 (unpublished).
- de la Puente GS, Rubinstein CV. 2013. Ordovician chitinozoans and marine phytoplankton of the Central Andean Basin, northwestern Argentina: a biostratigraphic and paleogeographic approach. *Review of Palaeobotany and Palynology*. 198:14–26.
- de la Puente GS, Paris F, Vaccari NE. 2020. Latest Ordovician–earliest Silurian chitinozoans from the Puna region, northwestern Argentina. *Bulletin of Geosciences*. 95(4):1–28.
- Dean WT, Martin F. 1978. Lower Ordovician acritarchs and trilobites from Bell Island, eastern Newfoundland. *Geological Survey of Canada*. 284: 1–35.
- Deflandre G, Deflandre-Rigaud M. 1962. Nomenclature et systématique des hystrichosphères (sensu lato); observations et rectifications. *Revue de Micropaléontologie*. 4(4):190–196.
- Delabroye A, Munnecke A, Vecoli M, Copper P, Tribouvillard N, Joachimski MM, Desrochers A, Servais T. 2011. Phytoplankton dynamics across the Ordovician/Silurian boundary at low palaeolatitudes: correlations with carbon isotopic and glacial events. *Palaeogeography, Palaeoclimatology, Palaeoecology*. 312(1-2):79–97.
- Delabroye A, Vecoli M, Hints O, Servais T. 2011. Acritarchs from the Ordovician–Silurian boundary beds of the Valga–10 drill core, southern Estonia (Baltica) and their stratigraphical and palaeobiogeographical implications. *Palynology*. 35(1):4–45.
- Deunff J. 1954. *Veryhachium* genre nouveau d'Hystrichosphères du Primaire. *Compte Rendu Sommaire de la Société géologique de France*. 13:305–306.
- Deunff J. 1977. Un microplancton à Acritarches dans les schistes Llanvirniens de l'Anti-Atlas (Zagora Maroc). *Notes du Service Géologique du Maroc*. 38(268):141–151.
- Deunff J, Evitt WR. 1968. *Tunisphaeridium*, a new acritarch genus from the Silurian and Devonian. *Stanford University Publications Geological Sciences*. 12:1–13.
- Deunff J, Massa D. 1975. Palynologie et stratigraphie du Cambro-Ordovicien (Libye nord-occidentale). *Comptes Rendus de l'Académie des Seances de Paris*. 281:21–24.
- Downie C. 1963. 'Hystrichosphères' (acritarchs) and spores of the Wenlock Shales (Silurian) of Wenlock, England. *Palaeontology*. 6(4): 625–652.
- Downie C. 1984. Acritarchs in British stratigraphy. *Geological Society of London, Special Paper*. 17:1–26.
- Duffield SL. 1985. Land-derived microfossils from Jupiter Formation (Upper Llandoveryan) Anticosti Island, Quebec. *Journal of Paleontology*. 59:1005–1010.
- Eisenack A. 1931. Neue Mikrofossilien des Baltischen Silurs. I. *Paläontologische Zeitschrift*. 13(1-2):74–118.
- Eisenack A. 1934. Neue Mikrofossilien des baltischen Silurs. III. und neue Mikrofossilien des böhmischen Silurs. I. *Paläontologische Zeitschrift*. 16(1-2):52–76.
- Eisenack A. 1938. Hystrichosphären und verwandten Formen im baltischen Silur. *Geschiebeforsch*. 14(1):1–30.
- Eisenack A. 1939. Chitinozoen und Hystichosphaerideen im Ordovizium des Rheinischhen Schiefergebirges. *Senckenbergiana*. 21:135–152.
- Eisenack A. 1958. Mikroplankton aus dem norddeutschen Apt nebst einigen Bemerkungen über fossile Dinoflagellaten. *Neues Jahrbuch für Geologie und Paläontologie, Abhandlungen*. 106(3):383–422.
- Eisenack A. 1959. Neotypen baltischer Silur–Chitinozoen und neue Arten. *Neues Jahrbuch für Geologie und Paläontologie, Abhandlungen*. 108(1):1–20.

- Eisenack A. 1962. Neotypen baltischer Silur-Chitinozoen und neue Arten. *Neues Jahrbuch für Geologie und Paläontologie, Abhandlungen*. 114: 291–316.
- Eisenack A. 1963. Mitteilungen zur Biologie der Hystrichosphären und über neue Arten. *Neues Jahrbuch für Geologie und Paläontologie, Abhandlungen*. 118:207–216.
- Eisenack A. 1965. Die Mikrofauna der Ostseekalke. 1. Chitinozoen, Hystrichosphären. *Neues Jahrbuch für Geologie und Paläontologie, Abhandlungen*. 123(2):115–148.
- Eisenack A. 1968a. Mikrofossilien eines Geschiebes der Borkholmer Stufe, baltisches Ordovizium F2. Mitteilungen aus dem Geologischen Staatsinstitut in Hamburg. 37:81–94.
- Eisenack A. 1968b. Über Chitinozoen des Baltischen Gebietes. *Paläontographica Abteilung A*. 131:137–198.
- Eisenack A. 1969. Zur Systematik einiger paläozoischer hystrichosphären (Acritarcha) des baltischer Gebietes. *Neues Jahrbuch für Geologie und Paläontologie, Abhandlungen*. 133:115–145.
- Eisenack A. 1972. Beiträge zur Chitinozoen-Forschung. *Paläontographica Abteilung A*. 140:117–130.
- Eisenack A, Cramer FH, Díez M. 1976. Katalog der fossilen Dinoflagellaten, Hystrichosphären und verwandten Mikrofossilien. Band IV Acritarcha 2, Teil 3. Stuttgart (Germany): E. Schweizerbart'sche Verlagsbuchhandlung; p. 863.
- Eisenack A, Cramer FH, Díez M. 1979. Katalog der fossilen Dinoflagellaten, Hystrichosphären und verwandten Mikrofossilien. Band VI Acritarcha 3, Teil 3. Stuttgart (Germany): E. Schweizerbart'sche Verlagsbuchhandlung; p. 533.
- Eiserhardt KH. 1989. Baltisphären aus Gotländer Öjlemyrflint (Acritarcha, Oberordoviz, Geschiebe, Schweden). Mitteilungen aus dem Geologisch Paläontologischen Institut der Universität Hamburg. 68: 79–129.
- Eiserhardt KH. 1992. Die Acritarcha des Öjlemyrflintes. *Paläontographica, Abteilung A*. 226: 1–132.
- Elaouad-Debbaj Z. 1978. Acritarches de l'Ordovicien Supérieur du Synclinal de Bucao (Portugal). *Bulletin de la Société Géologique et Mineralogique de Bretagne*. 10:1–101.
- Elaouad-Debbaj Z. 1984. Acritarches et chitinozoaires de l'Arenig-Lianvirn de l'Anti-Atlas (Maroc). *Review of Palaeobotany and Palynology*. 43(1-3):67–88.
- Elaouad-Debbaj Z. 1986. Chitinozoaires de la formation du Ktaoua inférieur, Ordovicien supérieur de l'Anti-Atlas (Maroc). *Hercynica*. 2(1): 35–55.
- Elaouad-Debbaj Z. 1988. Acritarches et chitinozoaires du Trémadoc de l'AntiAtlas Central (Maroc). *Revue de Micropaléontologie*. 31:85–128.
- Evitt WR. 1963. A discussion and proposals concerning fossil dinoflagellates, hystrichospheres, and acritarchs, I, II. *Proceedings of the National Academy of Sciences of the United States of America*. 49: 158–164 and 298–302.
- Fensome RA, William GL, Barss MS, Freeman JM, Hill JM. 1990. Acritarchs and fossil prasinophytes: an index to genera, species, and intraspecies taxa. *American Association of Stratigraphic Palynologists Contributions Series*. 25:67–88.
- Gansser A, Huber H. 1962. Geological observations in Central Elburz, Iran. *Schweizerische Mineralogische und Petrographische Mitteilungen*. 42(2):583–630.
- Ghavidel-Syooki M. 1990. The encountered acritarchs and chitinozoans from Mila, Ilebek and Zard Kuh Formation in Tang-e-Ilebek at Zard Kuh and their correlation with the Palaeozoic sequence at Chal-i-Sheh area. In: *Symposium on Diapirism Bandar Abbas, Iran*; p. 139–215.
- Ghavidel-Syooki M. 1995. Palynostratigraphy and paleogeography of a Lower Palaeozoic sequence in the Hasanakdar area, Central Alborz, northern Iran. *Review of Palaeobotany and Palynology*. 86(1-2): 91–109.
- Ghavidel-Syooki M. 1996. Acritarch biostratigraphy of the Paleozoic rock units in the Zagros Basin, southern Iran. In: *Fatka O, Servais T, editors. Acritarcha in Praha Proceedings of International Meeting and Workshop*. Vol. 40. *Acta Universitatis Carolinae, Geologica*; p. 385–411.
- Ghavidel-Syooki M. 1997. Palynostratigraphy and paleogeography of Early Permian strata in the Zagros Basin, Southeast-Southwest, Iran. *Journal of Sciences, Islamic Republic of Iran*. 8:243–261.
- Ghavidel-Syooki M. 2000. Palynostratigraphy and palaeobiogeography of Lower Palaeozoic strata in the Ghelli area, northeastern Alborz Range of Iran (Kopet-Dagh Region). *Journal of Sciences, Islamic Republic of Iran*. 11(4):305–318.
- Ghavidel-Syooki M. 2001. Palynostratigraphy and paleobiogeography of the Lower Paleozoic sequence in Iran's northern Alborz Range (Kopet-Dagh Region). In: *Goodman DK, Clarke RT, editors. Proceedings of the IX International Palynological Congress Houston, Texas, U.S.A., 1996*. *American Association of Stratigraphic Palynologists Foundation*; p. 17–35.
- Ghavidel-Syooki M. 2003. Palynostratigraphy and paleoecology of lower Paleozoic strata at Kuh-e Boghou, southwest of Kashmar City, in Eastern Central Iran. *Iranian International Journal of Science*. 4(2): 181–207.
- Ghavidel-Syooki M. 2006. Palynostratigraphy and paleogeography of the Cambro-Ordovician strata in the southwest of Shahrud City (Kuh-e-Kharbash near Deh-Molla), Central Alborz Range, northern Iran. *Review of Palaeobotany and Palynology*. 139(1-4):81–95.
- Ghavidel-Syooki M. 2008. Palynostratigraphy and paleogeography of the Upper Ordovician Gorgan Schists (Southeastern Caspian Sea), eastern Alborz Mountain Ranges, Northern Iran. *Comunicações Geológicas*. 95:123–155.
- Ghavidel-Syooki M. 2016. Biostratigraphy of acritarchs and chitinozoa in Ordovician strata from the Fazel Abad area, southeastern Caspian Sea, Alborz Mountains, northern Iran: stratigraphic and paleogeographic implications. In: *Sorkhabi R, editor. Tectonic evolution, collision, and seismicity of Southwest Asia: in honor of Manuel Berberian's forty-five years of research contributions*. USA: *Geological Society of America Special Paper*. Vol. 525; p. 1–32.
- Ghavidel-Syooki M. 2017a. Cryptospore and trilete spore assemblages from the Late Ordovician (Katian–Hirnantian) Ghelli Formation, Alborz Mountain Range, Northeastern Iran: palaeophytogeographic and palaeoclimatic implications. *Review of Palaeobotany and Palynology*. 244:217–240.
- Ghavidel-Syooki M. 2017b. Biostratigraphy of acritarchs and chitinozoans in Ordovician Strata from the Fazel Abad Area, Southeastern Caspian Sea, Alborz Mountains, Northern Iran: stratigraphic implications. *Journal of Sciences, Islamic Republic of Iran*. 28(1):37–57.
- Ghavidel-Syooki M. 2017c. Stratigraphic evidence for Hirnantian glaciation in the Alborz Mountain Ranges, northeastern Iran. *Palaeogeography, Palaeoclimatology, Palaeoecology*. 485:879–898.
- Ghavidel-Syooki M. 2019. Middle-Late Cambrian acritarchs from the Zardkuh area in the High Zagros Mountains, southern Iran: stratigraphic and paleogeographic implications. *Journal of the Science Islamic Republic of Iran*. 30(4):331–353.
- Ghavidel-Syooki M. 2021. Peri-Gondwanan acritarchs, chitinozoans, and miospores from Paleozoic succession in the High Zagros Mountains, southern Iran: regional stratigraphic significance and paleogeographic implications. *Review of Palaeobotany and Palynology*. 292:104457.
- Ghavidel-Syooki M. 2023. Biostratigraphy and palaeogeographic implications of Ordovician and Silurian chitinozoa from the High Zagros Mountains, northern Persian Gulf, Iran. *Palynology*. 47(2):2149631.
- Ghavidel-Syooki M, Álvaro JJ, Popov L, Ghobadi-Pour M, Ehsani MH, Suyarkova A. 2011b. Stratigraphic evidence for the Hirnantian (latest Ordovician) glaciation in the Zagros Mountains, Iran. *Palaeogeography, Palaeoclimatology, Palaeoecology*. 307(1-4):1–16.
- Ghavidel-Syooki M, Borji S. 2018. Chronostratigraphy of acritarchs and chitinozoans from upper Ordovician strata from the Robat-e Gharabil Area, NE Alborz Mountains, Northern Khorasan Province: stratigraphic and paleogeographic implications. *Journal of the Sciences Islamic Republic of Iran*. 29(1):35–51.
- Ghavidel-Syooki M, Hassanzadeh J, Vecoli M. 2011a. Palynology and isotope geochronology of the Upper Ordovician–Silurian successions (Ghelli and Soltan Maidan Formations) in the Khoshyeilagh area, eastern Alborz Range, northern Iran; stratigraphic and palaeogeographic implications. *Review of Palaeobotany and Palynology*. 164(3-4): 251–271.
- Ghavidel-Syooki M, Hoseinzadeh-Moghadam M. 2005. Biostratigraphy of Palaeozoic sediments in the Ali-Abad area in the Gorgan province,

- southeastern the Caspian Sea, northern Iran [Msc thesis]. Iran, Tehran: Shahid Beheshti University; p. 111.
- Ghavidel-Syooki M, Piri-Kangarshahi MH. 2021. Biostratigraphy of acritarchs, chitinozoans, and miospores from Upper Ordovician sequences in Kuh-e Boghou, southwest of Kashmar, eastern central Iran: stratigraphic and palaeogeographic implications. *Review of Palaeobotany and Palynology*. 284:104337.
- Ghavidel-Syooki M, Piri-Kangarshahi MH. 2023. Peri-Gondwanan acritarchs and chitinozoans from the Lower–Middle Ordovician Lashkarak Formation in the Alborz Mountain Ranges, northern Iran: regional stratigraphical significance and palaeogeographical implications. *Palynology*. 47(3):2214191.
- Ghavidel-Syooki M, Piri-Kangarshahi MH. 2024. The biostratigraphy and palaeobiogeography of Cambrian and Ordovician acritarchs and chitinozoa from the Simeh-Kuh, NW Damghan City, the Alborz Mountains, northern Iran. *Palynology*. 48(4):2341324.
- Ghavidel-Syooki M, Popov LE, Álvaro JJ, Ghobadi Pour M, Tolmacheva TY, Ehsani M-H. 2014. Dapingian–lower Darriwilian (Ordovician) stratigraphic gap in the Faraghan mountains, Zagros ranges, south-eastern Iran. *Bulletin of Geosciences*. 89(4):679–706.
- Ghavidel-Syooki M, Rahman-Reresht A. 1994. Palynostratigraphy and palaeoecology of the Milla Formation, at the Shahmirzad area, Alborz Mountain Ranges [Unpublished Thesis for M.Sc. degree in Stratigraphy and Palaeontology]. Tehran (Iran): Islamic Azad University, Branch North Tehran; p. 124. (Persian).
- Ghavidel-Syooki M, Vecoli M. 2007. Latest Ordovician–early Silurian chitinozoans from the eastern Alborz Mountain Range, Kope-Dagh Region, northeastern Iran: biostratigraphy and paleobiogeography. *Review of Palaeobotany and Palynology*. 145(1-2):173–192.
- Ghavidel-Syooki M, Vecoli M. 2008. Palynostratigraphy of Middle Cambrian to lowermost Ordovician stratal sequences in the High Zagros Mountains, southern Iran: regional stratigraphic implications and palaeobiogeographic significance. *Review of Palaeobotany and Palynology*. 150(1-4):97–114.
- Ghavidel-Syooki M, Winchester-Seeto T. 2002. Biostratigraphy and palaeogeography of Late Ordovician chitinozoans from the northeastern Alborz Range. Iran. *Review of Palaeobotany and Palynology*. 118(1-4):77–99.
- Górka H. 1969. Microorganisms de l'Ordovicien de Pologne. *Acta Palaeontologia Polonica*. 22:1–102.
- Górka H. 1979. Les acritarches et Prasinophyceae de l'ordovicien Moyen d'Olsztyn IG 2 (Pologne). *Acta Palaeontologica Polonica*. 24(3):351–376.
- Górka H. 1987. Acritarches et Prasinophyceae de l'ordovicien Moyen (Viruen) de sondage de Smedsby Gard no. 1 (Götland, Suède). *Review of Palaeobotany and Palynology*. 52(4):257–297.
- Grahn Y. 1980. Early Ordovician chitinozoa from Öland. *Sveriges Geologiska Undersökning Serie, C*. 775:1–41.
- Grahn Y. 1981. Ordovician chitinozoa from the Stora Asbotorp boring in Vistergtland, south-central Sweden. *Sveriges Geologiska Undersökning Serie, C*. 787:1–40.
- Grahn Y. 1982. Caradocian and Ashgillian chitinozoa from the subsurface of Götland. *Sveriges Sveriges Geologiska Undersökning Serie, C*. 788: 1–66.
- Grahn Y, Bergström SM. 1984. Lower-Middle Ordovician chitinozoa from the southern Appalachians of the United States. *Review of Palaeobotany and Palynology*. 43(1-3):89–122.
- Grahn Y, Idil S, Østvedt AM. 1994. Caradocian and Ashgillian chitinozoan biostratigraphy of the Oslo-Asker and Ringerike districts, Oslo region, Norway. *Geologiska Foereningens i Stockholm Foerhandlingar*. 116(3): 147–160.
- Grahn Y, Nölvak J. 2007. Ordovician chitinozoa and biostratigraphy from Skåne and Bornholm, southernmost Scandinavia – an overview and update. *Bulletin of Geosciences*. 82(01):11–26.
- Gray J. 1985. The microfossil record of early land plants; advances in the understanding of early terrestrialisation. In Chaloner WG, Lawson JD, editors. *Evolution and environment in the Late Silurian and Early Devonian*. *Philosophical Transactions of the Royal Society of London B, Biological Sciences*. vol. 309, p. 167–195.
- Gray J. 1988. Land plant spores and the Ordovician–Silurian boundary. *Bulletin of the British Museum (Natural History) Geology*. 43:351–358.
- Gray J, Boucot AJ. 1989. Is *Moyeria* a euglenoid? *Lethaia*. 22(4):447–456.
- Hagstrom J. 1997. Land-derived palynomorphs from the Silurian of Gotland, Sweden. *GFF*. 119:301–316.
- Heuse T, Erdtmann B–D, Kraft P. 1994. Early Ordovician microfossils (acritarchs, chitinozoans) and graptolites from the Schwarzburg Anticline, Thuringia (Germany). *Veröffentlichungen Naturhistorisches Museum Schleusingen*. 9:41–68.
- Hill PJ, Molyneux SG. 1988. Biostratigraphy, palynofacies and provincialism of Late Ordovician–Early Silurian acritarchs from Northeast Libya. In: El-Arnauti A, Owens B, Thusu B, editors. *Subsurface palynostratigraphy of Northeast Lybia*. Benghazi (Lybia): Garyounis University; p. 27–43.
- Hill PJ, Paris F, Richardson JB. 1985. Silurian palynomorphs. *Journal of Micropalaeontology*. 4(1):27–48.
- Hints L, Hints O, Kaljo D, Kiipli T, Männik P, Nölvak J, Pärnaste H. 2010. Hirnantian (latest Ordovician) bio- and chemostratigraphy of the Stirnas-18 core, western Latvia. *Estonian Journal of Earth Sciences*. 59(1):1–24.
- Jachowicz M. 1995. Ordovician acritarch assemblages from central and northwestern Saudi Arabia. *Review of Palaeobotany and Palynology*. 89(1-2):19–25.
- Jacobson SR, Achab A. 1985. Acritarch biostratigraphy of the *Dicellograptus complanatus* graptolite zone from the Vaureal formation (Ashgillian), Anticosti Island, Québec, Canada. *Palynology*. 9(1): 165–198.
- Jansonius J. 1964. Morphology and classification of some chitinozoa. *Bulletin of Canadian Petroleum Geology*. 12(4):901–918.
- Jardiné S, Combaz A, Magloire L, Peniguel G, Vachey G. 1974. Distribution stratigraphique des acritarches dans le Paléozoïque du Sahara algérien. *Review of Palaeobotany and Palynology*. 18(1-2): 99–129.
- Jenkins WAM. 1967. Ordovician chitinozoa from Shropshire. *Palaeontology*. 10:436–488.
- Jenkins WAM. 1969. Chitinozoa from the Ordovician Viola and Fernvale limestones of the Arbuckle Mountains, Oklahoma. *Special Papers in Palaeontology*. 5:1–44.
- Jenkins WAM. 1970. Chitinozoa from the Ordovician Sylvan Shale of the Arbuckle Mountains, Oklahoma. *Palaeontology*. 13:261–288.
- Jenny J. 1977. Géologie et stratigraphie de l'Elburz oriental entre Aliabad et Shahrud, Iran [PhD thèse]. Geneva (Switzerland): University of Geneva.
- Johnson NG. 1985. Early Silurian palynomorphs from the Tuscarora Formation in Central Pennsylvania and their paleobotanical and geological significance. *Review of Palaeobotany and Palynology*. 45(3-4): 307–359.
- Keegan JB, Rasul SM, Shaheen Y. 1990. Palynostratigraphy of Lower Palaeozoic, Cambrian to Silurian, sediments of the Hashemite Kingdom of Jordan. *Review of Palaeobotany and Palynology*. 66(3-4): 167–180.
- Kjellström G. 1971. Middle Ordovician microplankton from the Grötlingbo Borehole no. 1 in Götland, Sweden. *Sveriges Geologiska Undersökning, Series C*. 65(669):1–35.
- Laufeld S. 1967. Caradocian chitinozoa from Dalarna, Sweden. *Geologiska Föreningen i Stockholm Förhandlingar*. 89(3):275–349.
- Laufeld S. 1971. Chitinozoa and correlation of the Moldova and Restevo Beds of Podolia: USSR. *Mémoires du Bureau de Recherches Géologiques et Minières*. 73:291–300.
- Le Hérisse A, Al-Ruwaili M, Miller M, Vecoli M. 2007. Environmental changes reflected by palynomorphs in the early Middle Ordovician Hanadir, a Member of the Qasim Formation, Saudi Arabia. *Revue de Micropaléontologie*. 50(1):3–16.
- Le Hérisse A, Melo JHG, Quadros LP, Grahn Y, Steeman P. 2001. Palynological characterization and dating of the Tinguá Formation, Serra Grande Group, northern Brazil. *Science Technical Petroleum*. p. 20.
- Le Hérisse A, Molyneux SG, Miller MA. 2015. Late Ordovician to early Silurian acritarchs from the Qusaiba-1 shallow core hole, central Saudi Arabia. *Review of Palaeobotany and Palynology*. 212:22–59.

- Le Hérisse A, Paris F, Steemans P. 2013. Late Ordovician–earliest Silurian palynomorphs from northern Chad and correlation with contemporaneous deposits of southeastern Libya. *Bulletin of Geosciences*. 88(3): 483–504.
- Le Hérisse A, Vecoli M, Guidat C, Not F, Breuer P, Wellman C, Steemans P. 2017. Middle Ordovician acritarchs and problematic organic microfossils from the Saq-Hanadir transitional beds in the QSIM-801 well, Saudi Arabia. *Revue de Micropaléontologie*. 60(3):289–318.
- Le Heron DP, Craig J. 2008. First-order reconstructions of a Late Ordovician Saharan Ice Sheet. *Journal of the Geological Society*. 165(1):19–29.
- Legault JA. 1982. First report of Ordovician (Caradoc -Ashgill) palynomorphs from Orphan Knoll, Labrador Sea. *Canadian Journal of Earth Sciences*. 19(9):1851–1856.
- Li J. 1987. Ordovician acritarchs from the Meitan Formation of Guizhou Province, southwest China. *Palaeontology*. 30(3):613–634.
- Li J, Wang Y. 1997. Ordovician acritarchs from boreholes in the Tarim Basin. *Acta Micropalaeontologica Sinica*. 14(2):175–190.
- Li J, Wicander R, Yan K, Zhu H. 2006. An Upper Ordovician acritarch and prasinophyte assemblage from Dawangou, Xinjiang, northwestern China: biostratigraphic and palaeogeographic implications. *Review of Palaeobotany and Palynology*. 139(1-4):97–128.
- Liang Y, Paris F, Tang P. 2017. Middle-Late Ordovician chitinozoans from the Yichang area, South China. *Review of Palaeobotany and Palynology*. 244:26–42.
- Liang Y, Servais T, Tang P, Liu J, Wang W. 2017. Tremadocian (Early Ordovician) chitinozoan biostratigraphy of South China: an update. *Review of Palaeobotany and Palynology*. 247:149–163.
- Liang Y, Tang P, Wang GX, Yan GZ, Wang Q. 2023. Middle-Late Ordovician chitinozoans from Songliang of Qiaojia, western South China, and their biostratigraphic implications. *Palaeoworld*. 32(2): 287–302.
- Lister TR. 1970. The acritarchs and chitinozoa from the Wenlock and Ludlow Series of the Ludlow and Millichope areas, Shropshire. *Monographs of the Palaeontographical Society*. 124(528):1–100.
- Loeblich AR, Jr. 1970. Morphology, ultrastructure and distribution of Paleozoic acritarchs. *Proceedings of the North American Paleontological Convention, Chicago, 1969, Part G*, p. 705–788.
- Loeblich AR, Jr, Tappan H. 1976. Some new and revised organic-walled phytoplankton microfossil genera. *Journal of Palaeontology*. 50:301–308.
- Loeblich AR, Jr, Tappan H. 1978. Some Middle and Late Ordovician microphytoplankton from Central North America. *Journal of Paleontology*. 52(6):1233–1287.
- Loeblich AR, Jr, Wicander ER. 1976. Organic walled microplankton from the Lower Devonian Late Gedinnian Haragan and Bois d'Arc Formations of Oklahoma, USA, Part I. *Paleontographica Abteilung B*. 159:1–39.
- Loydell DK, Männik P, Nestor V. 2003. Integrated biostratigraphy of the lower Silurian of the Aizpute-41 cores, Latvia. *Geological Magazine*. 140(2):205–229.
- Mahmoudi M, Saburi J, Alimohammadian H, Majidifard MR. 2014. The first cryptospore assemblages of Late Ordovician in Iran, Ghelli Formation, eastern Alborz. *Geopersia*. 4:125–140.
- Martin F. 1969. Les acritarches de l'Ordovicien et du Silurien belges. *Determination et valeur stratigraphique*. *Bulletin Institut royal des sciences naturelles de Belgique, Brussels*. 160:1–175.
- Martin F. 1973. Les acritarches de l'Ordovicien Inférieur de la Montagne Noire (Hérault, France). *Bulletin de l'Institut Royal des Sciences Naturelles de Belgique, Sciences de la Terre*. 48(10):1–61.
- Martin F. 1980. Quelques Chitinozoaires et Acritarches ordoviens supérieurs de la Formation d'White Head en Gaspésie, Québec. *Canadian Journal of Earth Sciences*. 17(1):106–119.
- Martin F. 1983. Chitinozoaires et acritarches ordoviens de la plateforme du Saint-Laurent (Québec et sud-est de l'Ontario). *Commission géologique du Canada, Geological Survey of Canada Bulletin*. 310: 1–59.
- McClure HA. 1988. Chitinozoan and acritarch assemblages, biostratigraphy, and biogeography of the Early Palaeozoic of Northwest Arabia. *Review of Palaeobotany and Palynology*. 56(1-2):41–60.
- Miller MA. 1991. *Paniculaferum missouriensis* gen. et sp. nov., a new Upper Ordovician acritarch from Missouri, USA. *Review of Palaeobotany and Palynology*. 70(3):217–223.
- Miller MA, Al-Ruwaili MH. 2007. Preliminary palynological investigation of Saudi Arabian Upper Ordovician glacial sediments. *Revue de Micropaléontologie*. 50(1):17–26.
- Miller MA, Eames LE. 1982. Palynomorphs from the Silurian Medina Group (Lower Llandovery) of the Niagara Gorge, Lewiston, New York, U.S.A. *Palynology*. 6:221–254.
- Miller MA, Vecoli M, Cesari C. 2017. New palynomorphs from the Ordovician–Silurian boundary interval: Eastern North America and Saudi Arabia. *Palynology*. 41(sup1):106–120.
- Molyneux SG, Barron HF, Smith RA. 2008. Upper Llandovery-Wenlock (Silurian) palynology of the Pentland Hills inliers, Midland Valley of Scotland. *Scottish Journal of Geology*. 44(2):151–168.
- Molyneux SG, Delabroye A, Wicander R, Servais T. 2013. Biogeography of early to mid-Palaeozoic (Cambrian–Devonian) marine phytoplankton. In: Harper DAT, Servais T (eds). *Early Palaeozoic Biogeography and Palaeogeography*. Geological Society, London, Memoirs; vol. 38, p. 365–397.
- Molyneux SG, Le Hérisse A, Wicander R. 1996. Paleozoic phytoplankton. In: Jansonius J, McGregor DC, editors. *Palynology: principles and applications*. Vol. 2. American Association of Stratigraphic Palynologists Foundation; p. 493–529.
- Molyneux SG, Paris F. 1985. Late Ordovician palynomorphs. In: Thusu B, Owens B, editors. *Palynostratigraphy of Northeast Libya*. Vol. 4. *Journal of Micropalaeontology*; p. 11–26.
- Molyneux SG, Raevskaya E, Servais T. 2007. The *messauoudensis-trifidum* acritarch assemblage and correlation of the base of Ordovician Stage 2 (Floian). *Geological Magazine*. Cambridge University Press. 144(1): 143–156.
- Mullins GL, Loydell DK. 2002. Integrated lower Silurian chitinozoan and graptolite biostratigraphy of Buttington Brick Pit, Wales. *Geological Magazine*. 139(1):89–96.
- Navidi-Izad N, Benachour H, Kroeck DM, Steemans P, Servais T. 2022. *Virgatasporites* and *Attritasporites*: the oldest land plant derived spores, cryptospores or acritarchs? *Botany Letters*. 169(4):495–509.
- Navidi-Izad N, Hashemi H, Régner S, Kroeck D, Yan K, Servais T. 2020. Revision of the Middle-Upper Ordovician acritarch genus *Orthosphaeridium* Eisenack 1968 nov. emend. *Review of Palaeobotany and Palynology*. 273:104127.
- Nestor V. 1980. New chitinozoan species from the lower Llandovery of Estonia. *The Estonian Academy of Sciences, Geology*. 29:98–107.
- Nölvak J. 1980. Chitinozoans in biostratigraphy of the Northern East Baltic Ashgillian. A Preliminary report. *Acta Palaeontologica Polonica*. 25(2):253–260.
- Nölvak J, Grahm Y. 1993. Ordovician chitinozoan zones from Baltoscandia. *Review of Palaeobotany and Palynology*. 79(3-4): 245–269.
- Nölvak J, Liang Y, Hints O. 2019. Early diversification of Ordovician chitinozoans on Baltica: new data from the Jägala waterfall section, northern Estonia. *Palaeogeography, Palaeoclimatology, Palaeoecology*. 525: 14–24.
- Nölvak J, Liang Y, Hints O. 2022. Early and early Middle Ordovician chitinozoans from the Baldone drill core, central Latvia. *Estonian Journal of Earth Sciences*. 71(1):25–43.
- Nölvak J, Meidla T, Uutela A. 1995. Microfossils in the Ordovician erratic boulders from southwestern Finland. *Bulletin of the Geological Society of Finland*. 67(2):3–26.
- Oktay B, Wellman CH. 2019. Palynological analysis of Upper Ordovician to Lower Silurian sediments from the Diyarbakir Basin, southeastern Turkey. *Review of Palaeobotany and Palynology*. 263:28–46.
- Oulebsir L, Paris F. 1995. Chitinozoaires ordoviens du Sahara algérien: biostratigraphie et affinités paléogéographiques. *Review of Palaeobotany and Palynology*. 86(1-2):49–68.
- Paris F. 1979. Les Chitinozoaires de la Formation de Louredo, Ordovicien Supérieur du Synclinal de Bucaco (Portugal). *Paleontographica, Abteilung A*. 164(1-3):24–51.
- Paris F. 1981. Les Chitinozoaires dans le Paléozoïque du Sud-Ouest de l'Europe. *Société Géologique et Minéralogique de Bretagne*. 26:1–496.

- Paris F. 1988. New chitinozoans from the Late Ordovician – Late Devonian of northeast Libya. In: El-Arnauti A, Owens B, Thusu B, editors. Subsurface palynostratigraphy of northeast Libya. Benghazi (Libya): Garyounis University Publishing; p. 77–87.
- Paris F. 1990. The Ordovician chitinozoan biozones of the northern Gondwana Domain. Review of Palaeobotany and Palynology. 66(3-4): 181–209.
- Paris F. 1996. Chapter 17 Chitinozoan biostratigraphy and palaeoecology. In: Jansonius J, McGregor DC, editor. Palynology: principal and applications. Vol. 2. USA: American Association Stratigraphic Palynologists Foundation; p. 531–552.
- Paris F. 1999. Palaeobiodiversification of Ordovician chitinozoans from northern Gondwana. Acta Universitatis Carolinae, Geologica. 43: 283–286.
- Paris F, Bourahrouh A, Hérisse AL. 2000a. The effects of the final stages of the Late Ordovician glaciation on marine palynomorphs (chitinozoans, acritarchs, and leiospheres) in well NI-2 (N.E. Algerian Sahara). Review of Palaeobotany and Palynology. 113(1-3):87–104.
- Paris F, Grahn Y, Nestor V, Lakova I. 1999. A revised chitinozoan classification. Journal of Paleontology. 73(4):549–570.
- Paris F, Le Hérisse A, Monod O, Kozlu H, Ghienne J-F, Dean WT, Vecoli M, Günay Y. 2007. Ordovician chitinozoans and acritarchs from southern and southeastern Turkey. Revue de Micropaleontologie. 50(1):81–107.
- Paris F, Verniers J, Al-Hajri S. 2000b. Ordovician chitinozoans from Central Saudi Arabia. In: Al-Hajri S, Owens B, editors. Stratigraphic palynology of the Palaeozoic of Saudi Arabia. Special GeoArabia Publication. Manama (Bahrain): Persian Gulf PetroLink; p. 42–56.
- Paris F, Verniers J, Miller MA, Al-Hajri S, Melvin J, Wellman CH. 2015. Late Ordovician–earliest Silurian chitinozoans from the Qusaiba-1 core hole (North Central Saudi Arabia) and their relation to the Hirnantian glaciation. Review of Palaeobotany and Palynology. 212:60–84.
- Playford G, Wicander R. 2006. Organic-walled microphytoplankton of the Sylvan Shale (Richmondian: Upper Ordovician), Arbuckle Mountains, southern Oklahoma, U.S.A. Bulletin of the Oklahoma Geological Survey. 148:1–116.
- Rauscher R. 1970. Les Chitinozoaires de l'Ordovicien du Synclinal de May-sur-Orne (Clavados). Bulletin de la Société Linnéenne de Normandie. 101:101–117.
- Rauscher R. 1973. Recherches micropaléontologiques et stratigraphiques dans l'Ordovicien et le Silurien en France. Étude des acritarches, des chitinozoaires et des spores. Sciences Géologiques, Université Louis Pasteur (Strasbourg), Institut de Géologie. 38:1–224.
- Rauscher R, Doubinger J. 1967. Associations de chitinozoaires de Normandie et comparaisons avec les faunes déjà décrites. Sciences Géologiques, Bulletins et Mémoires. 20(4):307–328.
- Richardson JB. 1988. Late Ordovician and Early Silurian cryptospores and miospores from northeast Libya. In El-Arnauti A, Owens B, Thusu B. (eds). Subsurface Palynostratigraphy of Northeast Libya. Benghazi, Libya: Garyounis University Publications; p. 89–110.
- Richardson JB. 1996a. Taxonomy and classification of some new Early Devonian cryptospores from England. In: Cleal CJ, editor. Studies on early land plant spores from Britain. Special Papers in Palaeontology. Vol. 55; p. 7–40.
- Richardson JB. 1996b. Palaeozoic spores and pollen: chapter 18A-Lower and Middle Palaeozoic records of terrestrial palynomorphs. In: Jansonius J, McGregor DC, editors. Palynology: principles and applications. Houston (TX): American Association of Stratigraphic Palynologists Foundation; p. 555–574.
- Richardson JG, Ausich WI. 2007. Late Ordovician–Early Silurian cryptospore occurrences on Anticosti Island (Île d'Anticosti), Quebec, Canada. Canadian Journal of Earth Sciences. 44(1):1–7.
- Riding JB. 2021. A guide to preparation protocols in palynology. Palynology. 45(sup1):1–110.
- Ross RJ. 1982. The Ordovician system in the United States: correlation chart and explanatory notes. Vol 12. Paris (France): International Union Geological Sciences; p. 73.
- Rubinstein CV, Gerrienne P, de la Puente GS, Astini RA, Steemans P. 2010. Early–Middle Ordovician evidence for land plants in Argentina (eastern Gondwana). The New Phytologist. 188(2):365–369.
- Rubinstein CV, Vaccari NE. 2004. Cryptospore assemblages from the Ordovician/Silurian Boundary in the Puna Region, North-west Argentina. Palaeontology. 47(4):1037–1061.
- Rubinstein CV, Vajda V. 2023. High diversity and early radiation of organic-walled phytoplankton in southern Baltica during the Middle–Late Ordovician – evidence from the Borensult-1 drill core of south Sweden. GFF. 145(1–2):50–83.
- Rubinstein CV, Vecoli M, Astini RA. 2011. Biostratigraphy and palaeo-environmental characterization of the Middle Ordovician from the Sierras Subandinas (NW Argentina) based on organic-walled microfossils and sequence stratigraphy. Journal of South American Earth Sciences. 31(1):124–138.
- Sarjeant WAS, Stancliffe RPW. 1994. The *Michrystidium* and *Veryhachium* complexes (Acritarcha: Acanthomorphae and Polygonomorphae): a taxonomic reconsideration. Micropaleontology. 40(1):1–77.
- Servais T, Harper DA, Munnecke A, Owen AW, Sheehan PM. 2009. Understanding the Great Ordovician Biodiversification Event (GOBE): influences of palaeogeography, paleoclimate, or paleoecology? GSA Today. 19(4):4–10.
- Servais T, Li J, Molyneux SG, Rubinstein CV, Vecoli M, Yan K. 2014. The palaeobiogeographical spread of the acritarch *Veryhachium* in the Early and Middle Ordovician and its impact on biostratigraphic applications. Geologiska Föreläsningarna i Stockholm Föreläsning. 136(1): 234–237.
- Servais T, Maletz J. 1992. Lower Llanvirn (Ordovician) graptolites and acritarchs from the “assise de Huy”, Brande de Sambre-et-Meuse, Belgium. Annales de la Société Géologique de Belgique. 115(1): 265–285.
- Servais T, Molyneux SG, Li J, Nowak H, Rubinstein CV, Vecoli M, Wang W, Yan K. 2018. First Appearance Datums (F.A.D.s) of selected acritarch taxa and the correlation between Lower and Middle Ordovician stages. Lethaia. 51(2):228–253.
- Siesser WG, Hendley IJ, Kessler TE, Marler JC, Wehner ET. 1998. Caradocian chitinozoans from the Central Basin, Tennessee. Review of Palaeobotany and Palynology. 102(3-4):213–222.
- Smelror M, Cocks LRM, Mørk A, Neuman BEE, Nakrem HA. 1997. Upper Ordovician–Lower Silurian strata and biota from offshore South Norway. Norsk Geologisk Tidsskrift. 77:251–268.
- Soufiane A, Achab A. 1993. Some chitinozoan assemblages from the Ordovician of the Tedla Basin, Morocco. Geobios. 26(5):535–553. [Mismatch]
- Soufiane A, Achab A. 2000. Upper Ordovician and Lower Silurian chitinozoans from central Nevada and Arctic Canada. Review of Palaeobotany and Palynology. 113(1-3):165–187.
- Spina A, Vecoli M. 2009. Palynostratigraphy and vegetational changes in the Siluro-Devonian of the Ghadamis Basin, North Africa. Palaeogeography Palaeoclimatology Palaeoecology. 282:1–18.
- Stampfli GM. 1978. Etude géologique general de l'Elburz oriental au S de Gonbad-e-Qabus, Iran, Iran NE [thesis no.1868]. Switzerland: Univerite de Geneve; p. 328.
- Staplin FL, Jansonius J, Pocock SAJ. 1965. Evaluation of some acritarcheous hystrichosphere genera. Neues Jahrbuch für Geologie und Paläontologie, Abhandlungen. 123(2):167–201.
- Stemans P. 2000. Miospore evolution from the Ordovician to Silurian. Review of Palaeobotany and Palynology. 113(1-3):189–196.
- Stemans P. 2001. Ordovician cryptospores from the Oostduinkerke borehole, Brabant Massif, Belgium. Geobios. 34(1):3–12.
- Stemans P, Higgs KT, Wellmans CH. 2000. Cryptospores and trilete spores from the Llandoverly, Nuayyin-2 Borehole, Saudi Arabia. In: Al-Hajri S, Owens B, editors. Stratigraphic palynology of the Palaeozoic of Saudi Arabia. Manama, Bahrain: GeoScienceWorld; p. 92–115.
- Stemans P, Le Hérisse A, Bozdogan N. 1996. Ordovician and Silurian cryptospores and miospores from southeastern Turkey. Review of Palaeobotany and Palynology. 93(1-4):35–76.
- Stemans P, Wellman CH, Filatoff J. 2007. Palaeophytogeographical and palaeoecological implications of a miospore assemblage of earliest Devonian (Lochkovian) age from Saudi Arabia. Palaeogeography, Palaeoclimatology, Palaeoecology. 250(1-4):237–254.
- Stockmans F, Willièrre Y. 1963. Les Hystrichosphères ou mieux les Acritarches du Silurien Belge. Sondage de la Brasserie Lust à Courtrai

- (Kortrijk). Bulletin de la Société belge de géologie, de paléontologie et d'hydrologie. 71:450–481.
- Strother PK. 1991. A classification scheme for the cryptospores. *Palynology*. 15(1):219–236.
- Strother PK, Al-Hajri S, Traverse A. 1996. New evidence for land plants from the lower Middle Ordovician of Saudi Arabia. *Geology*. 24(1): 55–58.
- Strother PK, Taylor WA, van de Schootbrugge B, Leander BS, Wellman CH. 2020. Pellicle ultrastructure demonstrates that *Moyeria* is a fossil euglenid. *Palynology*. 44(3):461–471.
- Strother PK, Traverse A. 1979. Plant microfossils from the Llandoveryan and Wenlockian rocks of Pennsylvania. *Palynology*. 3(1):1–21.
- Strother PK, Traverse A, Vecoli M. 2015. Cryptospores from the Hanadir Shale Member of the Qasim Formation, Ordovician (Darriwilian) Saudi Arabia. *Review of Palaeobotany and Palynology*. 212:97–110.
- Strother PK, Wood GD, Taylor WA, Beck JH. 2004. Middle Cambrian cryptospores and the origin of land plants. *Memoirs of the Association of Australasian Palaeontologists*. 29:99–113.
- Sutherland SJE. 1994. Ludlow chitinozoans from the type area and adjacent regions. *Palaeontographical Society Monograph*. 148(594):1–104.
- Tammekänd M, Hints O, Nõlvak J. 2010. Chitinozoan dynamics and biostratigraphy in the Vão Formation (Darriwilian) of the Uuga Cliff, Pakri Peninsula, NW Estonia. *Estonian Journal of Earth Sciences*. 59(1): 25–36.
- Tappan H, Loeblich AR. 1971. Surface sculpture of the wall in Lower Paleozoic acritarchs. *Micropaleontology*. 17(4):385–410.
- Taugourdeau P. 1966. Les Chitinozoaires. Techniques d'Études, morphologies et classification. *Mémoires de la Société Géologique*. 104:64.
- Taugourdeau P, de Jehowsky B. 1960. Répartition et description des chitinozoaires siluro-dévonien de quelques sondages de la CREPS, de la CFPA et de la SN Repal au Sahara. *Institut Français du Pétrole*. 15:1199–1260.
- Taylor WA. 1995. Ultrastructure of *Tetrahedraletes medinensis* (Strother and Traverse) Wellman and Richardson, from the upper Ordovician of southern Ohio. *Review of Palaeobotany and Palynology*. 85(3-4):183–187.
- Taylor WA, Strother PK. 2008. Ultrastructure of some Cambrian palynomorphs from the Bright Angel Shale, Arizona, USA. *Review of Palaeobotany and Palynology*. 151(1-2):41–50.
- Taylor WA, Strother PK. 2009. Ultrastructure, morphology, and topology of Cambrian palynomorphs from the Lone Rock Formation, Wisconsin, USA. *Review of Palaeobotany and Palynology*. 153(3-4):296–309.
- Tomescu AM, Pratt LM, Rothwell GW, Strother PK, Nardon GC. 2009. Carbon isotopes support the presence of extensive land floras predating the origin of vascular plants. *Palaeogeography, Palaeoclimatology, Palaeoecology*. 283(1-2):46–59.
- Tongiorgi M, Lei-Ming Y, Di Milia A. 1995. Arenigian acritarchs from the Daping section (Yangtze Gorges area, Hubei Province, Southern China) and their palaeogeographic significance. *Review of Palaeobotany and Palynology*. 86(1-2):13–48.
- Tongiorgi M, Yin L, Di Milia A. 2003. Lower Yushanian to lower Zhejiangian palynology of the Yangtze Gorges area (Daping and Huanghuachang sections), Hubei province, South China. *Palaeontographica Abteilung B*. 266(1-6):1–160.
- Torsvik TH, Cocks LR. 2017. *Earth history and palaeogeography*. England: Cambridge University Press.
- Trythall RJB, Eccles C, Molyneux SG, Taylor WEG. 1987. Age and controls of ironstone deposition (Ordovician) North Wales. *Geological Journal*. 22(S1):31–43.
- Turner RE. 1984. Acritarchs from the type area of the Ordovician Caradoc Series, Shropshire, England. *Palaeontographica Abteilung B*. 190(4-6): 87–157.
- Turner RE. 1985. Acritarchs from the type area of the Ordovician Llandeilo Series, South Wales. *Palynology*. 9(1):211–234.
- Umnova NI. 1975. Ordovician and Silurian acritarchs of the Moscow Basin and the Prebaltic. Moscow (Russia): Izdatelskva Nedra.
- Uutela A, Tynni R. 1991. Ordovician acritarchs from Rapla borehole, Estonia. *Bulletin of the Geological Survey of Finland*. 353:1–135.
- Van Nieuwenhove N, Vandenbroucke TRA, Verniers J. 2006. Chitinozoan biostratigraphy of the Upper Ordovician Greenscoe section, southern Lake District, UK. *Review of Palaeobotany and Palynology*. 139(1-4): 151–169.
- Vandenbroucke T. 2004. Chitinozoan biostratigraphy of the Upper Ordovician Fagelsang GSSP, Scania, southern Sweden. *Review of Palaeobotany and Palynology*. 130(1-4):217–239.
- Vandenbroucke TRA. 2005. Upper Ordovician Global Stratotype Section and points and British historical type area: a chitinozoan point of view [unpublished PhD thesis]. Ghent (Belgium): Ghent University; 33, pls.
- Vandenbroucke TRA. 2007. Upper Ordovician chitinozoans from the British Historical Type Area and adjacent key sections. *Monographs of the Palaeontographical Society*. 161(628):1–110.
- Vandenbroucke TRA, Gabbot SE, Paris F, Aldridge RJ, Theron JN. 2009. Chitinozoans and the age of the Soom Shale, an Ordovician black shale in Lagerstätte, South Africa. *Journal of Micropalaeontology*. 28(1):53–66.
- Vandenbroucke TRA, Williams M, Zalasiewicz J, Davies JR, Waters RA. 2008. Integrated Upper Ordovician graptolite chitinozoan biostratigraphy of the Cardigan and Whitland areas, southwest Wales. *Geological Magazine*. 145(02):199–214.
- Vanmeirhaeghe J. 2006. Chitinozoan biostratigraphy of the Upper Ordovician of Faulxles-Tombes (central Condroz Inlier, Belgium). *Review of Palaeobotany and Palynology*. 139(1-4):171–188.
- Vanmeirhaeghe J, Storme A, Van Noten K, Van Grootel G, Verniers J. 2005. Chitinozoan biozonation and new lithostratigraphical data in the Upper Ordovician of the Fauquez and Asquempont areas (Brabant Massif, Belgium). *Geologica Belgica*. 8(4):145–159.
- Vavrdová M. 1966. Paleozoic microplankton from central Bohemia. *Časopis pro Mineralogii a Géologii*. 11(4):409–414.
- Vavrdová M. 1972. Acritarchs from the Klabava Shales (Arenig). *Věstník Ústředního Ústavu Geologického*. 47:79–86.
- Vavrdová M. 1974. Geographical differentiation of Ordovician acritarch assemblages in Europe. *Review of Palaeobotany and Palynology*. 18(1-2):171–175.
- Vavrdová M. 1977. Acritarchs from the Šárka Formation (Darriwilian). *Věstník Ústředního Ústavu Geologického*. 52:109–118.
- Vavrdová M. 1988. Further acritarchs and terrestrial plants remain from the Late Ordovician at Hlánská Třeban (Czechoslovakia). *Časopis pro Mineralogii a Geologii*. 33(1):1–10.
- Vavrdová M. 1989. New acritarchs and miospores from the Late Ordovician of Hlánská Třeban, Czechoslovakia. *Časopis pro Mineralogii a Geologii*. 34(4):403–419.
- Vavrdová M. 1990. Coenobial acritarchs and other palynomorphs from the Arenig/Llanvirn boundary Prague Basin. *Vestník Ustredniho ustavu Geologického*. 65:237–242.
- Vavrdová M. 1997. Early Ordovician provincialism in acritarch distribution. *Review of Palaeobotany and Palynology*. 98(1-2):33–40.
- Vecoli M. 1999. Cambro-Ordovician palynostratigraphy (acritarchs and prasinophytes) of the Hassi-R' Mel area and northern Rhadames Basin, North Africa. *Palaeontographica Italica*. 86:1–112.
- Vecoli M. 2000. Palaeoenvironmental interpretation of microphytoplankton diversity trends in the Cambrian-Ordovician of the northern Sahara Platform. *Palaeogeography, Palaeoclimatology, Palaeoecology*. 160(3-4):329–346.
- Vecoli M. 2004. Stratigraphic and palaeoenvironmental distribution of organic-walled microfossils in Cambrian-Ordovician transitional strata of borehole Bir Ben Tartar-1 (Tr-1; Ghadamis Basin, southern Tunisia). *Memoir of the Association of Australasian Palaeontologists*. 29:13–30.
- Vecoli M, Cesari C. 2019. Palynological correlation of the Late Cambrian to Middle Ordovician Saq Formation in Saudi Arabia and equivalent strata in Oman manuscript title. In: SPE Middle East Oil and Gas Show and Conference, SPE, Manama, Bahrain; p. D021S004R001.
- Vecoli M, Delabroye A, Spina A, Hints O. 2011. Cryptospore assemblages from Upper Ordovician (Katian-Hirnantian) strata of Anticosti Island, Québec, Canada, and Estonia: palaeophytogeographic and palaeoclimatic implications. *Review of Palaeobotany and Palynology*. 166(1-2):76–93.
- Vecoli M, Le Hérisse A. 2004. Biostratigraphy, taxonomic diversity, and patterns of morphological evolution of Ordovician acritarch organic-walled microphytoplankton) from the northern Gondwana margin to

- palaeoclimatic and palaeogeographic changes. *Earth Science Reviews*. 67(3-4):267–311.
- Vecoli M, Riboulleau A, Versteegh GJM. 2009. Palynology, organic geochemistry and carbon isotope analysis of the latest Ordovician through Silurian clastic succession from borehole Tt1, Ghadamis Basin, southern Tunisia, North Africa: palaeoenvironmental interpretation. *Palaeogeography, Palaeoclimatology, Palaeoecology*. 273(3-4): 378–394.
- Verschaeve D. 2004. Biostratigrafie met Chitinozoa van de GSS Pkandidaat voor de basis van “Etage Zes” van het Ordovicium, in Hartfell Score (Southern Uplands, Scotland) [unpublished MSc thesis]. Gent (Belgium): Laboratorium voor Paleontologie, Universiteit Gent.
- Videt B, Paris F, Rubino JL, Boumendjel K, Dabard MP, Loi A, Ghienne JF, Marante A, Gorini A. 2010. Biostratigraphical calibration of third-order Ordovician sequences on the northern Gondwana platform. *Palaeogeography, Palaeoclimatology, Palaeoecology*. 296(3-4):359–375.
- Wang X, Chen X. 2004. Ordovician chitinozoan diversification events in China. *Science in China Series D: Earth Sciences*. 47(10):874–879.
- Wang Y, Li J, Wang R. 1997. Latest Ordovician cryptospores from southern Xinjiang, China. *Review of Palaeobotany and Palynology*. 99(1): 61–74.
- Webby BD, Cooper RA, Bergström SM, Paris F. 2004. Stratigraphic framework and time slices. In: Webby BD, Paris F, Droser ML, Percival IG, editors. *The Great Ordovician Biodiversification Event*. New York (NY): Columbia University Press; p. 41–47.
- Wellman CH. 1993. A land plant microfossil assemblage of mid Silurian age from the Stonehaven group, Scotland. *Journal of Micropalaeontology*. 12(1):47–66.
- Wellman CH, Gray J. 2000. The microfossil record of early land plants. *Philosophical Transactions of the Royal Society of London. Series B, Biological Sciences*. 355(1398):717–732.
- Wellman CH, Higgs KT, Steemans P. 2000. Spore assemblages from a Silurian sequence in Borehole-151 from Saudi Arabia. In: Al-Hajri S, Owens B, editors. *Stratigraphic Palynology of the Palaeozoic of Saudi Arabia*. USA: Stratigraphic palynology of the Palaeozoic of Saudi Arabia. p. 116–133.
- Wellman CH, Osterloff PL, Mohiuddin U. 2003. Fragments of the earliest land plants. *Nature*. 425(6955):282–285.
- Wellman CH, Richardson JB. 1993. Terrestrial plant microfossils from Silurian inliers of the Midland Valley of Scotland. *Palaeontology*. 36(1):155–193.
- Wellman CH, Richardson JB. 1996. Terrestrial plant microfossils from Silurian inliers of the Midland Valley of Scotland. *Palaeontology*. 36: 155–193.
- Wellman CH, Steemans P, Miller MA. 2015. Spore assemblages from Upper Ordovician and Lowermost Silurian sediments recovered from Qusaiba-1 shallow core hole, Qasim region, Central Saudi Arabia. *Review of Palaeobotany and Palynology*. 212:111–126.
- Wicander ER. 1974. Upper Devonian-lower Mississippian acritarchs and prasinophycean algae from Ohio, U.S.A. *Palaeontographica Abteilung B*. 148:9–43.
- Wicander R, Playford G, Robertson EB. 1999. Stratigraphic and paleogeographic significance of an Upper Ordovician acritarch flora from the Maquoketa Shale, northeastern Missouri, USA. *Memoir of the Paleontological Society*; p. 1–38.
- Wicander R. 1981. Systematics and biostratigraphy of the organic-walled microphytoplankton from the Middle Devonian (Givetian) Silica Formation, Ohio, USA. *American Association of Stratigraphic Palynologists, Contributions Series*. 8:1–137.
- Winchester-Seeto T, Foster C, O’Leary T. 2000. Chitinozoan from the Middle Ordovician (Darriwilian) Goldwyer and Nita Formations, Canning basin (Western Australia). *Acta Palaeontologica Polonica*. 45: 271–300.
- Wood GD, Turnau E. 2001. New Devonian coenobial Chlorococcales (Hydrodictyaceae) from the Holy Cross Mountains and Random-Lublin Region of Poland: their paleoenvironmental and sequence stratigraphic implications. In: Goodman DK, Clarke, RT, editors. *Proceedings of the IX International Palynological Congress*. Houston (TX): American Association of Stratigraphic Palynologists Foundation; p. 53–63.
- Wright RP, Meyers WC. 1981. Organic-walled microplankton in the subsurface Ordovician of northeastern Kansas. *Kansas Geological Survey, Subsurface Geology Series*. 4:1–53.
- Xiaofeng W, Xiaohong C. 2004. Ordovician chitinozoan diversification events. *China Science in China Series D: Earth Sciences*. 47:874–987.
- Yin L. 1995. Early Ordovician acritarchs from Hunjiang region, Jilin and Yichang region, Hubei province, China. *Palaeontologia Sinica, Series A*. 185(12):1–170. (In Chinese with English summary).
- Zalasiewicz J, Rushton A, Vandenbroucke T, Verniers J, Stone P, Floyd J. 2004. Submission of Hartfell Score (south Scotland) as a GSSP for the base of the middle stage of the Upper Ordovician Series. Report for the ISOS GSSP Discussion site, UK p. 1–22.